GEOSCIENCE APPLICATIONS OF GEOGRAPHIC INFORMATION SYSTEMS FOR THE STRAND FIORD AREA, WEST AXEL HEIBERG ISLAND, NUNAVUT

Sheri Ann Lyon

Submitted in Partial Fulfillment of the Requirements
For the Degree of Bachelor of Science, Honours
Department of Earth Sciences
Dalhousie University, Halifax, Nova Scotia
April 2005

Dalhousie University

Department of Earth Sciences
Halifax, Nova Scotia
Canada B3H 3J5
(902) 494-2358
FAX (902) 494-6889

DATE: April 28/05

AUTHOR: Sheri Ann Lyon

TITLE: Geoscience Applications of Geographic Information Systems for the Strand Fiord Area, west Axel Heiberg Island, Nunavut

Degree: BSC Convocation: May Year: 2006

Permission is herewith granted to Dalhousie University to circulate and to have copied for non-commercial purposes, at its discretion, the above title upon the request of individuals or institutions.

ABSTRACT

This study uses Geographic Information Systems (GIS) as a tool to assess the geological processes associated with igneous rocks and salt structures within the Strand Fiord area, Axel Heiberg Island, Nunavut. This area was the subject of petroleum exploration with disappointing results, and this study attempted to provide practical tools to provide an explanation for that failure. Remote access of the area has limited field mapping to reconnaissance maps at 1:250,000 scale, compiled by the Geological Survey of Canada. A GIS, the first for Nunavut in areas north of the 75th parallel, allows more geological detail to be added, particularly in the case of igneous rocks. To produce the GIS, digital elevation models, aeromagnetic data, gravity, and lithological data were integrated with geological and topographic maps. As an example of how petrological data can be integrated into such a GIS, lithological data for the Strand Fiord Formation (Index Ridge on the Kanguk Peninsula) and a large sill exposed at the head of Expedition Fiord (Wolf Intrusion) were compiled.

Queries of the database prove that the characterizations and classifications are true for a certain structure within the GIS by providing information on the shape and morphology of the structures, nature of geological contacts, attitude, and extent of faults, and relative percentage of igneous material "rafted" in the evaporite domes.

Analysis of aeromagnetic data integrated with geology and DEM layers helps better define the distribution of igneous rocks, and reveals a north to northwest-trending high that coincides with the trends of salt diapirs and some important regional faults. Magnetic data help ascertain whether diapirs are shallow or deep bodies, and allow to speculate the presence of salt under a region where salt is covered by the Muller Ice Cap. A gravity low in the eastern portion of the study area is interpreted to represent a region of intense folding and faulting rooted by a décollement and cored by low-density salt structures, topographically expressed as the Princess Margaret Range.

Key words: Strand Fiord, Axel Heiberg Island, GIS, salt diapirs, igneous intrusions, resource potential

TABLE OF CONTENTS

TABLE OF FIGURES

TABLE OF TABLES

ACKNOWLEDGEMENTS

I would like to thank Drs. Marie-Claude Williamson and Marcos Zentilli, my thesis supervisors, for their continued support and guidance throughout the year. They kept me motivated and I am grateful for all the time and effort they put in. Special thanks to Roxane Déry, Gordon Oakey, and Sheila Hynes (GSC Atlantic), who initiated the GIS work on the Strand Fiord area. I am grateful to Tracy Lynds (GSC Ottawa) for advice on geophysical databases and to Frank Dostlar who helped with aeromagnetic and gravity data. Paul Budkewitsch, of the Canada Centre for Remote Sensing, kindly gave us access to Earth Observation data for the study area and Axel Heiberg Island. Gordon Brown (Dalhousie University), Gavin Manson and Frank Thomas (GSC Atlantic) assisted with thin section preparation, file conversions, and spectral analysis, respectively. Without the contributions of all the persons above, I would never have completed a thesis. Thank you to all of you for your help and time.

Support for the project was provided by the NEON project of the Earth Sciences Sector, Natural Resources Canada. This thesis is also a contribution to CRD project "Geothermal Anomalies Associated with Salt Structures" funded by the Natural Sciences and Engineering Research Council of Canada (NSERC) and Petroleum Research Atlantic Canada (PRAC), awarded to Dr. M.Zentilli.

CHAPTER 1 INTRODUCTION

1.1 General statement

Geographic Information Systems (GIS) are a relatively recent technology that can help geologists present and interpret their data in new ways. The GIS is set up to capture, store, manipulate, display, and analyze many databases that are all spatially referenced to the Earth with known coordinates.

GIS are used in various fields such as science, government, hospital administration, etc. and can be very useful tool in geology because it helps the geologist understand geological formations, structures, and processes. Data can be represented by two different databases. The first shows data spatially by using layers (themes) such as topographical data or location points on a map. The next type of database is an attribute table and assigns meaning to the location within the theme. The table displays information such as the coordinates or lithologies of the samples. GIS software can manipulate and analyze this data by performing operations on themes and attributes such as queries and overlays.

Limited outcrop exposure due to ice cover and remoteness creates difficulties while field mapping in the Arctic. Through manipulation of data within a GIS, results will give a better representation of the stratigraphic formations and structures within the study area. The application of GIS to perform various operations and queries will help solve questions in this study relating to basaltic magmatism and salt structures for the Strand Fiord area of West Axel Heiberg Island, Nunavut. Due to short field seasons and high travel costs, using GIS to aid geological interpretation proves to be beneficial for areas such as Axel Heiberg Island.

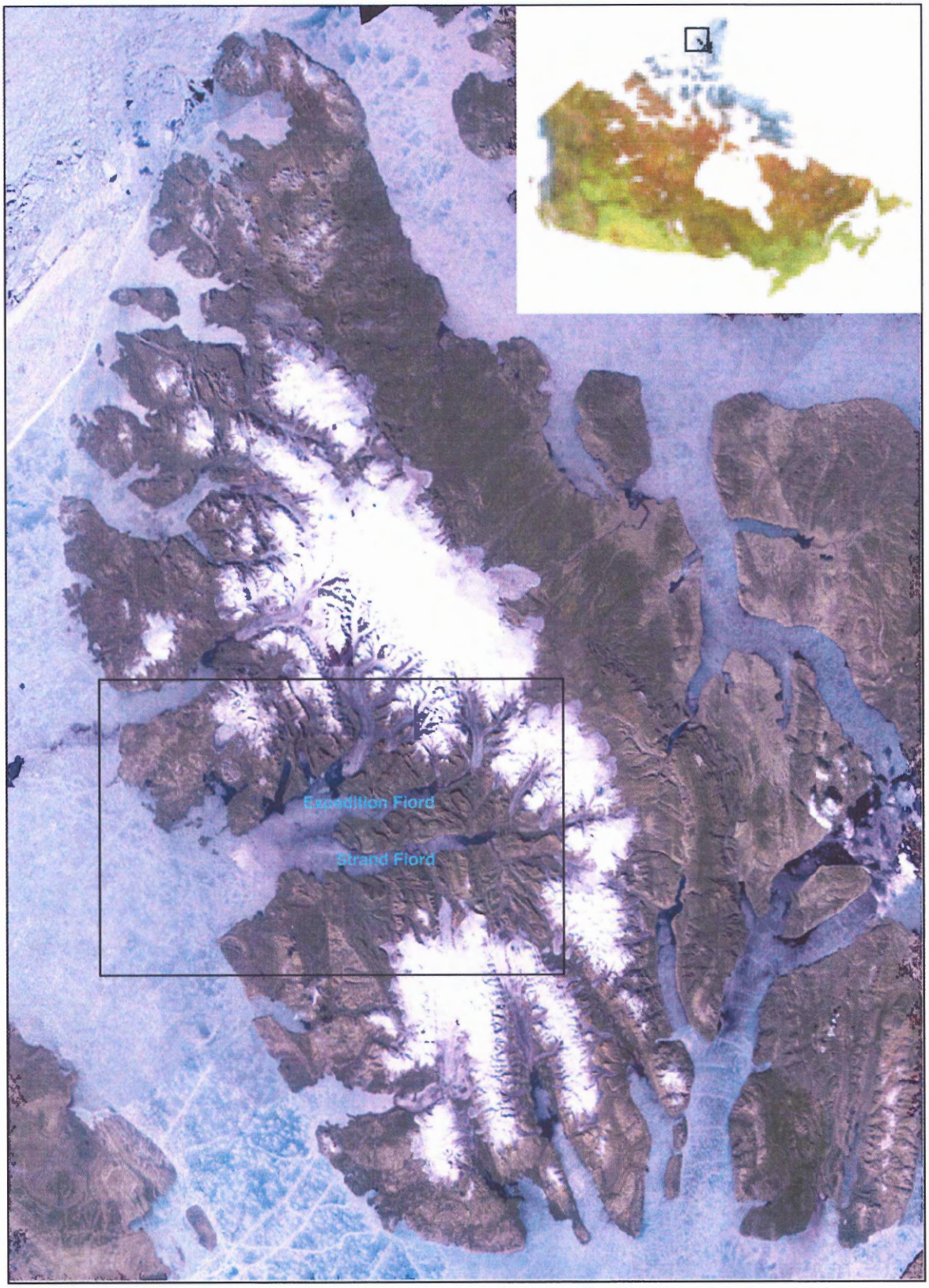

Figure 1.1 Study area location; Strand Fiord, Axel Heiberg Island, Nunavut, Canada. LandSAT image of Axel Heiberg Island courtesy of Paul Budkewitsch (CCRS). Satellite image of Canada courtesy of NRCAN.

1.2 Study Area

The study area is located within the Canadian Arctic Archipelago, Nunavut, at W 96-88 and N 79-80. Two east-west fiords, Strand and Expedition, constitute important landmarks for the study area and are located on Axel Heiberg Island, Nunavut, within the Canadian Arctic Archipelago (Figure 1.1).

This work will build upon a collaborative study, initiated in 2001, between Dr. Marie-Claude Williamson of the Geological Survey of Canada and Dr. Marcos Zentilli, Department of Earth Sciences, Dalhousie University. A full list of contributors can be found under Acknowledgments.

1.3 Previous Work

The first work completed in the Canadian Arctic Archipelago was during the late 1800's when explorers such as Robert Peary started the push to the North Pole or Per Shei was part of the famous Fram expedition (Trettin, 1989). Arctic geological research continued into the 1950's. Geographers and geologists used boats and dog sleds, to document the geology in the Canadian Arctic Archipelago. In 1955, the Geological Survey of Canada started 'Operation Franklin' in order to publish comprehensive studies of Arctic geology. The first stratigraphic outline was published in 1955 and over 65,000 km of seismic reflection lines were taken. The first geological map of Axel Heiberg Island and surrounding islands was published in 1959 showing stratigraphic formations and cross sections from gravity and deep refraction surveys were also published in the 1950s (Trettin, 1989).

During the late 1950s to early 1960s, McGill University began the Jacobsen-McGill Arctic Research Expedition and published reports related to the evaporite diapirs and igneous rocks of the Strand Fiord area.

Petroleum exploration of the Arctic Islands has also been investigated. During 1960-1987, over 176 wells were drilled within the Sverdrup Basin, of which 18 appear to be favourable for oil and gas (Trettin, 1989).

In recent years, many studies have been completed. Of significance to this work are fission track studies initiated by Dr. Marcos Zentilli to understand hydrocarbon generation and predict the thermal history using vitrinite reflectance (e.g. Arne et al., 1998); and the geochemical and petrological study of Cretaceous mafic igneous rocks of the Sverdrup Basin accomplished by Williamson (1988). A complete list of all relevant literature for the Strand Fiord area can be found in Table 1.1.

There are still many unanswered questions about the geology of the Arctic Archipelago due to ice cover and remoteness. Through manipulation of data within a GIS, results will help solve questions in this study relating to basaltic magmatism and salt structures for the Strand Fiord area.

1.4 Scientific Questions

Much of Axel Heiberg Island and other areas of the Canadian Arctic Archipelago are ice covered, isolated and have complex geology, creating difficulties when mapping. In 1971, the GSC published 1:250,000 geological maps for the Strand and Middle Fiords. Due to the limited access, air photos were used to map most of the island. Many questions still remain about the geology and volume of salt diapirs. The main objective of this study is to produce a GIS in order to help answer the following questions.

Year	Reference	Subject of Study
1961	Hoen, E.W.	Descriptions of salt diapirs of the Strand Fiord area.
1961	Kranck, E.H.	Descriptions of salt diapirs of the Strand Fiord area.
1963	Fricker, P.E.	Descriptions of the geology of the Strand Fiord area.
1963	Kranck, E.H.	Descriptions of salt diapirs of the Strand Fiord area.
1966	Schwerdtner, W.M et al.	Structural development of evaporite diapirs in Axel Heiberg Island
1966	Schwerdtner, W.M.	Identification of evaporite diapirs formed under the influence of horizontal compression.
1967	Schwerdtner, W.M. & Clark, A.R.	Structural analysis of Mokka Fiord and South Fiord domes.
1969	Thorsteinsson, R. and Tozer, E.T.	Descriptions of the geology of the Arctic Archipelago.
1971	Thorsteinsson, R.	Geological Map compilation Strand Fiord region,1:250.000.
1971	Thorsteinsson, R.	Geological Map compilation Strand Fiord region,1:250.000.
1982	Balkwill, H.R., and Fox, F.G.	Overview of the Incipient Rift Zone of Western Sverdrup Basin.
1984	Schwerdtner, W.M. & van Kranendonk, M.	Structure of the Stolz Diapir - a well-exposed salt dome on Axel Heiberg Island.
1984	van Berkel, J.T., Schwerdtner, W.M., and Torrance, J.G.	Descriptions of salt diapirs of the Sverdrup Basin.
1988	Embry. A and Osadetz, K.G.	Stratigraphy of volcanic rocks in the east-central Sverdrup Basin.
1988	Williamson, M-C.	Descriptions of igneous rocks of the Strand Fiord area.
1989	Trettin, H.P.	Overview of geology and tectonic history of the Arctic Islands.
1991	Davies, G.R. and Nassichuk, W.W.	Carboniferous and Permian history of the Sverdrup Basin.
1991	Embry, A.F.	Mesozoic history of the Arctic Islands.
1992	Stephenson, R.A., van Berkel, J.T., and Cloetingh, S.	Descriptions of salt diapirs of the Sverdrup Basin.
1998 2002	Arne, D. et al.	Apatite fission track evidence for the timing of Eurekan deformation in the Sverdrup Basin
1999 2002	Pollard W. et al. & Andersen and Pollard	Descriptions and interpretation of perennial spring occurrences in the Expedition Fiord area.
In press	Villeneuve, M., and Williamson, M-C.	$^{40}Ar/^{39}Ar$ dating of mafic rocks from the Sverdrup Basin Magmatic Province.

Table 1.1 – Relevant literature to Strand Fiord area.

1.4.1 Can GIS help assess properties of igneous rocks in the study area?

The sedimentary succession within the study area is heavily intruded by sills that are not currently included in the 1:250,000 maps of the area. Using GIS, comparing and manipulating various attributes and themes will produce a better representation of the extrusive bodies, and their intrusive equivalents.

1.4.2 Can GIS help determine depth and volume of salt structures in the study area?

Previous exploration in the Arctic Archipelago has identified several potential salt related petroleum systems, making the classification and identification of salt structures vital. These are discussed briefly in Chapter 3. By performing operations on various attributes and themes within the GIS, the classification, characteristics, and geometry of the salt structures can be determined.

Answering the above questions will provide an improved understanding of the geology for the Strand Fiord area. As a result, a more accurate geological map will show a better representation of the stratigraphic formations and structures for the study area. The assemblage of a GIS for the study area is the first attempt to integrate multiple databases in areas north of the 75th parallel. The Strand Fiord, Axel Heiberg Island is an excellent study area because of the significant number of geological and geophysical studies that were carried out by the Geological Survey of Canada in this region, over the past 50 years. There is also a renewed interest in the resource potential of this area, linked to the interaction of Cretaceous igneous rocks with evaporite diapirs that intrude the Mesozoic and Tertiary succession of the Sverdrup Basin. The GIS is a useful tool to characterize and classify the igneous rocks and salt diapirs, by providing

information on the shape and morphology of the structures, nature of geological contacts, attitude, and extent of faults, and relative percentage of igneous material "rafted" in the salt domes.

1.5 Scope and Organization

This study is divided into chapters pertaining to the geological setting, methods, GIS applications, discussion, conclusion and appendices. Chapter 2 will describe the methods used in conjunction with the GIS, petrography, and electron scanning microscope. Chapter 3 is a description of the geological setting of the Sverdrup Basin and Axel Heiberg Island in terms of tectonism, stratigraphic formations, and structures. Chapter 4 will explain all the databases and the results obtained from each. Chapter 5 will discuss the application of GIS to solve the questions posed pertaining to the igneous bodies and salt intrusions of the study area. Discussion will follow examining the use of GIS for interpreting geology and future implications.

1.6 Summary

GIS is a tool to help geologists and geographers show and interpret their data in new ways through capturing, storing, manipulating, querying, displaying, and analyzing data. These data is represented in the GIS as layers (themes) and attributes.

Data collected by Dr. Marie-Claude Williamson, Dr. Marcos Zentilli, CCRS, and GSC will be inputted into the GIS and used to answer two main questions:

- Can GIS help assess properties of igneous rocks in the study area?
- Can GIS help determine depth and volume of salt structures in the study area?

Limited outcrop exposure due to ice cover and remoteness creates difficulties while field mapping in the Arctic. GIS is a very important tool for the management and interpretation of data. Through manipulation of data within a GIS, results can give a better representation of the geological features. The study will produce a geological map showing a better representation of the stratigraphic formations and structures for the study area. The assemblage of a GIS for the study area is the first attempt to integrate multiple databases in areas north of the 75^{th} parallel. The Strand Fiord, Axel Heiberg Island is an excellent study area because of the significant number of geological and geophysical studies carried out in previous years and because of the renewed interest in the resource potential of this area.

CHAPTER 2 METHODS

2.1 Building a Geographic Information System (GIS)

Assessing characteristics of igneous bodies and salt diapirs within the Strand Fiord requires a compilation of all available data. During the summer of 2004, a student hired by Dr. Marie-Claude Williamson started preliminary work on the GIS by adding data collected by Dr. Williamson and Dr. Zentilli and previously published data into ArcMap. ArcMap allows the management of multiple databases and allows the operator to perform basic queries upon the attributes of the database.

To produce the GIS, aeromagnetic and gravity data were integrated with geological and topographic maps (1:250,000 scale) made available through the Government of Canada. The Earth Sciences Sector of Natural Resources Canada (NRCAN) offers a data repository site complete with all available aeromagnetic, geochemical, gravity, radioactivity, and topographical data for most parts of Canada; however, only aeromagnetic, gravity, and topographic data were available for the Strand Fiord due to the remoteness of the area. Scanned geological maps are also made available through NRCAN and of particular interest to this study are the 1971 geological maps of Strand Fiord and Middle Fiord by Thorsteinsson. These geological maps are the basis for the geological point, line, and polygon data for the present study.

In addition, satellite imagery and Digital Elevation Models (DEMs) were provided by Paul Budkewitsch of the Canadian Centre for Remote Sensing (CCRS). These images allow for more precise identification of igneous intrusions sampled during field work.

Lithological data was also integrated into the GIS. One volcanic succession of the Strand Fiord Formation on the Kanguk Peninsula (Index Ridge) and a large sill exposed at the head of Expedition Fiord (Wolf Intrusion) show characteristics of extrusive and intrusive bodies. The attributes within the GIS for the two samples include: geographic location, lithology, petrography, and textural characteristics.

The integration of all of the databases, along with information on the samples collected by Dr. Williamson and Dr. Zentilli, will help answer questions posed in the Introduction. Chapter 4 carries out assessment of the various databases.

2.2 Lithological Data

During field seasons in 2003 and 2004, Williamson and Zentilli collected samples from the Strand Fiord region. Extrusive and intrusive samples were cut into polished and normal thin sections. At the MicroAnalysis laboratory of the Bedford Institute of Oceanography (BIO), petrography and ESEM analyses were completed.

2.2.1 Petrography

Using an optical microscope, observations of mineral type, textures, and per cent cover will help show characterizations of the six extrusive samples and five intrusive samples. Observations will be displayed within a table for easy reference. All photomicrographs were captured digitally using a Nikon CoolPix camera available at the MicroAnalysis facility at BIO and a graticule was used for scale. Note that in all photomicrographs the scale is illustrated by the long axis of the yellow box. Observations and digital images will be hotlinked to the GIS database.

2.2.2 Environmental Scanning Electron Microscope (ESEM)

The ElectroScan E3 Environmental Scanning Electron Microscope situated at BIO acts like a scanning electron microscope (SEM) as it creates a beam of electrons that travels through a sample producing a greyscale image (Thomas and Williamson, 2004). The ESEM differs from your typical SEM because ESEMs have a lower vacuum state compared the SEMs that have a high vacuum state (Thomas and Williamson, 2004). The ESEM analyzed selected polished thin sections in order to confirm mineral phases present in selected samples. Frank Thomas, operator of the ESEM, helped prepare and analyze the samples. Spectral analysis identifies the principal mineral phases of the intrusive sill while grey scale images displays the textures present. A comparison of the ESEM and petrography observations will confirm the mineral phases present.

The prepared samples show different mineral phases via shades of grey. A grey scale image was obtained for each area analyzed in order to record the spectra analysis and is hotlinked to the GIS database. Where ever a different phase exists, a qualitative spectral analysis gives a spectrum of elements comprising the grain. Examining the proportions of elements leads to the identification of the grain. For this study, a fresh unaltered sample is used as a reference slide. Analysis of mineral phases of the reference slide are used for comparison with the grains from an intrusive sample.

The grayscale images and spectral analysis are added to the GIS database in attempt too illustrate the textures and minerals present in the samples.

2.2.3 Compositional Maps

Another function of the ESEM at BIO is producing compositional maps showing the abundance of selected elements within an area. Compositional mapping is an easy way to investigate the presence of sulphides and other important trace elements. Each element is represented on its own map using a different colour. A concentration of dots within an area, indicate a high proportion of the specific element within an area. To show the ESEM capability, an area previously examined with the qualitative spectral analysis will be chosen and elements including Fe, Ca, Ti, and Ni will be examined. It was beyond the scope of this study to link photomicrographs and compositional maps to location points in the GIS. The objective of this work was to demonstrate the usefulness of the method, and how the information can be integrated with other databases.

2.3 Two-dimensional cross-sections

Throughout the study area, the Mesozoic strata of the fiord contain intrusions of basaltic lavas, chemically equivalent sills, and salt resulting in magnetic highs and lows. Cross sections across known intrusions show varying magnetic signatures across different features of the area. ArcMap outputs values and using Microsoft Excel the distance in metres (X-Axes) and the magnetic values in nanoteslas (Y-Axes) be plotted. Analysis of the two-dimensional cross-sections classify and characterize the igneous and salt structures.

2.4 Remote Sensing

LANDSAT images and air photos provided by Paul Budkewitsch (Canada Centre for Remote Sensing) will show the boundaries of rafted igneous rocks within the South Fiord Dome in the western portion of the Strand Fiord. For specified areas, LANDSAT images have brightness and spectral information allowing the construction of a spectral reflectance signature for different materials through absorbing/reflecting wavelengths (Liew, 2001). LANDSAT images enhance textures and geometries of the geological features through shadows, colours, etc., allowing for easy identification. Knowing where the rafted igneous areas occur within the dome allows for a better representation of the boundaries between the two.

CHAPTER 3 GEOLOGICAL SETTING

3.1 Introduction: The Canadian Arctic Islands, Nunavut

The Canadian Arctic Islands and surrounding channels cover roughly 1.3 million square kilometres of Northern Canada. The Sverdrup Basin extends east to west from the Parry Islands to Ellesmere Island, and northward into the Arctic Ocean. The following sections discuss the geology and tectonism of Axel Heiberg Island and the Sverdrup Basin.

3.2 Sverdrup Basin

The Sverdrup Basin is an oval-shaped, regional, deep depression forming after a widespread rifting event in the Carboniferous (Balkwill and Fox, 1981). The basin measures 1,300 kilometres by 400 kilometres respectively.

3.2.1 Tectonic setting

Sedimentary and volcanic rocks of the Sverdrup Basin overly the Franklinian mobile belt, consisting of 3 kilometres of Palaeozoic strata, 9 kilometres of Mesozoic strata, and 3 kilometres of Cretaceous to Tertiary clastic sediments (Trettin, 1994). In between Late Carboniferous and Late Permian deposition, an event referred to in the literature as the "Melvillian Disturbance" occurred causing folding and faulting of the Sverdrup Basin to take place (Thorsteinsson and Tozer, 1960; Trettin 1991). This basin was over 2000 meters deep and finished forming by the Early Permian (Stephenson et al., 1992).

Igneous rocks are associated with the initial Carboniferous-early Permian rifting event (Cameron, 1982), and emplacement occurred episodically during the Cretaceous (Embry and Osadetz, 1988; Williamson, 1988). The mafic igneous

rocks are predominantly intrusive and of tholeiitic affinity, but some alkali extrusive basalts and associated intrusions are found (Williamson, 1988; Villeneuve and Williamson, 2003).

The last developmental influence affecting the Sverdrup Basin was the Eurekan Orogeny. This orogeny produced faulting, folding, and intrusion of evaporite bodies around Axel Heiberg Island and Ellesmere Island as a result of compressional tectonic activity (Thorsteinsson and Tozer, 1969; Miall, 1981). Uplift and erosion of the Princess Margaret Arch, Cornwall Arch, Stokerson Arch, Sverdrup Basin, and Franklinian mobile belt allowed alluvial, deltaic, and shallow marine deposition to take place in surrounding basins (Miall, 1981). The Eurekan Orogeny ended basin development and created the late Cretaceous to Paleogene Eureka Sound Group comprised of over 3 kilometres of mudrock and sandstone (Trettin, 1994).

3.2.2 The Cretaceous igneous province near Strand Fiord

Axel Heiberg Island, Northern Ellesmere Island, and other islands within close proximity show exposure of the Sverdrup Basin Magmatic Province (SBMP) (Williamson, 1988). The SBMP contains flood basalts, hypabyssal intrusive sheets, dykes and central volcanoes (Villeneuve and Williamson, 2003). Argon dating suggests that the emplacement of the volcanic succession occurred at 94-95 Ma (Villeneuve and Williamson, 2003).

3.2.3 Salt diapirism and thermal history

During the Permo-Triassic to Early Cretaceous, salt diapirs infused into the overburden due to of horizontal compression and small tabular anhydrite sills

and dykes rose because of horizontal compression in the Cretaceous and compression of plates during the Tertiary Eurekan Orogeny (Stephenson et al., 1992). Secondary driving forces such as differential loading, overburden and basement faulting, thermal contraction, and extension are believed to aid in the formation of diapirs since buoyancy cannot elevate the denser anhydrite alone (Stephenson et al., 1992). At the start of the Triassic, salt diapirs started to raise sporadically creating local unconformities and thinning of stratigraphic sequences that resulted in minor highs (Trettin, 1989). Exposure of the diapirs is excellent along the basin due to the dry cold climate of the basin that prevents erosion and along the Sverdrup Basin axis, evaporite diapirs are present consisting of 400 meters of anhydrite and an unknown depth of salt (Stephenson et al., 1992). The Sverdrup Basin consists of anhydrite in the upper portion ranging from 500-420 metres with thick small-interbedded limestones and a lower layer composed of salt with interbedded anhydrite (Stephenson et al., 1992). These diapirs form large dome shapes composed of gypsum and salt at depth, or dikes and sills composed of anhydrite (Hoen, 1961).

As mentioned in the Introduction, 176 wells have been drilled within the Sverdrup Basin from 1960-1987, while only 18 were promising (Trettin, 1989; Zentilli et al., 2003). Several of the petroleum plays drilled are salt cored and most were located on anticlinal structures consisting of Mesozoic clastic strata (Zentilli et al., 2003). Eurekan thrusting may have produced structural traps for hydrocarbons within the Tertiary strata, which were intruded by diapirs composed of Carboniferous salt, anhydrite and gypsum (Zentilli et al., 2003). Whereas

promising hydrocarbon fields occur in the Western Sverdrup Basin, wells in the region of Axel Heiberg Island are dry or have only small amounts of hydrocarbons. From apatite fission track evidence, Arne et al. (1998, 2002) suggested that hydrocarbon maturation and migration in the eastern Sverdrup Basin occurred well before the Palaeocene-Eocene Eurekan thrusting.

3.3 Central and western Axel Heiberg Island

Along the Strand Fiord area, Jurassic and Cretaceous sediments are heavily folded trending north south and northwest southeast with intersecting igneous flows and sills (Kranck, 1963). Synclines contain sediments within the folds and have broad limbs, while anticlines are narrow consisting of very steep limbs resulting in a generally symmetrical style of folding (Kranck, 1961). Tectonics from the north and south extremities of the island influence the tectonic styles of the Strand Fiord area (Kranck, 1961).

Central Axel Heiberg Island contains the strongest folding of the Innutian Belt (Kranck, 1961), where this folded and faulted strata gives Axel Heiberg its rough terrain (Hoen, 1961). The Strand Fiord area comprises of sequences of rocks called the Awingak Formation, Deer Bay Formation, Isachsen Formation, Christopher Formation, Hassel Formation, Kanguk Formation, and the lower portion of the Eureka Sound Formation (Balkwill et al., 1975). Section 3.4 describes individual formations.

3.3.1 Volcanic rocks of the Strand Fiord Formation

The Strand Fiord Formation constitutes the youngest basalts of the Strand Fiord area and argon dating confirms that 94-95 Ma emplacement of this volcanic succession occurred (Thorsteininsson and Tozer, 1969; Villeneuve and

Williamson, 2003). The flows occur as thick successions of ponds of lava with a well-defined flow top (Williamson and MacRae, 2001) comprising of *aa* and *pahoehoe* flows that reveal intraflow structures within the basalt (Villeneuve and Williamson, 2003). Also occurring in this area are volcanic breccias and lapilli tuffs, however they are not as common as the lava flows (Williamson, 1988). Several authors describe this area as being a Flood Basalt province due to the basalt composition, ponded lavas, and rapidly flowing lavas (Williamson and MacRae, 2001).

The Strand Fiord Formation occurs between the Bastion Ridge and Kanguk formations, described further in 3.4.

3.3.2 Dykes and sills

The emplacement of mafic dykes and sills occurred concurrently with the emplacement of the basaltic lavas, however, the dykes and sills have a wider aereal coverage and there is an increase north eastward through the basin in the amount of sills and dykes intruded into the country rock (Embry, 1991). These sills are Carboniferous to Late Cretaceous in age and are commonly up to 150 metres in thickness (Embry, 1991). Most formations of Axel Heiberg contain intrusions of sills and dykes, except the Upper Cretaceous Kanguk shales (Fricker, 1961). On parts of Axel Heiberg Island, dyke swarms occur (Thorsteinsson and Tozer, 1969).

3.3.3 Salt domes

Evaporite diapirs on Axel Heiberg Island have a source in the Carboniferous-Permian Otto Fiord Formation and tend to form as large isolated

domes or as ridges (Hoen, 1961). Large isolated domes are typically oval shaped, however sometimes they occur crescent shaped (Hoen, 1961). The strata tend to dip 60 to 70 degrees where it meets the dome and the sediments thin out as they approach the diapirs due to squeezing and dragging (Hoen, 1961). Salt usually occurs at depth in these diapirs, some of which are up to 10 kilometres wide (Stephenson et al., 1992). Mafic dykes have intruded some evaporite diapirs (Thorsteinsson and Tozer, 1969).

Dykes of gypsum are also found nearby varying in thickness approximately 15 metres and contain inclusions (Hoen, 1961). Gypsum ridges occur with smaller separated domes along strike while limited to the lenticular belt that trends northwest (Hoen, 1961). The largest ridges occur along this belt around the Strand Fiord Formation where the diapirs form within the sharp anticlines (Hoen, 1961). The ridges contain no bedding, minor limestone inclusions may occur, and the gypsum may become sheared showing the presence of flow structures (Hoen, 1961).

On Axel Heiberg, over 500 metres of anhydrite covers salt; however, the anhydrite thickness is believed to have been thicker before erosion (Stephenson et al., 1992).

3.3.4 Formations of the Strand Fiord

The Awingak Formation, Deer Bay Formation, Isachsen Formation, Christopher Formation, Hassel Formation, Kanguk Formation, and the lower portion of the Eureka Sound Formation are the rock sequences that make up the

Strand Fiord area (Balkwill et al., 1975). Further descriptions and discussion of the formations follow in Chapters 4 and 5.

3.3.4.1 Blaa Formation (Triassic)

This formation is composed of dark grey shales and minor siltstone occurrences (Thorsteinsson and Tozer, 1969).It occurs in the Strand Fiord and Expedition area with a thickness of 700m with a gradational contact with the Heiberg Formation (Fricker, 1963).

3.3.4.2 Heiberg Formation (Upper Triassic to Lower Jurassic)

The Heiberg formation is mainly composed of non-marine and consists of sandstone with minor amounts of siltstone and shale (Thorsteinsson and Tozer, 1969). In the region of the Strand Fiord, the Heiberg Formation is less than 1250 metres thick and has an abrupt contact with the overlying Savik Formation (Fricker, 1963).

3.3.4.3 Savik Formation (Middle Jurassic)

This marine formation contains shale with minor amounts of siltstone and clay ironstone (Fricker, 1963). On Axel Heiberg, the thickness ranges from 80 to 300 metres and there is a gradational contact with the Awinkgak Formation (Fricker, 1963).

3.3.4.4 Awingak Formation (Upper Jurassic)

The Awinkgak formation is mainly non-marine arenaceous sandstones and shales with varying thicknesses of 75 to 300 metres and has a gradational contact with the Deer Bay formation (Fricker, 1963).

3.3.4.5 Deer Bay Formation (Upper Jurassic to Lower Cretaceous)

This marine formation consists of shale, siltstone, and minor sandstone, has a thickness of 80-700 metres, and has a gradational contact with the Isachsen (Fricker, 1963).

3.3.4.6 Isachsen Formation (Lower Cretaceous)

The Isachsen formation comprises of sandstone with shales and intrusions of dikes and sills are common (Fricker, 1963). The contact with the overlying Christopher Formation is gradational (Thorsteinsson and Tozer, 1969).

3.3.4.7 Christopher Formation (Lower Cretaceous)

Grey shales dominate this formation with minor amounts of siltstone and sandstone forming a thickness as much as 1000 metres with intruding sills and dykes (Fricker, 1963). Superimposed on the Christopher Formation is the Hassel Formation forming a gradational contact (Fricker, 1963).

3.3.4.8 Hassel Formation (Lower to Upper Cretaceous)

The Hassel Formation includes medium to fine grained quartzose sandstone and siltstone (Thorsteinsson and Tozer, 1969). Along Axel Heiberg Island, the thickness can reach 430 metres and has a gradational contact with the overlying Kanguk Formation (Fricker, 1963).

3.3.4.9 Kanguk Formation (Upper Cretaceous)

The formation consists of shales, with minor siltstone, sandstone (Fricker, 1963) and a couple bentonitic tuff beds (Ricketts, 1991). The

Kanguk formation has a maximum thickness of 243 metres and has a gradational contact with the overlying Eureka Sound Formation (Ricketts, 1991).

3.3.4.10 Eureka Sound Formation (Upper Cretaceous to Tertiary)

This formation is the youngest of the Strand Fiord area consisting mainly of quartzose sandstones with siltstones, shales and some minor coal seams interbedded (Ricketts, 1991). The maximum thickness along the Strand Fiord area is 2900 metres (Ricketts, 1991).

3.4 Summary

In Northern Canada, the Canadian Arctic Islands and surrounding channels cover approximately 1.3 million square kilometres. Axel Heiberg Island is apart of the Canadian Arctic Archipelago and is within the extensive Sverdrup Basin. This basin's structure was influenced by Paleozoic and Mesozoic rifting or extensions, and by Tertiary compression.

The Sverdrup Basin Magmatic Province (SBMP) occurs along Axel Heiberg and Northern Ellesmere Islands and consists of flood basalts, intrusive sheets, dykes, and central volcanoes. Axel Heiberg exposes the oldest flows while showing an aphanitic and fine crystalline texture (Embry, 1991). This volcanism is thought to be associated with the rifting and drifting during the formation of the Amerasian Basin (Embry, 1991).

At the start of the Triassic, salt diapirs started to rise sporadically (Trettin, 1989) and Stephenson et al. (1992) are of the opinion that they were emplaced into the overlying overburden because of horizontal compression. Secondary driving forces are thought to

aid in the formation of diapirs since buoyancy cannot elevate the denser anhydrite alone (Stephenson et al., 1992).

Mafic dykes and sills occur along with the basaltic lavas, however, the dykes and sills have a wider aerial coverage and increase in amount moving north eastward through the Sverdrup Basin (Embry, 1991). Other types of sills and dykes that form are composed of tabular anhydrite that rose because of high horizontal compression during the Cretaceous to Tertiary (Stephenson et al., 1992).

A number of formations make up the Strand Fiord, the Blaa Formation, Heiberg Formation, Savik Formation, Awingak Formation, Deer Bay Formation, Isachsen Formation, Christopher Formation, Hassel Formation, Kanguk Formation, and Eureka Sound Formation.

CHAPTER 4 GEOLOGICAL AND GEOPHYSICAL DATA

4.1 Introduction

Chapter 4 introduces the layers and raster images used within the GIS database. Following the methodology described in Chapter 2, data and information are collected to understand the igneous bodies and salt structures for the Strand Fiord area. This chapter presents all of the data obtained throughout the study and the resulting geological map. Subsequent chapters, 5 and 6, will discuss the following results.

4.2 Databases used within the GIS

The compilation of a database links lithological data to the aeromagnetic, gravity, and field observation data. The following sub-sections describe the processes used to obtain the layers in this study and the subsequent analysis.

4.2.1 Geology

Geology layers (Figure 4.1) for the Strand Fiord area were obtained as AutoCAD files from Gordon Oakey of the GSC. The geology layers were created from digitizing lines from the 1971 geological maps of Strand Fiord and Middle Fiord by Thorsteinsson. An extension within the Arc program converted the AutoCAD files into layers that are operable in ArcMap. The geological polygons represent the various formations and units existing within the fiord, while the polylines display linear features such as faults, dykes, anticlines and synclines.

4.2.2 Topography

The topography shapefile, shown in Figure 4.2, appears as a polyline with a line spacing of 100m. The 1:250,000 layer came from the National Topographic

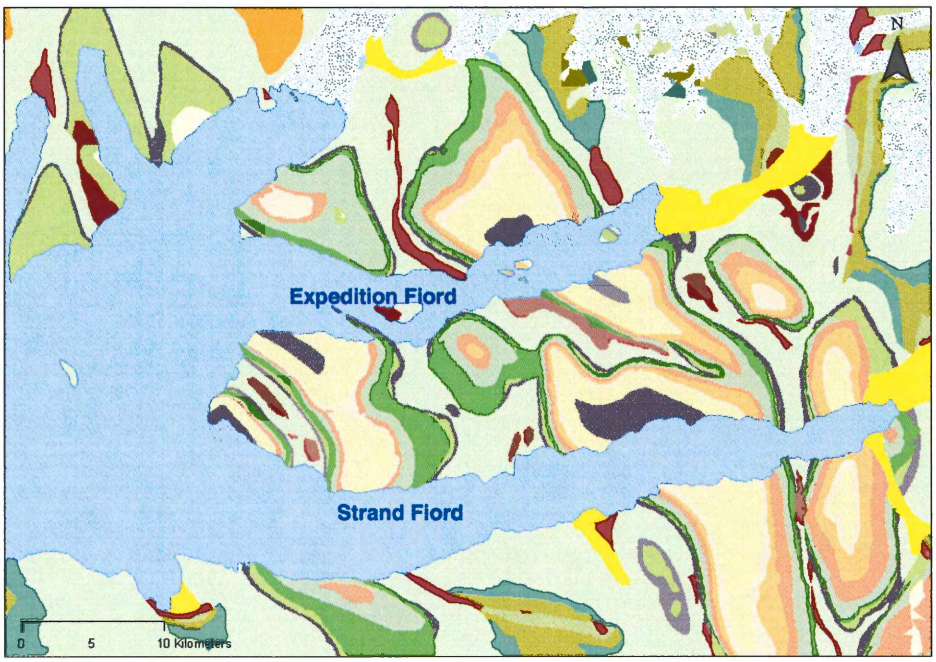

Figure 4.1 Geology layers used in GIS database obtained from Gordon Oakey of the GSC. The layers were created from digitizing lines from the 1971 geological maps of Strand Fiord and Middle Fiord by Thorsteinsson.

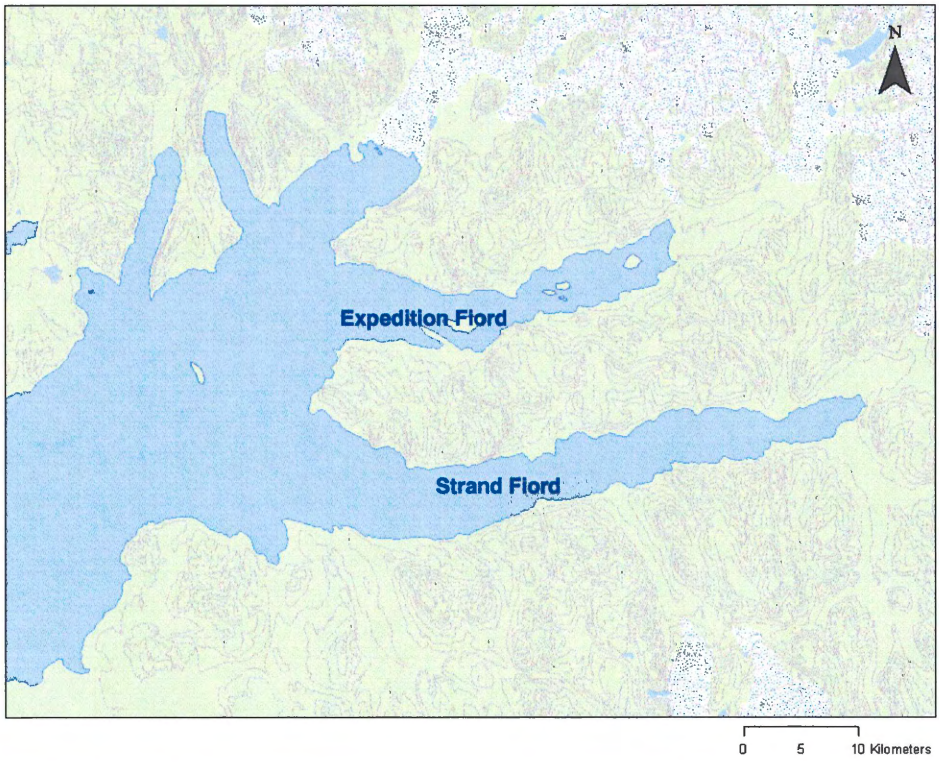

Figure 4.2 Topography obtained from the Natural Resources Canada National Topographic Data Base (1:250,000 made available through Natural Resources Canada, Geomatics Canada, 2004.

Data Base made available through Natural Resources Canada, Geomatics Canada, 2004.

4.2.3 Aeromagnetics

Frank Dostlar (GSC) supplied a raster image of aeromagnetic data with tables of all the aeromagnetic values acquired through geophysical surveys. The Canadian Aeromagnetic Data Base data is made available through the Continental Geoscience Division, Geological Survey of Canada, Earth Sciences Sector, Natural Resources Canada. The aeromagnetic raster of Axel Heiberg Island along with other geophysical data for the rest of Canada is also obtainable through the online Earth Science Sector's Geoscience Data Repository (GDR). The raster image (Figure 4.3) has a 200 metre resolution and is residual total field.

The aeromagnetic raster shows the extent of diapirs and igneous bodies in the Strand Fiord area by displaying different colour shades for different values of magnetism. Diapirs will show a low positive or negative anomaly, while igneous rocks display a high positive anomaly. The magnetism of a rock depends on the type of rock and the concentration of iron bearing minerals. Basalt contains magnetite/titanomagnetite and non-ferromagnetic minerals such as pyroxene that can generate a large magnetism.

Evaporite columns or diapirs should have a larger negative magnetic anomaly than rootless evaporite bodies. Rootless bodies overly basalts and sediments that have more minerals that are magnetic. This will cause an apparent magnetism, even though the evaporite body may not contain magnetic

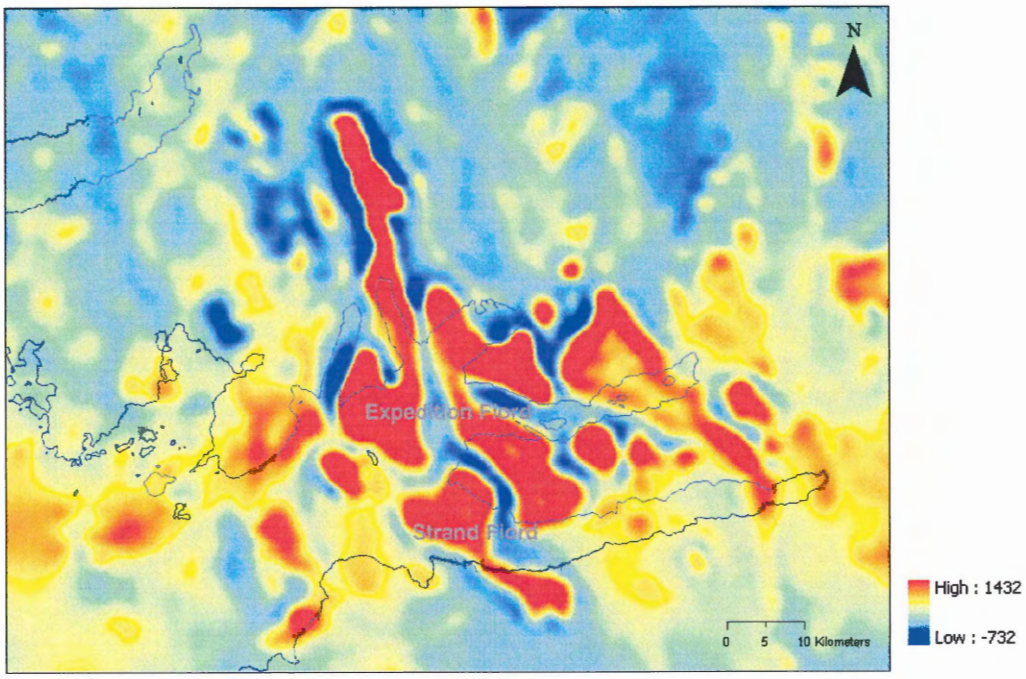

Figure 4.3 Aeromagnetic raster obtained from the Canadian Aeromagnetic Data Base, Continental Geoscience Division, Geological Survey of Canada, Earth Sciences Sector, Natural Resources Canada displays a 200 metre resolution and is residual total field.

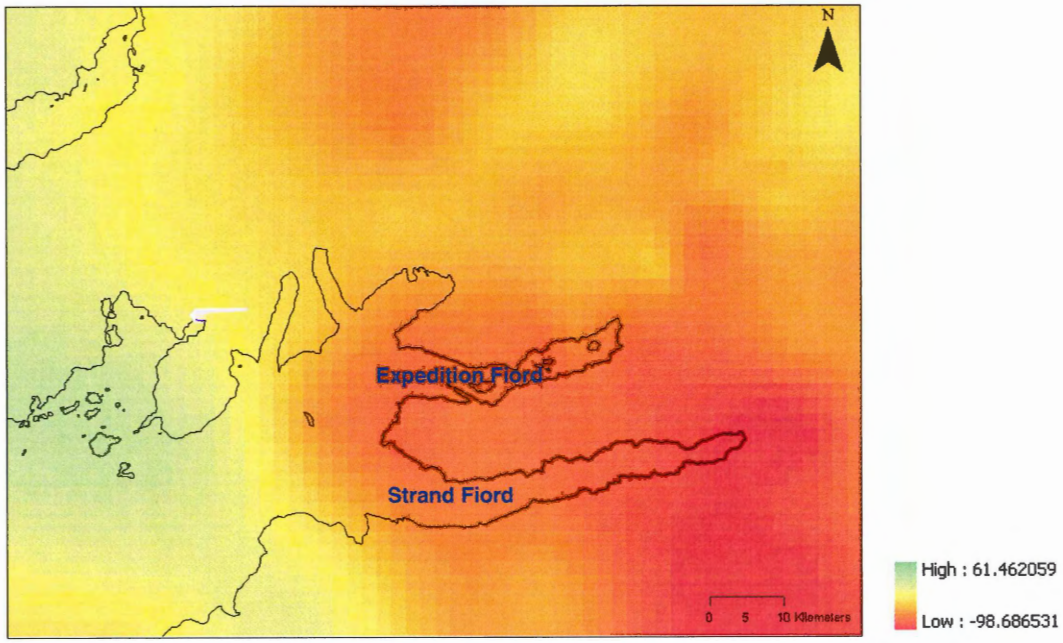

Figure 4.4 Gravity raster obtained from the Canadian Geodetic Information System, Geodetic Survey Division made available through Geomatics Canada, Earth Sciences Sector, of Natural Resources Canada. The raster has a 2-kilometre line spacing showing the gravity anomalies.

minerals itself. However, if columns or diapirs of evaporite have a higher magnetism associated with them, intrusions of dykes or igneous inclusions may be present. Analysis of the magnetics will determine the geometry, characteristics, and classification of the igneous and salt bodies and will produce a better representation of the units and formations.

4.2.4 Gravity

Frank Dostlar (GSC) supplied a gravity raster image (Figure 4.4) with 2-kilometre resolution. The raster image was obtained from the Canadian Geodetic Information System, Geodetic Survey Division made available through Geomatics Canada, Earth Sciences Sector, of Natural Resources Canada. The gravity raster is also obtainable through the online Earth Science Sector's Geoscience Data Repository (GDR). The raster image shows gravity anomalies throughout the fiord area, and gives an idea of the depth of the diapers. However, due to the 2 kilometre line spacing, the suggested depths will not be as accurate as using a high resolution gravity survey.

4.2.5 Digital Elevation Models (DEM)

The ASTER DEMs show the elevation of an area and can help determine geological boundaries between different formations (Figure 4.5). For Axel Heiberg Island, the DEMs were generated by Paul Budkewitsch of the Canadian Centre for Remote Sensing (CCRS) with bands of Visible Near Infra-Red (VNIR), paticularily the 3N (nadir-viewing) and 3B (backward-viewing). The band 3 data occur within spectrum ranging from 0.78- 0.86 um (P. Budkewitsch personal communication, 2005). Using the backward-viewing telescope assembly of the

VNIR, stereoscopic data is collected and has a base-to-height ratio (B/H) of 0.6 and a stereo intersection angle of 27.7° (P. Budkewitsch personal communication, 2005).

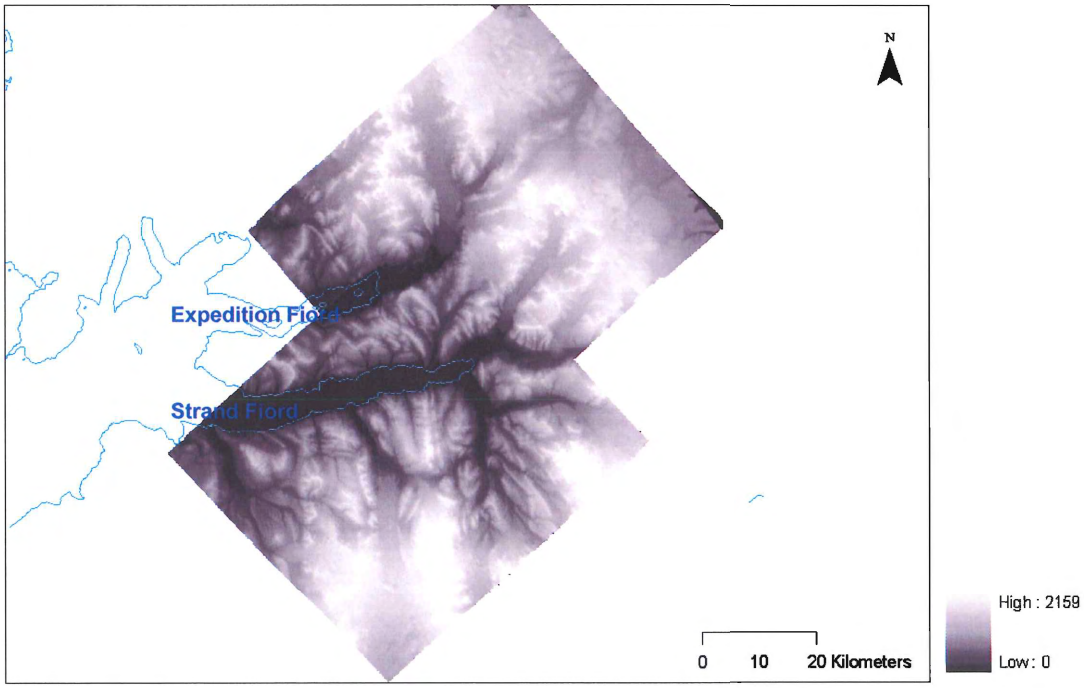

Figure 4.5 Digital Elevation Model (DEM) of the Strand Fiord area acquired from Paul Budkewitsch (CCRS).

4.3 Geological map and topographical data

The geological map (Figure 4.6) shows all geological formations and geological structures that constitute the fiord. The legend displays all the formations that are present (Figure 4.7). As discussed in Chapter 3, they are the Awingak Formation, Deer Bay Formation, Isachsen Formation, Christopher Formation, Hassel Formation, Strand Fiord Volcanic Formation, Kanguk Formation, the Eureka Sound Group, along with numerous intrusions of evaporite diapirs and mafic dykes.

The map displays a general orientation of east and north trending faults (Fricker,1963) and a north-south and northwest-southeast general trend of folding (Kranck, 1963). The topography contours display u- and v-shaped valleys occurring throughout the fiord along with a very rugged terrain.

4.4 Geophysical Data

4.4.1 Aeromagnetics

The first analysis divided the magnetic raster image into 5 intervals (Figure 4.8). There is a noticeably higher magnetic anomaly along the Strand Fiord area trending north-northwest. The Strand Fiord is known for abundant igneous bodies and salt structures that occur between the igneous bodies. In addition, low magnetic anomalies (shown in blue) occur throughout the Sverdrup Basin moving west from the Strand Fiord Area.

Two-dimensional cross sections show varying magnetic values across different features of the area. Two cross sections (Figure 4.9) trending from the Kanguk Peninsula to Bastion Ridge (A-A') and Twisted Ridge to Wolf Intrusion (B-B') were chosen for analysis. ArcMap extracted magnetic values across the

Figure 4.6 - Geological Map of the Strand Fiord Area. For formation descriptions, see Legend (Figure 4.7)

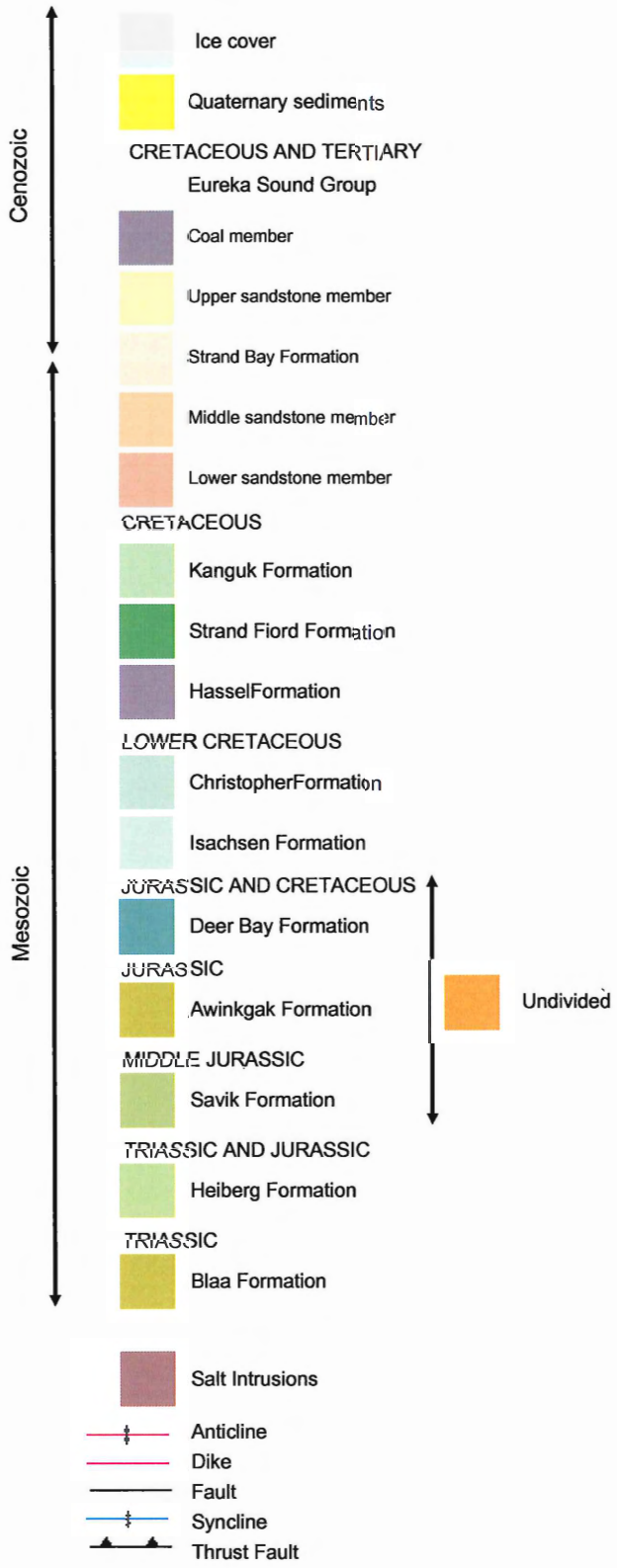

Figure 4.7 – Legend for Geological Map, after Thorsteinsson, 1971. See Section 3.3 for lithological descriptions.

trends, which were subsequently plotted using Microsoft Excel. The X-axes represent distance in metres, and the Y-axes represent the magnetic values in nanoteslas for the magnetic plots. The first trend from Kanguk Peninsula to Bastion Ridge yields an interesting magnetic plot. The peninsula is known for its salt structures, such as the Kanguk Diapirs, Twin Diapirs, and Bastion Ridge Diapirs. In addition, igneous flows are prominent and of particular interest are Index Ridge and Bastion Ridge; see section 4.5 for lithological descriptions. This distinct difference in rock types gives a magnetic plot (Figure 4.10), demonstrating a 'saw-tooth' type pattern as it moves across various salt structures and igneous flows with changing magnetic values.

The second trend from Twisted Ridge to Wolf Intrusion yields a similar magnetic plot (Figure 4.11). This peninsula is known for its salt structures, such as Colour Peak and Expedition Diapir. Various types of flows occur; particularly Twisted Ridge and the Wolf Intrusion Sill (see section 4.5 for lithological descriptions). The magnetic plot of this trend demonstrates another 'saw-tooth' pattern because of the distinct differences in rock types.

The two magnetic trends are used in section 5.1.2 to describe the suggested depth of the diapirs.

4.4.2 Gravity

The gravity raster (Figure 4.4) displays gravity lows in the highly folded and faulted portion of the eastern Strand Fiord while increasing to gravity highs moving towards the west into Strand Bay and the Arctic Ocean. The change in gravity values occurs where the highly folded mountainous terrain begins and the

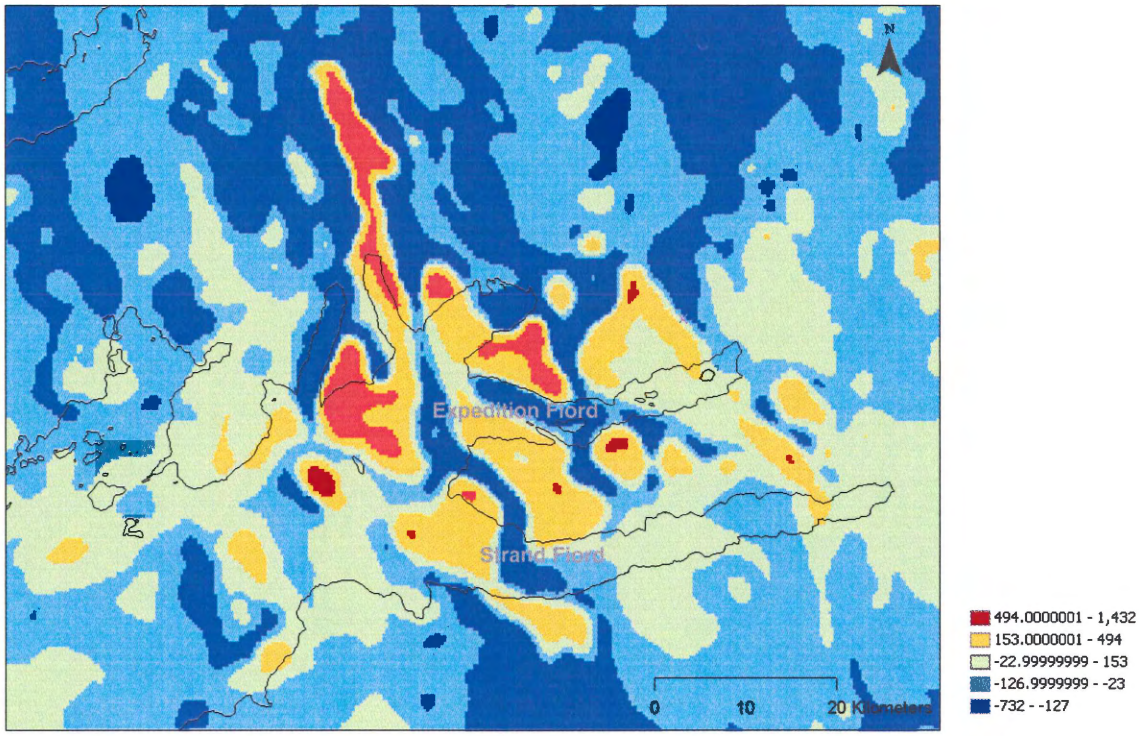

Figure 4.8 Magnetics divided into 5 intervals shows a north-northwest trend of high magnetic values within the Strand Fiord area.

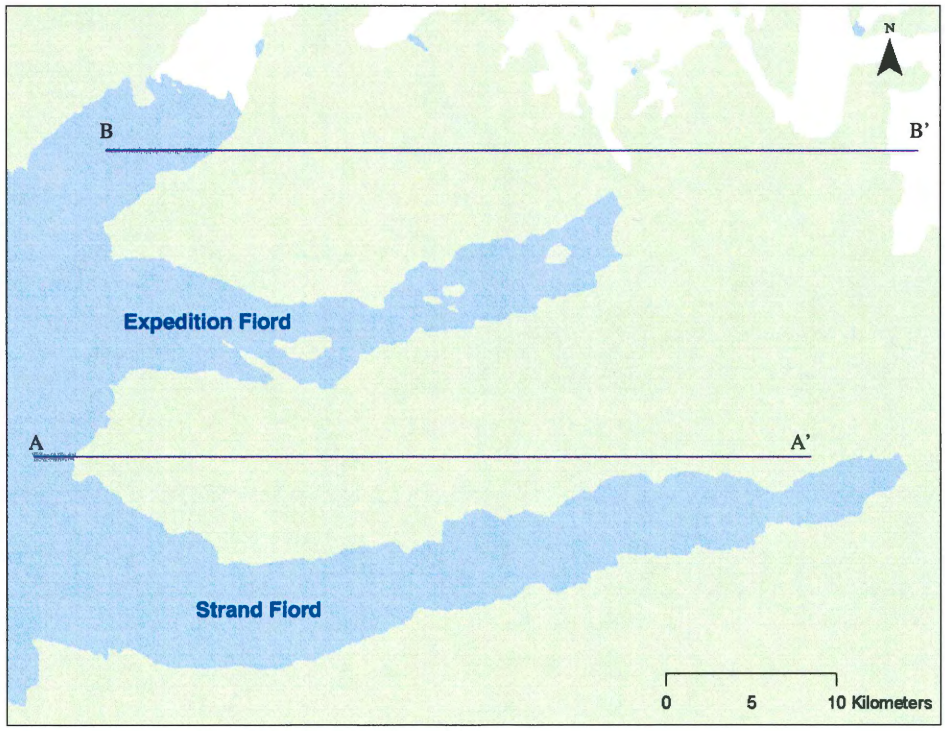

Figure 4.9 Cross sections across Kanguk Peninsula to Bastion Ridge (A-A') and Twisted Ridge to Wolf Intrusion (B-B').

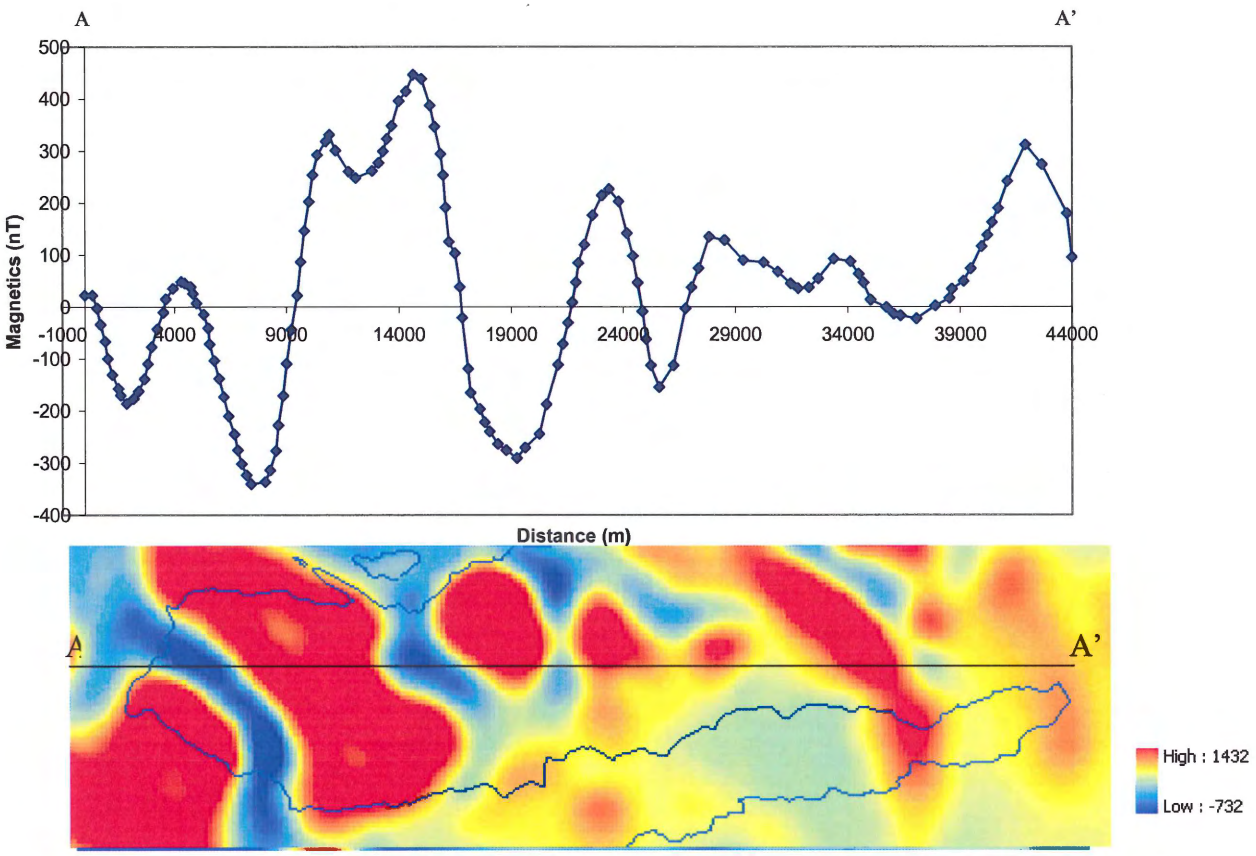

Figure 4.10 2D Cross-section across Kanguk Diapirs to Bastion Ridge. The values when plotted produce a saw-tooth pattern for the magnetics. The abrupt change from low magnetic values (salt diapirs) to high values of magnetic values (igneous intrusions) influence the pattern.

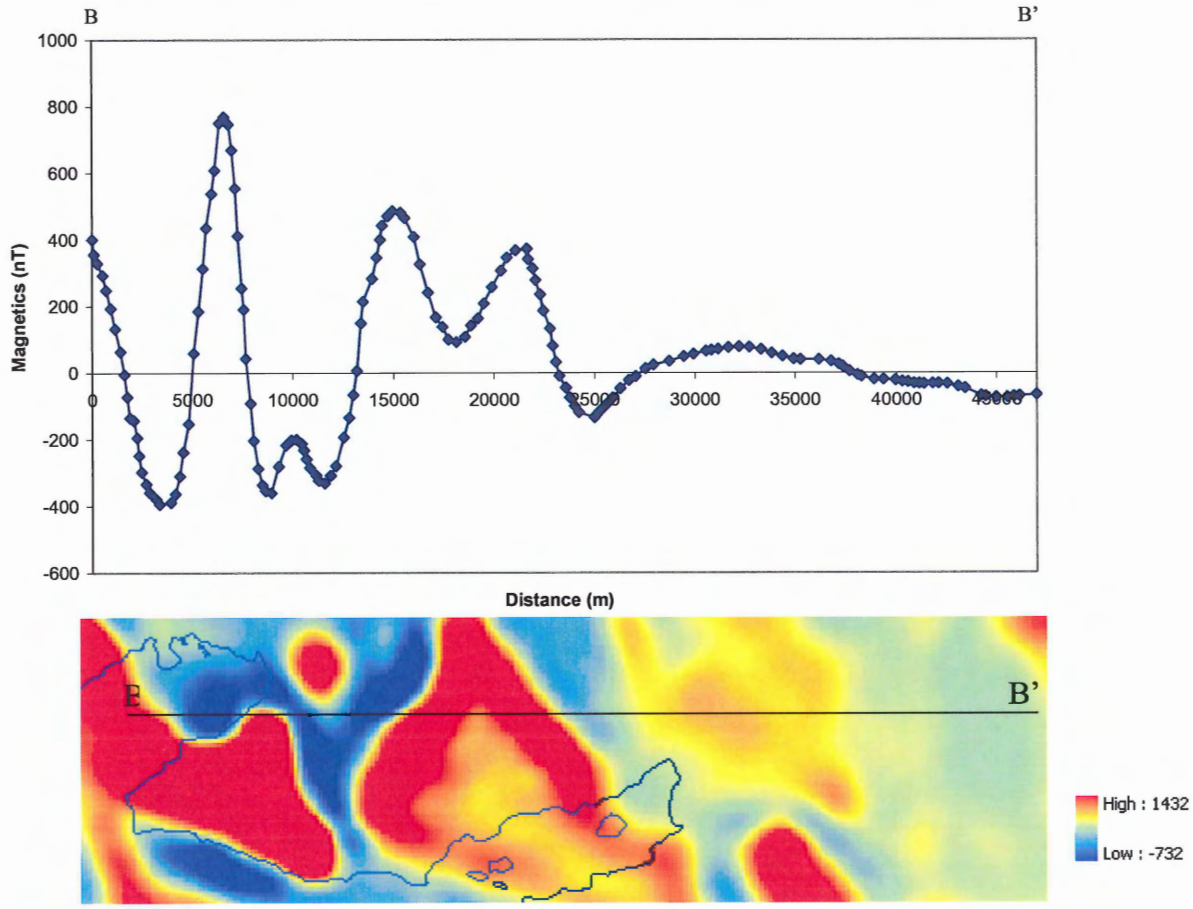

Figure 4.11 2D Cross-section across Twisted Ridge to Wolf Intrusion produces a saw-tooth magnetic plot caused by the abrupt change from low magnetic to high magnetic values.

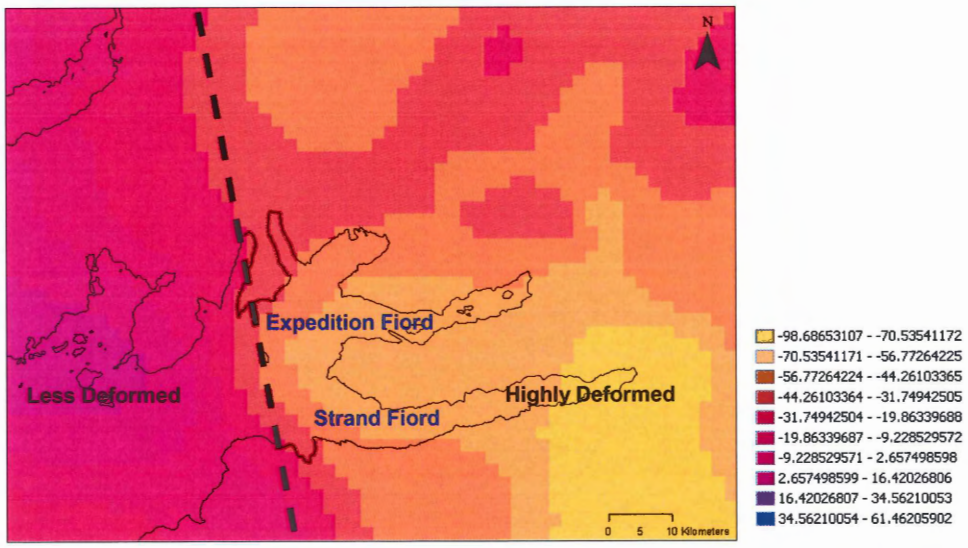

Figure 4.12 Gravity divided into 10 intervals shows a gradual increase moving east to west through the fiord. Line represents a break in gravity values showing the slightly and highly deformed portions of the fiord.

low-lying flat terrain ends. As mentioned previously, central Strand Fiord is heavily intruded by igneous bodies and salt structures. Salt has a lower density (2.16) compared to the surrounding igneous rocks (2.8-3.0), a 'gravity low' forms resulting from density contrast between the two rock types. Diapirs have exposed cap rocks composed of anhydrite (S.G. 2.98) and gypsum (2.32) plus rafted rocks, but these caps are probably not very thick, because they do not significantly affect their gravity expression.

Figure 4.12 shows the raster image divided into 10 intervals. The intervals portray a gradual increase of gravity lows to gravity highs moving east to west. The blue line represents an abrupt break in gravity values where the major folding and faulting stops and flat terrain begins.

4.5 Digital Elevation Models (DEMs)

The ASTER DEMs show the elevation of an area and can help determine geological boundaries between different formations.

In order to compare the outlines of the observed geological boundaries to the DEM, Bastion Ridge, an area largely composed of volcanics will help show the similarities. Figure 4.13a shows the DEM for the area surrounding Bastion Ridge. The geology for the area (Figure 4.13b) shows the shape of the formations seen in the field. When the geology and the DEM are combined (Figure 4.13c), the DEM shows an outline resembling the observed geological boundaries. The large oval shown on the DEM follows the shape of the geology around Bastion Ridge. Even though the DEM does not show what type of geology is present, it can give an idea of the shape of the landscape.

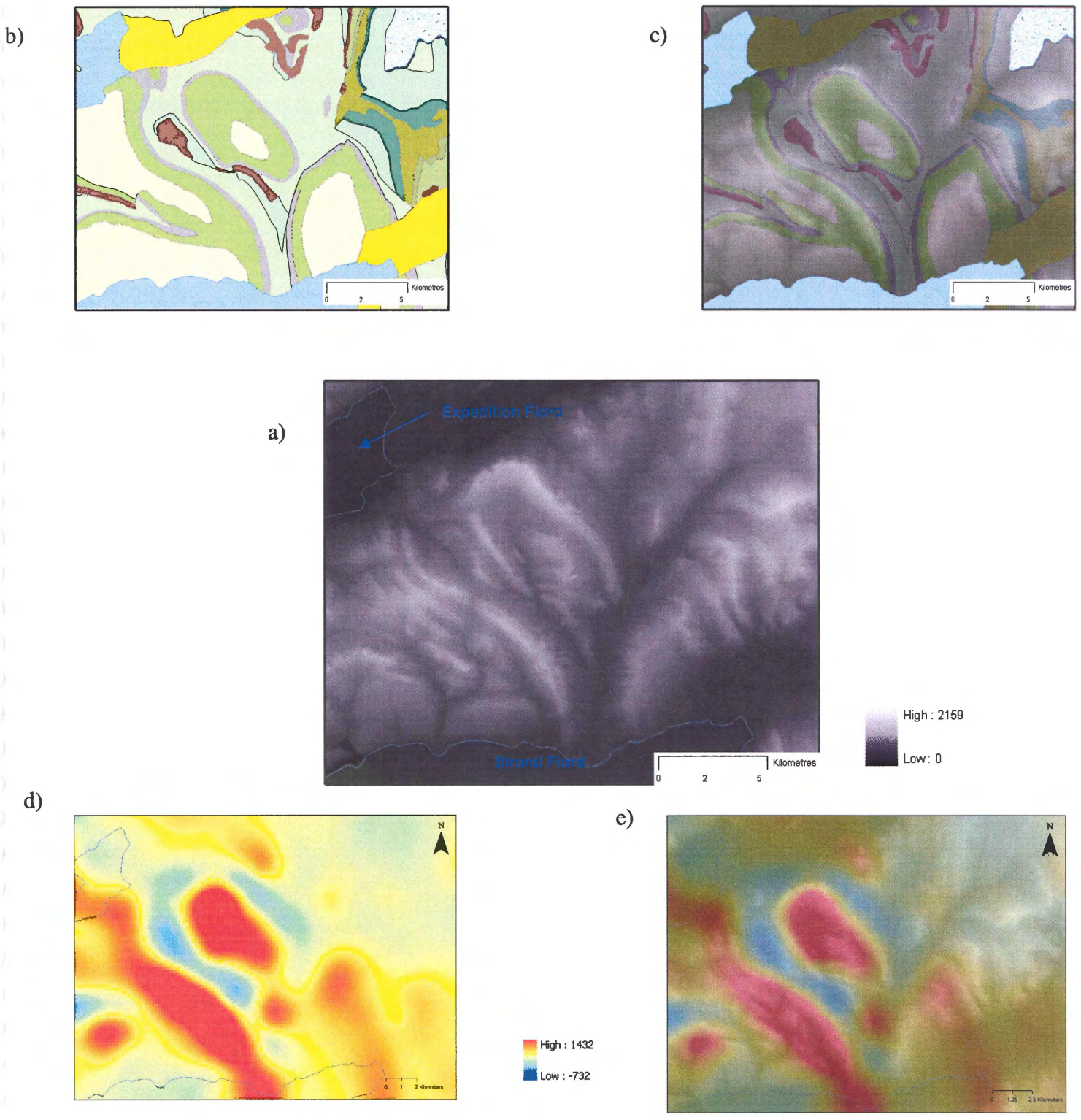

Figure 4.13 a) The geology surrounding Bastion Ridge; b) the DEM overlain with the geology; c) the DEM of Bastion Ridge; d) the magnetics surrounding Bastion Ridge; e) the magnetics overlying the DEM.

The magnetics (Figure 4.13d) can also be used in combination with the DEM. The DEM, as shown above can outline the shape of the formation, while the magnetics provides the magnetic value of the rock. An overlay of the magnetics onto the DEM (Figure 4.13e) suggests an outline of the units and shows where the salt structures and volcanics occur.

The use of the DEM, known geology, and magnetics gives a better representation of the units. Where outcrops and exposures are lacking in the field, the DEM and magnetics can help finish the boundaries of the units. This will allow for a more precise mapping especially in areas such as Axel Heiberg Island where poor exposure and difficult terrain occur.

4.6 Remote Sensing

LANDSAT is a multispectral imaging system comprising of several bands of data that make up a natural colour composite image (Liew, 2001). This image enhances the geological features and structures by displaying colours for different features and allowing for easy identification of different rock types.

The South Fiord Dome is a very complicated geological structure with evaporates, rafted igneous rocks, and rugged terrain. Figure 4.14 shows the location of the South Fiord Dome in respect to the study area. The map of the South Fiord Dome (Figure 4.15), created by Schwerdtner et al. (1967), displays the compiled structural and geological data for the area. A large area of igneous rock is shown along the east side of the fiord. The air photo of the same structure, Figure 4.16, shows a black and white aerial image of the dome with the same area of igneous rock occurring within the dome. The GIS uses the GSC maps and aerial images in order to produce the size and

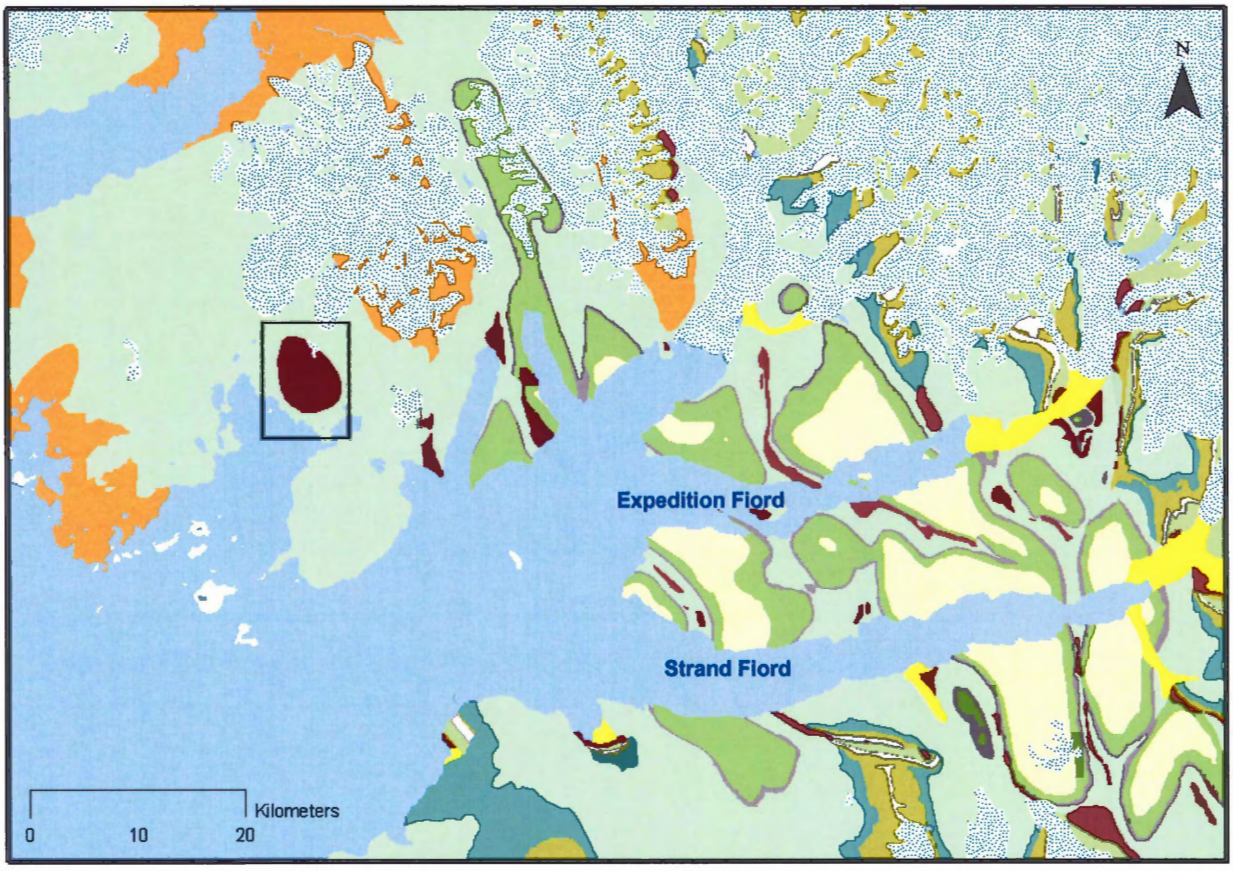

Figure 4.14 - Location of the South Fiord Dome (within boundary of the black square).

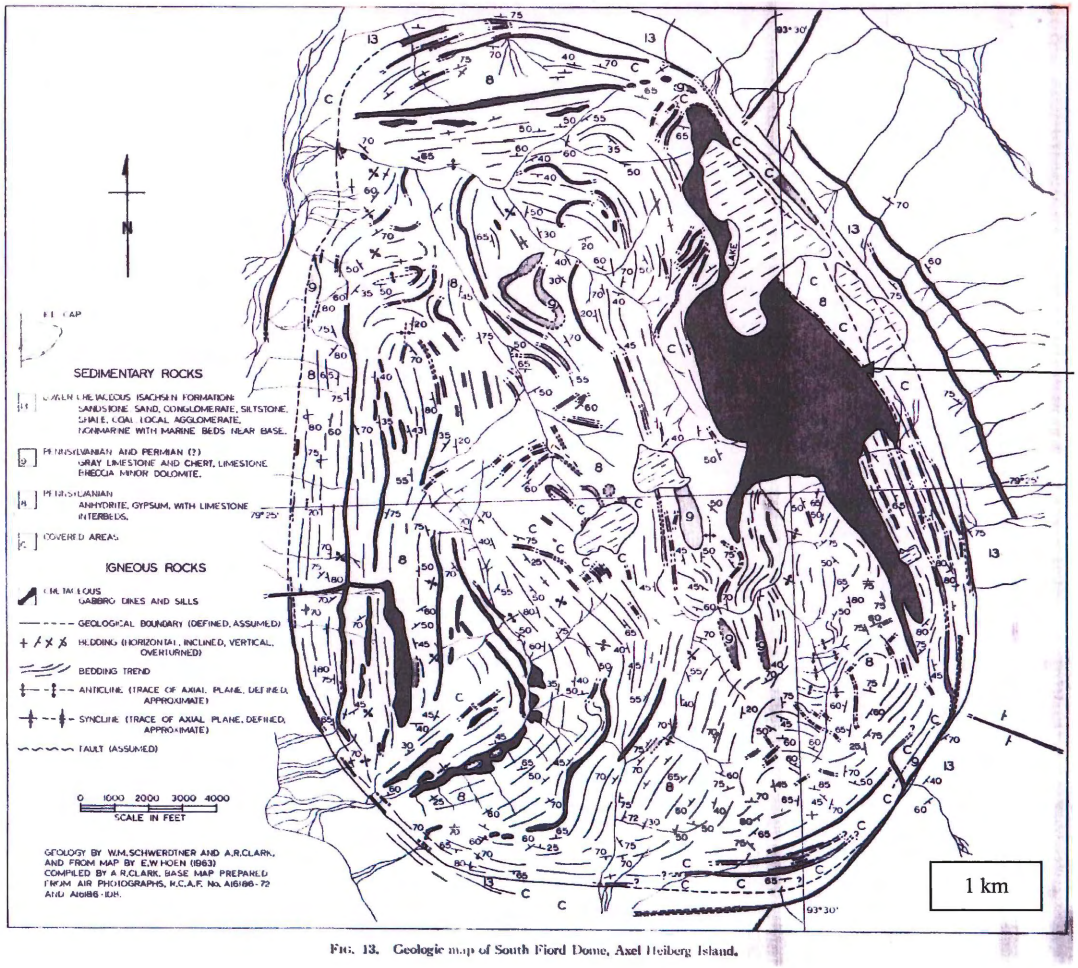

FIG. 13. Geologic map of South Fiord Dome, Axel Heiberg Island.

Figure 4.15 – shows the detailed structural and geological map of the South Fiord Dome compiled by Schwerdtner et al. (1967) identified above is an area of rafted igneous rock occurring within the dome.

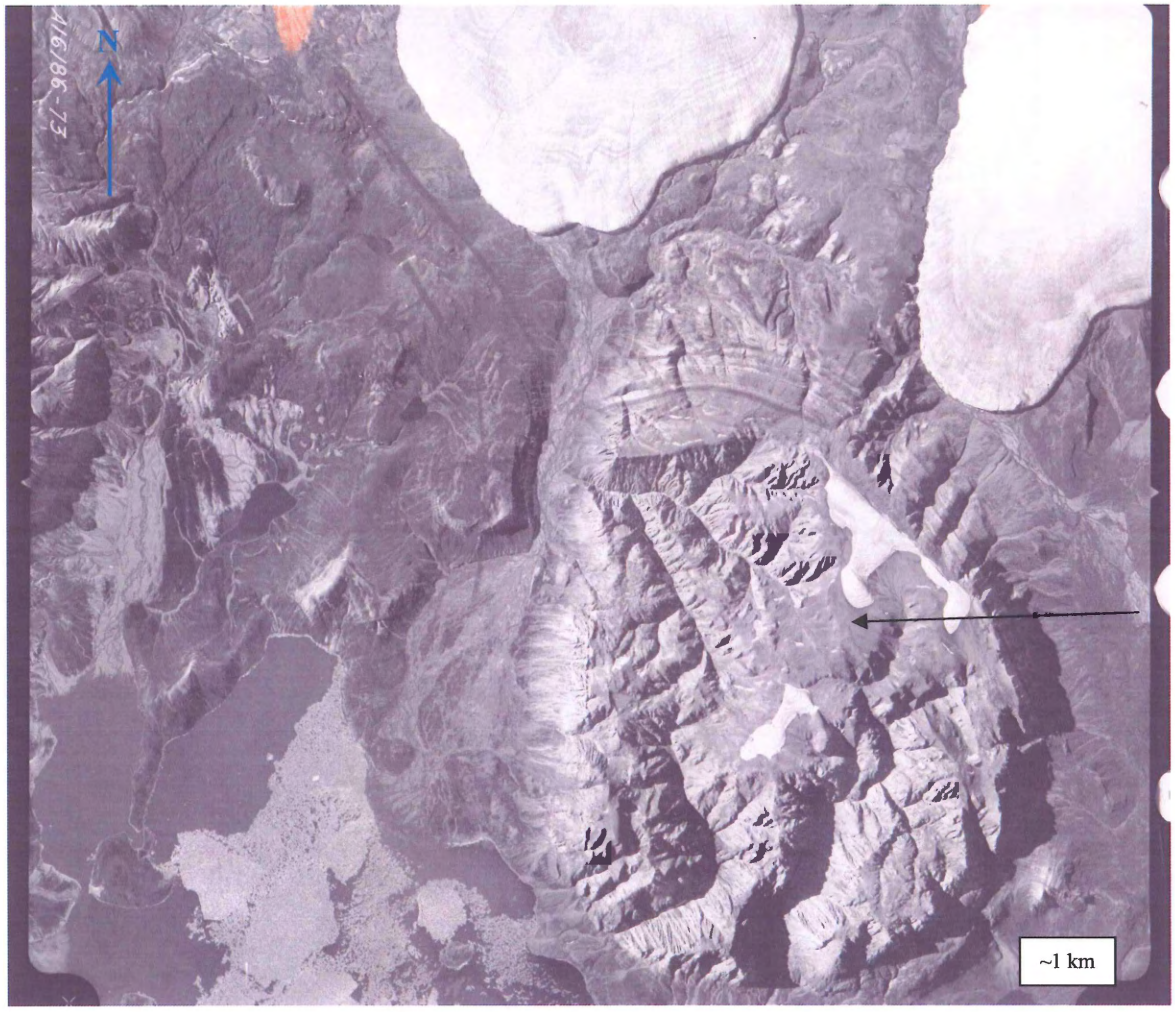

Figure 4.16 – The same area is illustrated on an air photo. Pointed out above is the same area comprised of rafted igneous rock (provided by Paul Budskewitsch CCRS).

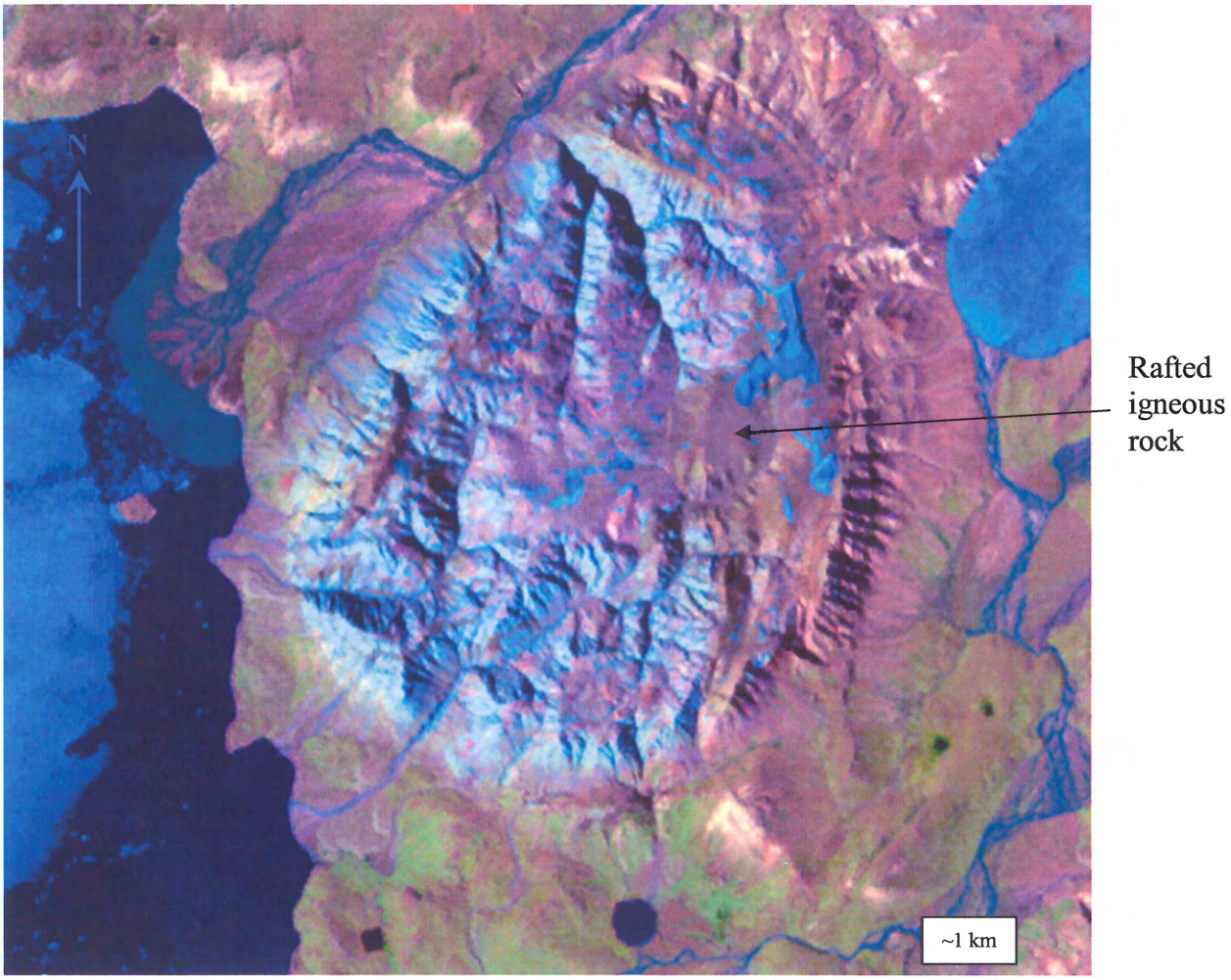

Figure 4.17 – LANDSAT image of the South Fiord dome showing the salt as blue and the igneous rock as brown (provided by Paul Budskewitsch CCRS).

shape of the structure. However, the tones, textures, patterns, and shadows of the air photos along with the large scaled GSC maps, create a challenge when distinguishing the limits of the rafted igneous rocks. In order to show a better representation of the rafted igneous rocks, LANDSAT images are used.

The LANDSAT image for the South Fiord Dome (Figure 4.17) displays salt as light cyan colour, vegetation as green, water as navy blue, ice as blue, the adjacent Isachsen Formation as brown and along the east side of the dome rafted igneous rock are a shade of dark brown. This outline of the rafted igneous rocks shows a definite boundary with the surrounding salt that is not as easily recognized in the air photo or 1:250,000 scaled maps. Knowing where the rafted igneous areas occur within the dome allows for a better representation of the boundaries between the two.
Textures of the land surface are also very important features in visual image interpretation. Textures can show whether an area is flat or rugged. The LANDSAT image of the South Fiord shows a very rugged terrain within the dome with very steep slopes. Whereas the colours around the dome are more homogenous with little to no shadow, indicating the area should be flat with minor amounts of hills and mountains. The LANDSAT, like an air photo, gives an idea of geometric features. For the South Fiord Dome, the structure is oval shaped and is approximately 6 kilometres in width.

4.7 Lithological Data

Throughout Strand Fiord, abundant extrusive flows and their chemical intrusive equivalents (sills, dikes) occur, and are very important factors within the stratigraphic succession. Two localities were chosen to show examples of extrusive and intrusive rocks, Index Ridge and the Wolf Intrusion (Figure 4.18). The first location, Index Ridge,

comprises of a basaltic flow termed the Strand Fiord Formation and is found along the Kanguk Peninsula at W 92-02 and N 79-17. The second location comprises of a large sill exposed at the head of Expedition Fiord called the Wolf Intrusion at W 90-52 and N 79-24. Lithological data for both samples were compiled and added into the GIS. Microscope and ESEM observations show textures and mineral properties of normal thin and polished thin sections. Integration of all data collected from petrography and ESEM are essential for a GIS application because it helps characterize and classify the igneous rocks especially in areas of the fiord where basaltic rocks raft into salt domes. Descriptions of the extrusive and intrusive samples follow in subsections.

4.7.1 Index Ridge

4.5.1.1 Petrography

Petrographical work allowed characterization and classification of thin sections for the Strand Fiord Formation of Index Ridge. Observations of six samples, AX83-89 to AX83-94, are listed within Table 4.1.
The samples are uniformly basalts consisting of a fine-grained texture (Figure 4.19). The samples display seriate, hypocrystalline, intergranular, and intersertal textures (Figure 4.20, 4.21) ranging from aphyric (no phenocrysts) to sparsely phyric (<1%) to moderately phyric (≥1%).

Phenocrysts present include plagioclase laths and clinopyroxene occurring locally as a sub-ophitic texture (Figure 4.22). In addition, Figure 4.23 shows a sub-fluidal arrangement of plagioclase with partial resorption of clinopyroxene. The groundmass consists dominantly of plagioclase and clinopyroxene, with minor amounts of olivine, opaque oxides, and

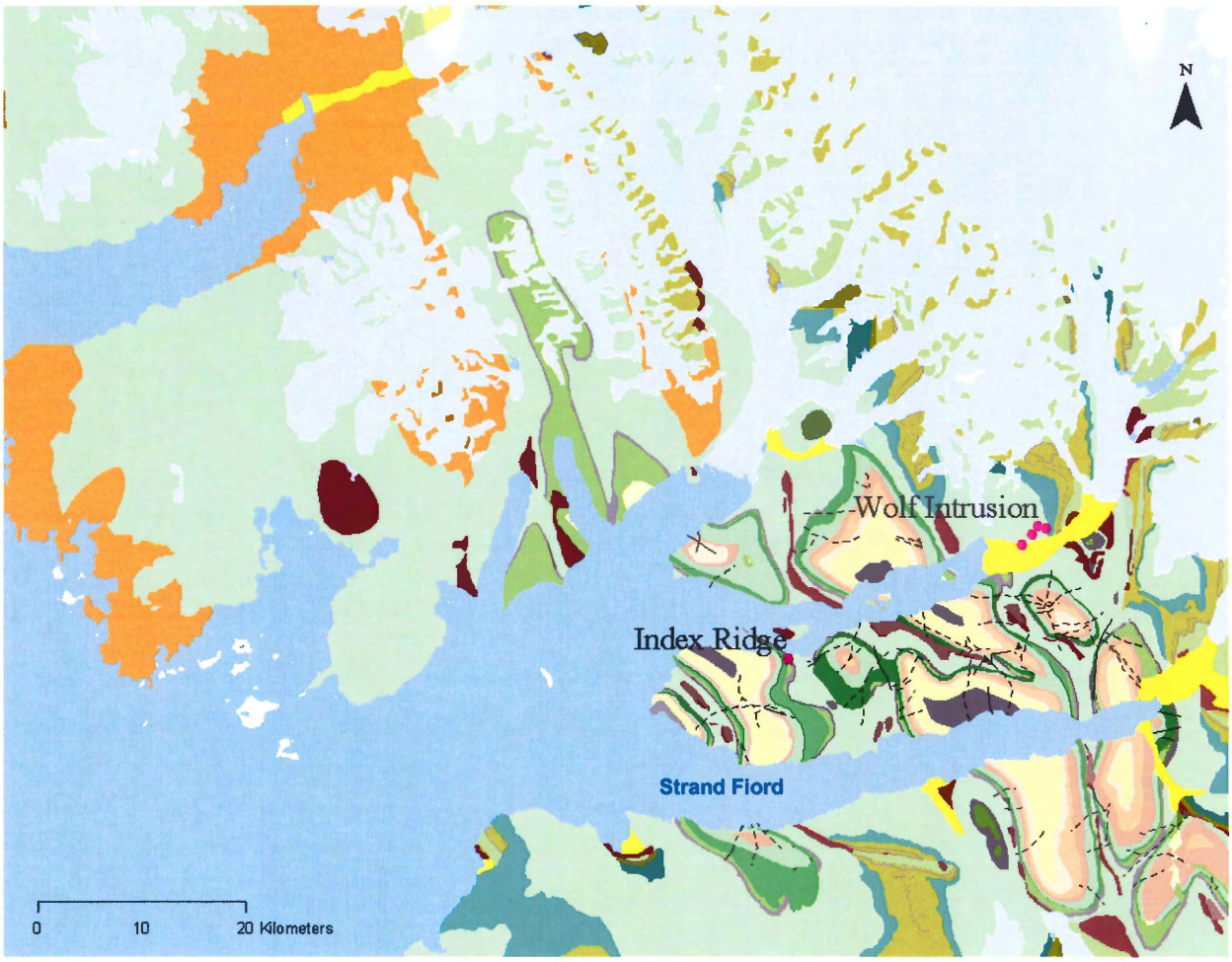

Figure 4.18 - Sample map showing locations of normal and polished thin sections used in the current study. At the end of the Kanguk Peninsula, Index Ridge represents a sample of the Strand Fiord Formation volcanics and the Wolf Intrusion is part of a large sill exposed at the head of Expedition Fiord.

	Phenocrysts						Groundmass													
	Clinopyroxene		Olivine		Plagioclase		Olivine			Clinopyroxene			Opaques			Plagioclase			Glass	
Sample Number	% Vol	Size (mm)	% Vol	Size (mm)	% Vol	Size (mm)	% Vol	Morph	Size (mm)	% Vol	Morph	Size (mm)	% Vol	Morph	Size (mm)	% Vol	Morph	Size (mm)	% Vol	Size (mm)
AX83-89							~15	subhedral	0.2	~25	subhedral	<0.1-0.5	~15	euhedral subhedral	<0.1-0.3	~40	euhedral laths	0.1-0.5	~5	<0.2
AX83-90					<1	0.7-1.0	~15	subhedral	0.2	~25	subhedral	<0.1-0.5	~15	euhedral subhedral	<0.1-0.3	~40	euhedral laths	0.1-0.6	~5	<0.2
AX83-91	<1	1			<1	0.8-1	~10	subhedral	0.2	~20	subhedral	<0.1-0.3	~10	euhedral subhedral	<0.1	~40	euhedral laths	0.1-0.5	~10-20	<0.2
AX83-92	<1	1	<1	<1	1	0.8-1.1	~15	subhedral	0.2	~25	subhedral	<0.1-0.5	~10	euhedral subhedral	<0.1-0.3	~40	euhedral laths	0.1-0.5	~5	<0.2
AX83-93	<1	0.8			<1	0.9	~10	subhedral	<0..2	~25	subhedral	<0.1-0.4	~15	euhedral subhedral	<0.1-0.3	~40	euhedral laths	0.1-0.5	~5	<0.1
AX83-94	<1	0.7	<1	1.2	1	0.8-1.3	~10	subhedral	0.2	~20	subhedral	<0.1-0.2	10	euhedral subhedral	<0.1-0.3	~35	euhedral laths	0.1-0.5	~10	<0.1

Table 4.1a - Observations of samples from Index Ridge describing the textures, minerals, and per cent cover present. Continued on following page.

Sample Number	Texture	Alteration
AX83-89	seriate, fine grained, hypocrystalline, intergranular, interstitial	All crystal phases are clear; olivine is partially preserved, however found mostly in the form of iddingsite (brownish-red material); minor amounts of green clays replace glass and are found within the groundmass
AX83-90	seriate, fine grained, hypocrystalline, intergranular, interstitial	All crystal phases are clear; olivine is partially preserved, however found mostly in the form of iddingsite; minor amounts of green clays replace glass and are found within the groundmass
AX83-91	seriate, fine grained, hypocrystalline, intergranular, interstitial	Olivine is pseudomorphed, iddingsite common; oxides and clays are abundant in groundmass
A83-92	seriate, fine grained, hypocrystalline, intergranular, interstitial	All crystal phases are clear; olivine is partially preserved, however found mostly in the form of iddingsite; minor amounts of green clays replace glass and are found within the groundmass
A83-93	seriate, fine grained, hypocrystalline, intergranular, interstitial	All crystal phases are clear; olivine is partially preserved, however found mostly in the form of iddingsite; very minor amounts of green clays replace glass and are found within the groundmass
AX83-94	very fine grained (<1mm), aphanitic, a couple of phenocrysts present sparsely phyric	All crystal phases are clear; olivine is partially preserved, however found mostly in the form of iddingsite; very minor amounts of green clays replace glass and are found within the groundmass

Table 4.1b - Observations of samples from Index Ridge describing the textures, minerals, and per cent cover present. Continued from previous page.

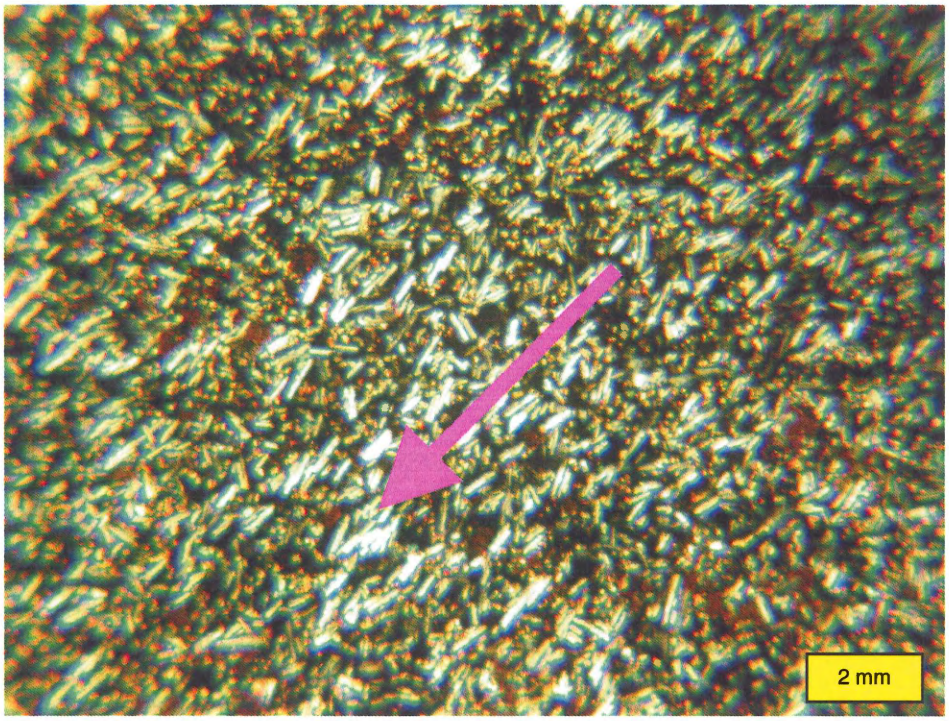

Figure 4.19 - Photomicrograph of a portion of basaltic flow from the Index Ridge succession. The lava flow is very fine-grained and aphyric. The groundmass assemblage consists of clinopyroxene, plagioclase, rare olivine, and opaque minerals, arranged in intergranular texture. Euhedral plagioclase laths locally display a sub-fluidal texture (AX-83-89; crossed polars). The arrow indicates flow direction and as mentioned in Chapter 2 the long axis of the yellow box illustrates the scale.

a)

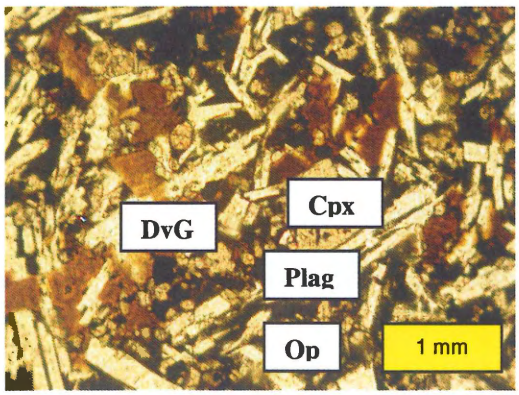

b)

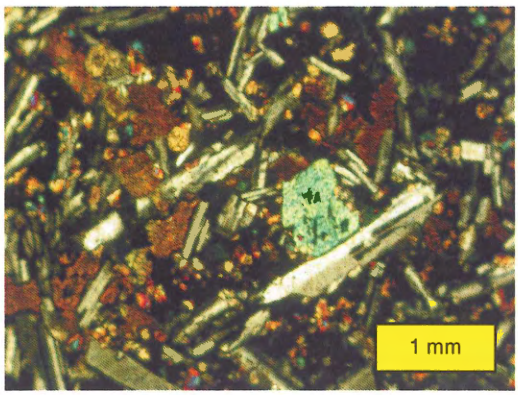

Figure 4.20 - Photomicrograph of a portion of basaltic flow from the Index Ridge succession, showing the intersertal texture of groundmass minerals. Volcanic glass altered to clays is brownish under plane-polarized light (a). The lava flow is very fine-grained and aphyric, with clinopyroxene and plagioclase displaying a seriate texture locally. (AX-83-89; a. plane-polarized light; b. crossed polars). Symbols are DvG = devitrified glass, Plag = plagioclase, Cpx = clinopyroxene, Op = opaques.

a)

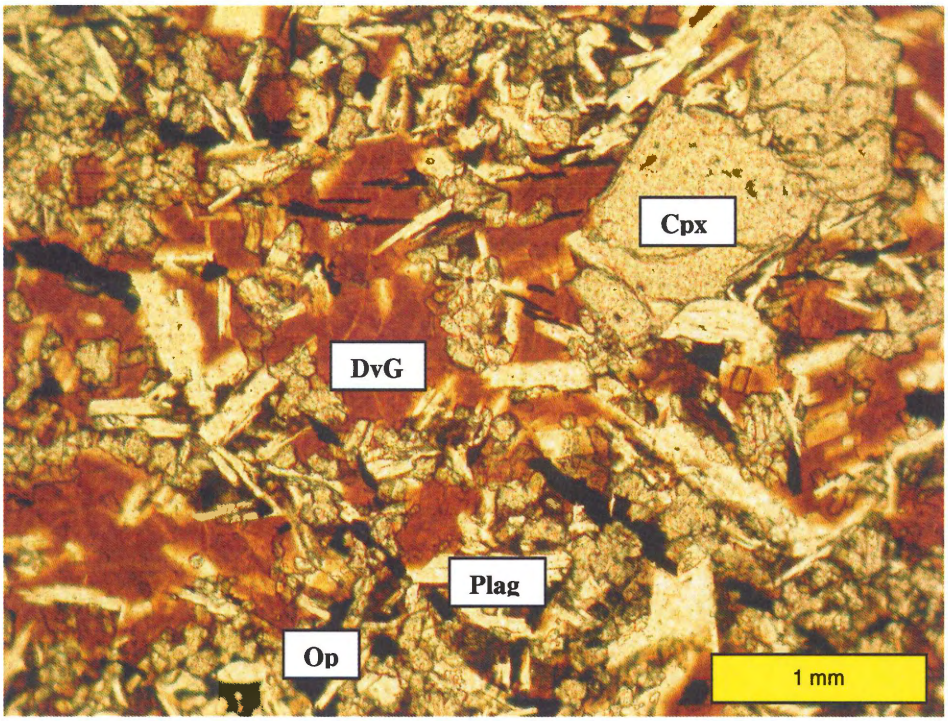

b)

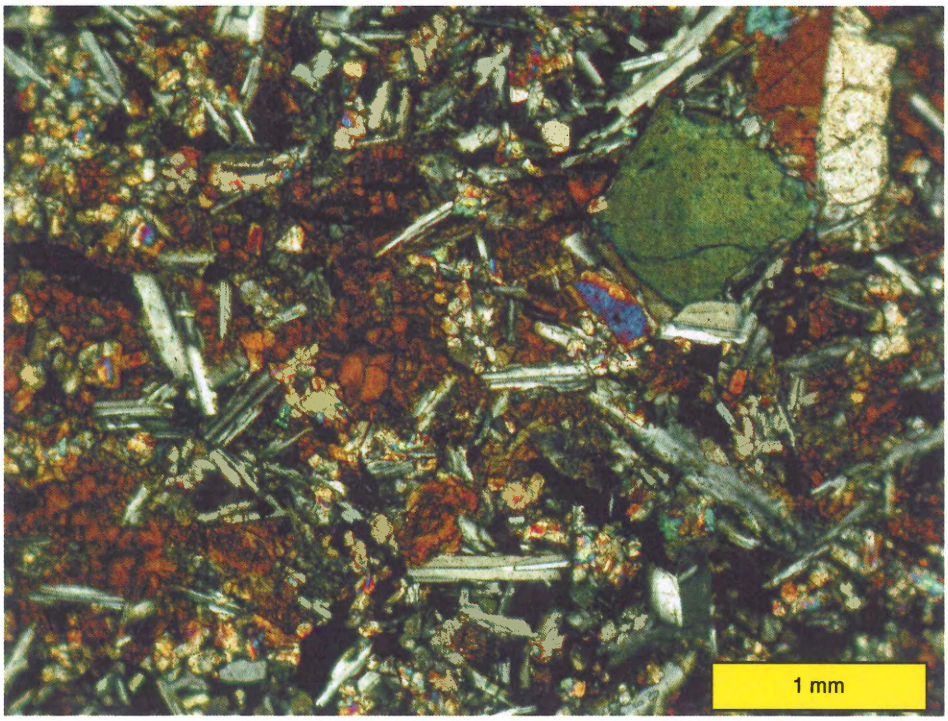

Figure 4.21 - Photomicrograph of a portion of basaltic flow from the Index Ridge succession, illustrating the microporphyritic, intersertal, and intergranular texture (AX-83-94). Volcanic glass altered to brownish clays is visible in plane-polarized light (a). The clinopyroxene microphenocryst at upper right shows twinning under crossed polars (b). Symbols as in Figure 4.20.

devitrified glass. In all samples, green clay particles are present in minor amounts existing within the groundmass. All crystal phases are altered to some extent, however, olivine can be partially preserved or pseudomorphed to the brown-red material iddingsite. Iddingsite suggests that oxidation and hydration of olivine has occurred.

4.5.2 Wolf Intrusion

4.5.2.1 Petrography

Petrographical work allowed characterization and classification of thin sections for the Wolf Intrusion. Observations of five samples are listed within Table 4.2.

Portions of the Wolf sill are fine to medium grained with equigranular, holocrystalline, and intergranular textures (Figure 4.24, 4.25). The minerals present are plagioclase and clinopyroxene. Some portions of the sill contain up to 5% olivine (Figure 4.26) with smaller amounts of opaques. In addition, large plagioclase laths (1.5 to 2 mm in length) appear and are locally saussuritized (Figure 4.27). Clinopyroxenes are well preserved, however, olivine is partially altered to the brown red material called iddingsite, and green clay is present.

4.5.2.2 Qualitative Spectral Analysis

Section 4.4.2.1 described principal mineral phases within the Wolf Intrusion. These apparently consist of pyroxene, plagioclase, some minor olivine, and opaque minerals. The sample AX03-68 (polished version) was chosen to undergo spectral analysis to confirm that these minerals are in

Sample Number	Mineralogy											
	Olivine			Pyroxene			Plagioclase			Opaques		
	% Vol	Morph	Size (mm)	% Vol	Morph	Size (mm)	% Vol	Morph	Size (mm)	% Vol	Morph	Size (mm)
AX03-60	1%	anhedral	Granular	~30%	anhedral	1-2mm	~30%	euhedral, laths	0.1-2mm	~15%	subhedral euhedral	1-2mm
AX03-63	1%	anhedral	Granular	~30%	anhedral subhedral	0.3-.5mm	~30%	euhedral, laths	0.3-.5mm	~10-15%	subhedral euhedral long slender	0.5 mm
AX03-66	1%	anhedral	Granular	~30%	anhedral subhedral	1-1.5 mm	~35%	euhedral, laths	1-1.5 mm	~20%	subhedral	1-1.5 mm
AX03-67	5%	Subhedral to rounded	0.5 mm	~25%	anhedral subhedral	<0.3-0.5 mm	~30%	euhedral, laths	0.3-1 mm	~20%	subhedral anhedral	0.1-5mm
AX03-68	5%	anhedral	0.5 mm	~25%	anhedral	<0.1-1.5mm	~35%	euhedral, laths	0.2-1.5mm	~15%	subhedral	0.2-2mm

Table 4.2a - Observations of five samples from the Wolf Intrusion, describing textures, minerals, and per cent cover.

Sample Number	Textures	Alteration	Notes	Photograph Number	Magnification
AX03-60	medium grained ~0.5-2mm, equigranular, intergranular, holocrystalline, no phenocrysts present, ophitic arrangement of cpx-plag (AX-03-60-24Feb05)	Plagioclase and ?relict olivine grains altered 2/3	some plagioclase grains demonstrates normal zoning	AX-83-60-2_5PPL and POL	2.5 and 10X
AX03-63	fine grained 0.3-0.5 mm, finer than AX03-60, equigranular, intergranular, holocrystallline, subophitic (AX-03-63-24Feb05)	Alteration 2/3 minor amounts of iddingsite occurring through slide; green material present, possible green clay	some plagioclase grains demonstrates normal zoning, most likely taken at chilled margin because it is finer grained then the other sills	AX-83-63-2_5PPL and POL	2.5 and 10X
AX03-66	medium grained ~1-4mm, equigranular, intergranular, no phenocrysts present, sometimes ophitic (AX-03-66_Feb2405 PPL and POL show large equant plagioclase with saussurite)	Alteration 1/3 olivine has altered to iddingsite (brown mineral); green material present, possible green clay	some plagioclase grains demonstrates normal zoning	AX-83-66-2_5PPL and POL	2.5 and 10X
AX03-67	medium grained ~1-5mm, equigranular, intergranular, holocrystalline, no phenocrysts present, sometimes ophitic (AX-03-67 24Feb05 series of x10 images show cpx and olivine in PPL and POL; followed by x2,5 textural assemblage of cpx-oliv)	olivine has altered to iddingsite (brown mineral); green material present, possible green clay Altered 2/3	some plagioclase grains demonstrates normal zoning	AX-83-67-2_5PPL and POL	2.5 and 10X
AX03-68	medium grained, ~1-3mm, equigranular, intergranular, holocrystalline, no phenocrysts present, sometimes ophitic (AX-03-68 24Feb05 Cracked olivine at x10, assoc. cpx; same view in PPL and POL at x2,5	olivine has altered to iddingsite (brown mineral); green material present, possible green clay Alteration 1/3	some plagioclase grains demonstrates normal zoning	AX-83-68-2_5PPL and POL	2.5 and 10X

Table 4.2b - Observations of five samples from the Wolf Intrusion, describing textures, minerals, and per cent cover.

a)

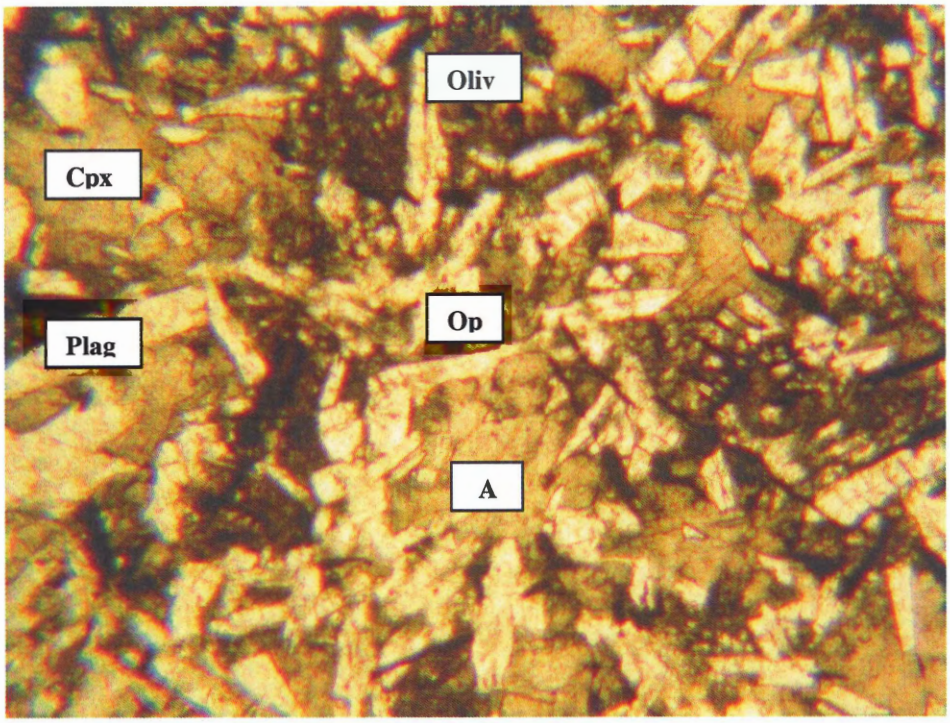

b)

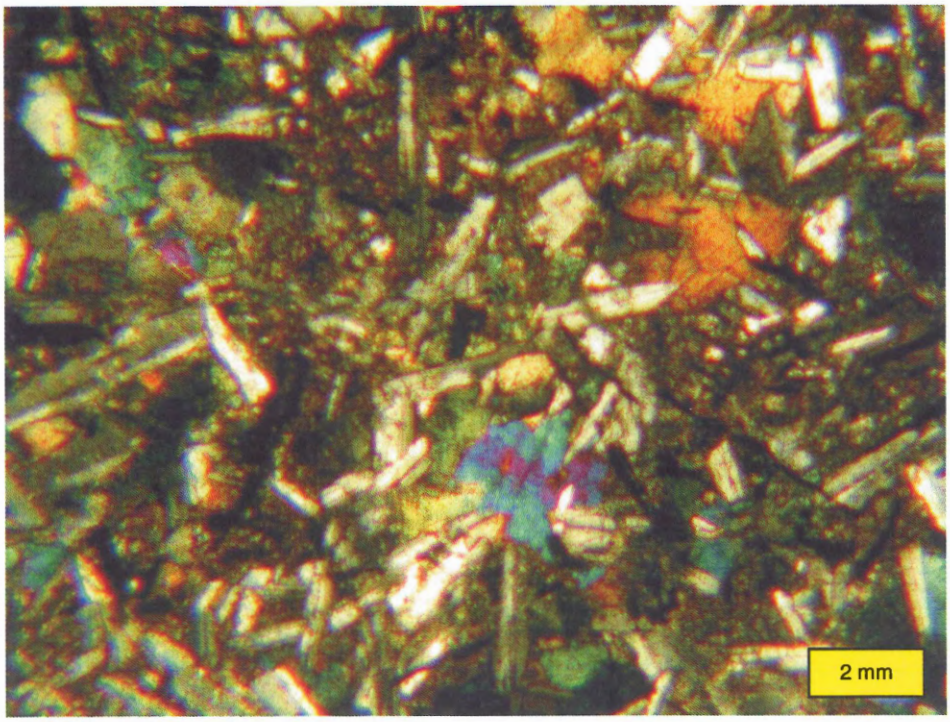

Figure 4.24 – Photomicrograph of a fine-grained sample of the chilled margin of the Wolf sill showing clinopyroxene and plagioclase in sub-ophitic texture, labelled A above (AX-03-63 a. plane-polarized light; b. crossed nichols). The coarse grained portions of the sill contain olivine. Symbols as in Figure 4.20, in addition Oliv = Olivine.

a)

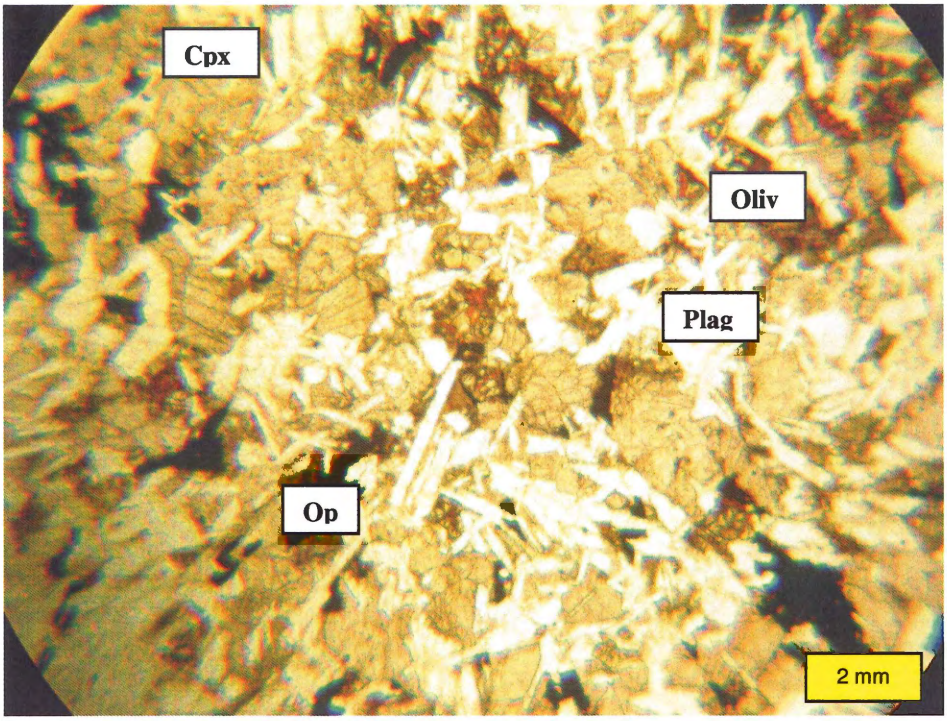

b)

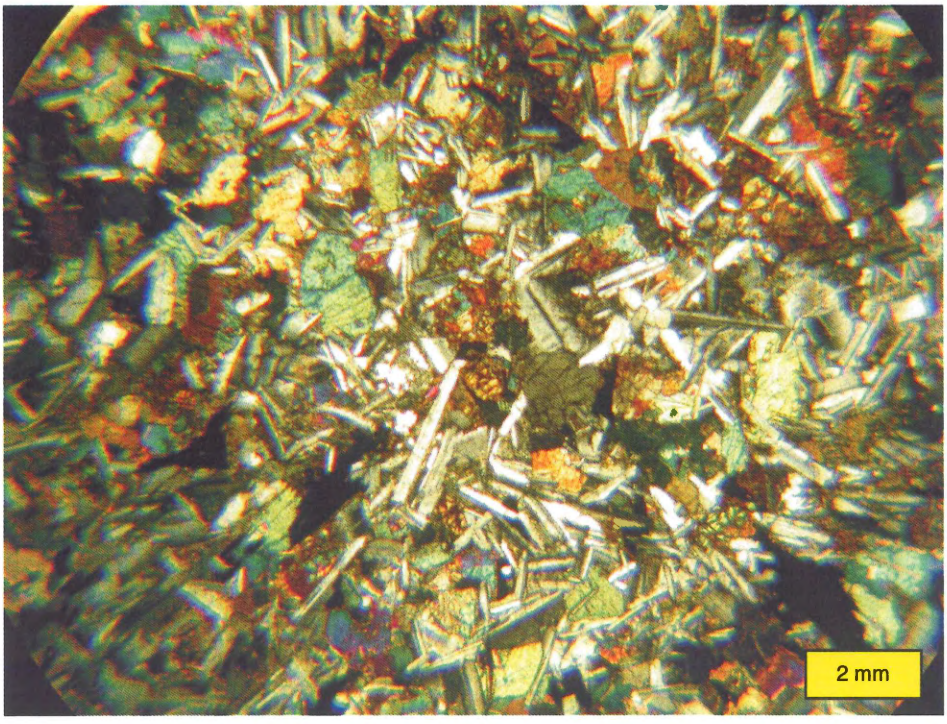

Figure 4.25 - Photomicrograph of a medium- to coarse-grained portion of the sill showing clinopyroxene, plagioclase, olivine, and opaques. Texture is equigranular and ophitic (AX-03-68 a. plane-polarized light; b. crossed nichols). Symbols as in Figure 4.20.

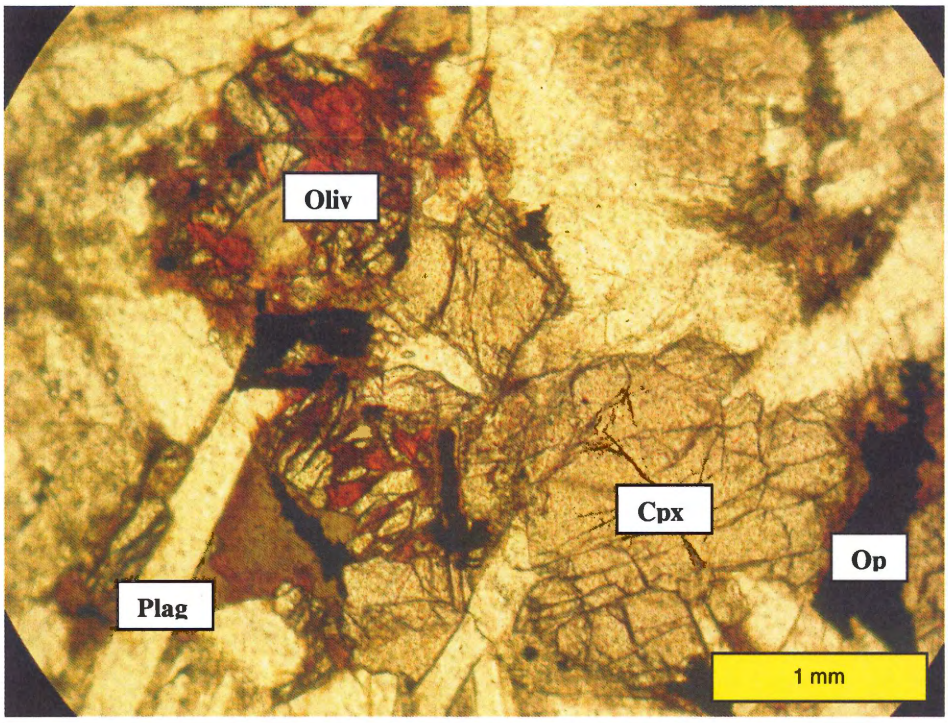

Figure 4.26 – Photomicrograph of a medium- to coarse-grained portion of the Wolf sill showing partially iddingsitized olivine and clinopyroxene (AX-03-68, plane-polarized light). Symbols as in Figure 4.20.

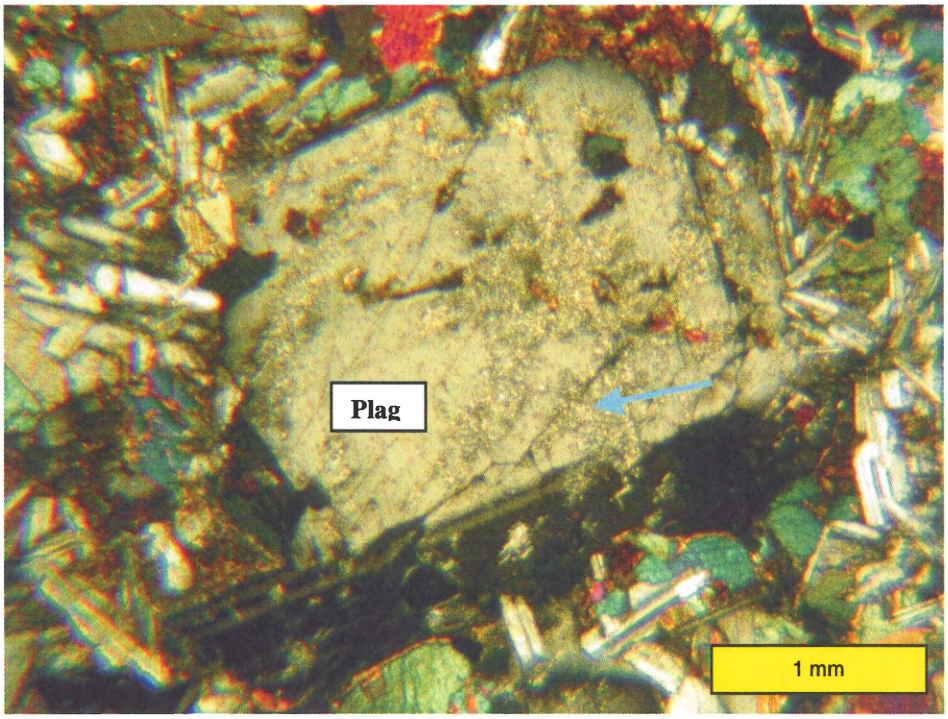

Figure 4.27 – Photomicrograph of a medium to coarse-grained portion of the Wolf sill showing equant, partially saussuritized (at arrow) plagioclase (AX-03-68, crossed nichols). Symbols as in Figure 4.20.

fact present. Since AX03-68 is a fairly altered portion of a gabbroic sill, a sample from a well-studied area, was chosen to act as a reference slide. Sample EL-84-50 is a portion of basaltic sill that was sampled on northern Ellesmere by Williamson (1988; Figure 4.29). The sample is characterized by a gabbroic mineralogy and texture. It was chosen as reference material for ESEM spectral analysis because of the exceptionally low degree of alteration, and well-documented mineralogy. Results of whole-rock, $^{40}Ar/^{39}Ar$ step-heating analyses performed by Avison (1987) on this sample yielded an age of 91 ± 2 Ma (1) and (2) represent the Dark Crystal and Mount Doom sills, respectively.

The preliminary analysis of the EL84-50 demonstrates a well-preserved freshly cut sill that has unaltered plagioclase crystals (Figure 4.30). In thin section, olivines are generally cracked and iddingsitized along the margins of these cracks. Figure 4.31 demonstrates that olivine is present. Using the analysis, a comparison of the EL84-50 mineral phases to those of the Wolf Intrusion sill (AX83-68), will help confirm the presence of olivine and other mineral phases in the altered rock. Appendix A shows all spectral analysis and greyscale images for EL84-50. The mineral phases present are titanomagnetite, clinopyroxene, plagioclase, and olivine. ESEM analysis of EL84-50 results in chemical spectrum and grey

Figure 4.28 – The *Star Intrusive* is a complex of feeder dykes and sills that intrudes an outlier of Permian strata in the area south of Piper Pass, on northern Ellesmere Island. Sample EL84-50 is a portion of Sill no. 4 reported in Williamson (1988).

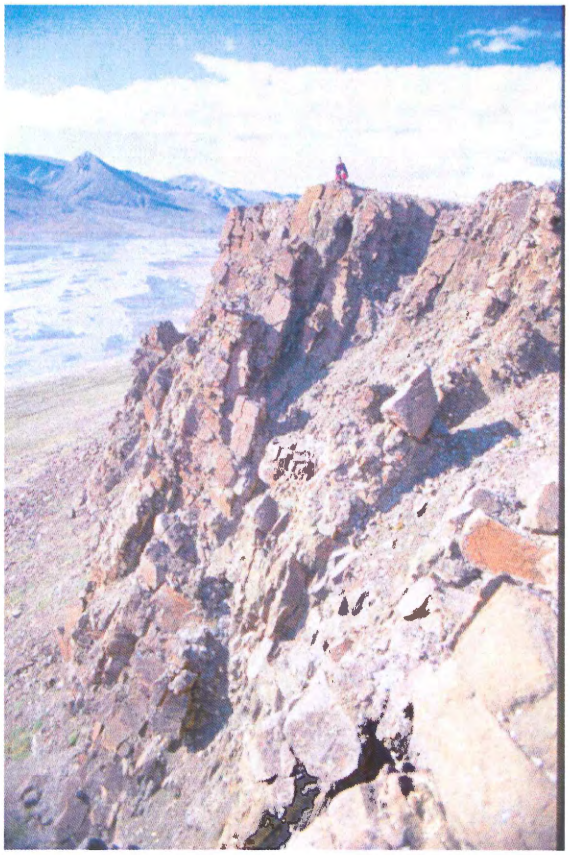

Figure 4.29 – The Wolf Intrusion is a sill that outcrops at the head of Expedition Fiord. The unit was chosen to illustrate what type of lithological data is routinely acquired for intrusive rocks and how these data can be displayed in a GIS. The photograph illustrates well-developed columnar jointing, below the point where Marie-Claude Williamson faces the camera. Very few concordant intrusions are exposed in the Strand Fiord-Expedition Fiord area; dykes are more abundant, and included on 1:250,000 scale geological maps. Photograph by Christopher Ferguson.

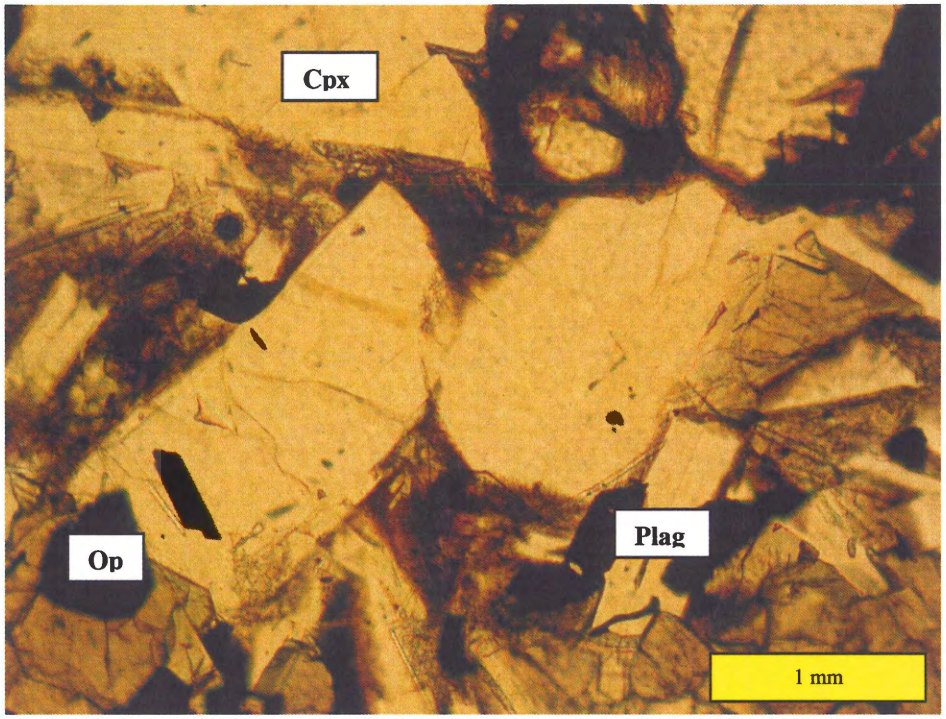

Figure 4.30 - Microphotograph displaying the well-preserved sill with plagioclase crystals unaltered in plane light (EL-84050, plane-polarized light). Symbols as in Figure 4.20.

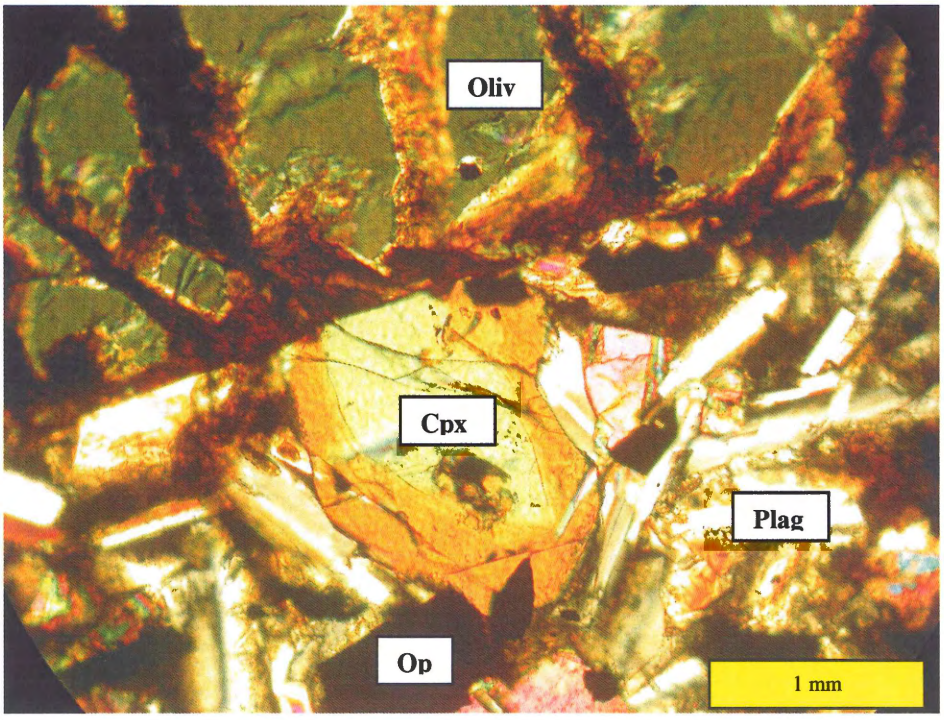

Figure 4.31 - Microphotograph showing a cracked olivine that is iddingsitized along the margins of these cracks. The small pyroxene crystal contains a large inclusion and is strongly zoned (EL84-050, crossed nichols). Symbols as in Figure 4.20.

scale images for the mineral phases and will be compared to the Wolf Intrusion sill (AX83-68).

Using the preliminary analysis of EL84-50 as a guide for the mineral phases present, the testing of the sample AX83-68 took place. In order to find a location where multiple mineral phases occur, a quick scan of AX83-68 showed an area with three phases occurring concurrently. This area, referred to as Area A (Figure 4.32a), shows light, medium, and dark grey grains. The first grain, shown in light grey, produced a spectrum comprising of titanium and iron (Figure 4.32b). The spectrum verifies that titanomagnetite is present and is comparable to the first grain of EL84-50 (Refer to Appendix A). The second grain, shown in medium grey, displays a spectrum with high silica and calcium values (Figure 4.32c). The spectrum is similar to the spectrum of grain two of EL84-50, confirming that clinopyroxene exists. Grain three, shown in dark grey, gives an analogous spectrum to that of grain three of EL84-50. The spectrum (Figure 4.32d) displays high Si, Ca, and Al values proving that plagioclase is in fact present.

Another scan of the slide revealed a cracked grain comprising of two different shades of grey. This area, is entitled Area B (Figure 4.33a). A spectrum analysis of both phases of the grain show similar compositions (Figure 4.33b and c). The lighter grey portion of the grain labelled 4a, shows high Si and Fe values along with the darker grey labelled 4b. These

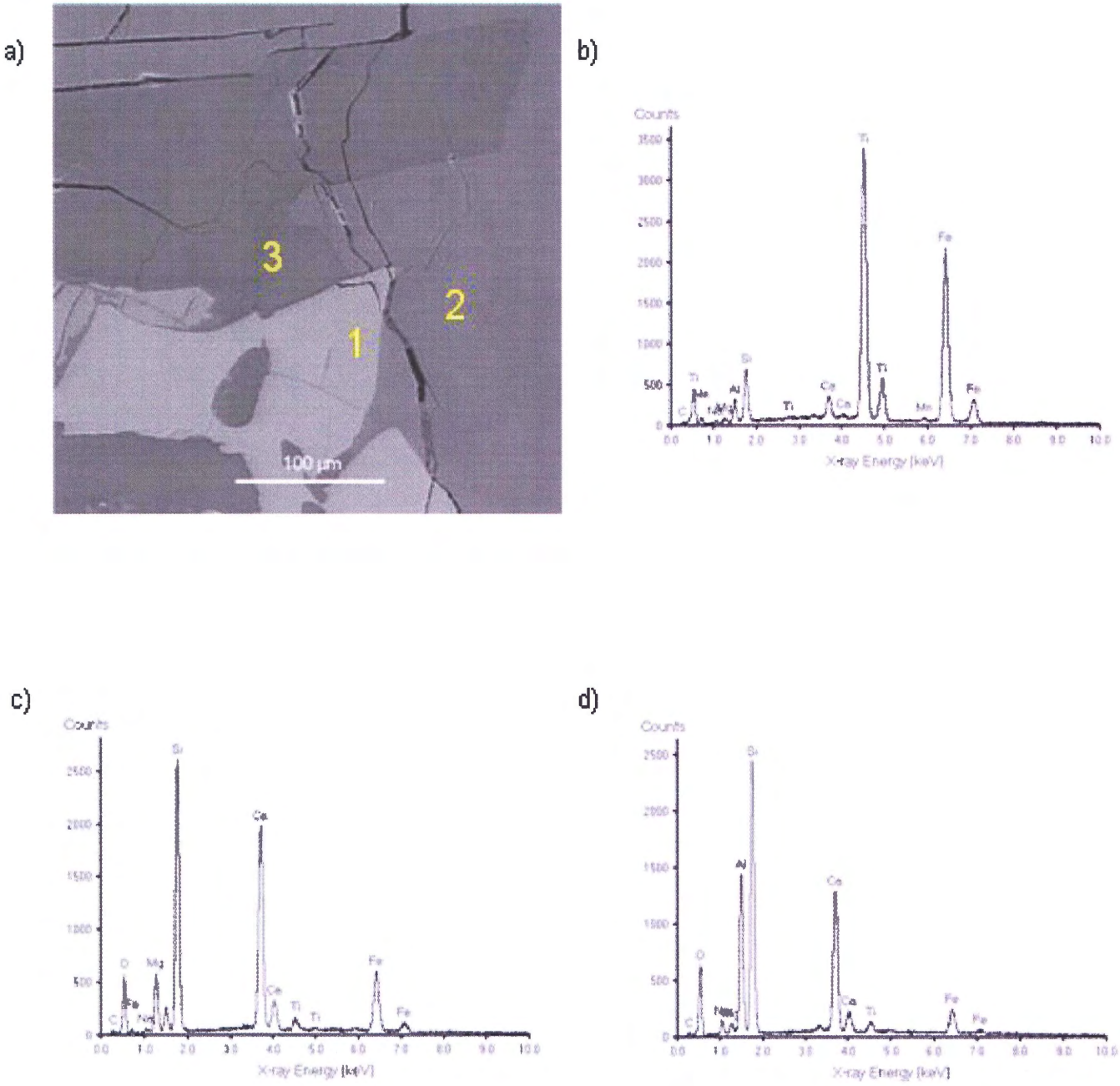

Figure 4.32 Grey scale image of area A with corresponding spectrum for AX83-68; a) Area A grey scale image displaying the three mineral phases, light, medium and dark; b) Spectrum analysis for grain 1; c) Spectrum analysis for grain 2; d) Spectrum analysis for grain 3. The above analysis confirms the identification of the mineral phases of Area A.

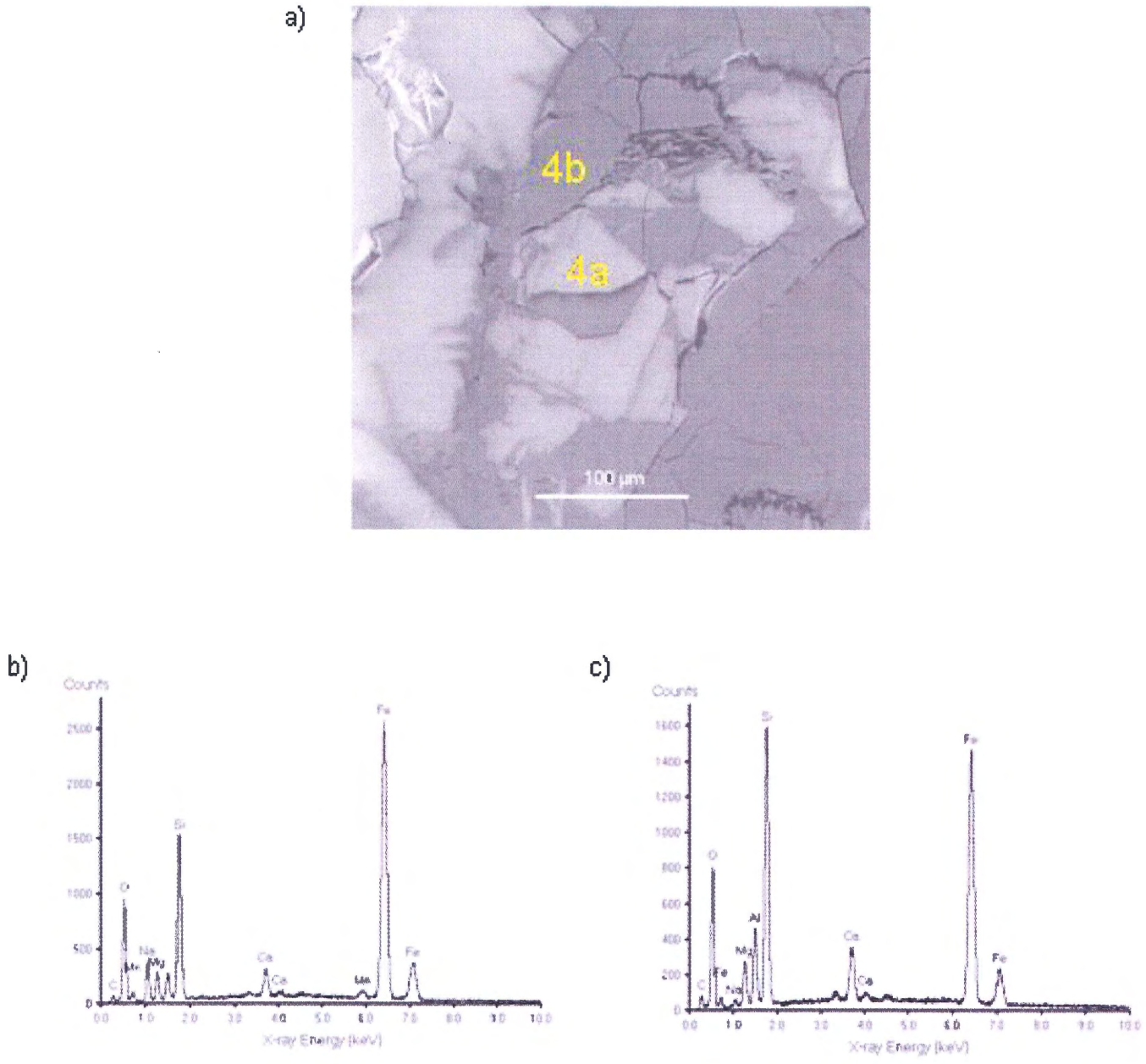

Figure 4.33 Grey scale image of area B with corresponding spectrum for AX03-68; a) Area B grey scale image displaying mineral phases for olivine, light and dark; b) Spectrum analysis for grain 4a ; c) Spectrum analysis for grain 4b.

spectra are similar to Grain 4 of the EL84-50 sample and suggest the presence of olivine in AX03-68.

4.4.2.3 Compositional Maps

Compositional mapping is an easy way to investigate the presence of elements and are most useful for med- to coarse grained intrusive rocks in the search for massive sulphides. Each element is represented independently with a different colour. Using the previously examined AX03-68 from the above qualitative spectral analysis, Area A (Figure 4.32a) was used to test for elements including Fe, Ca, Ti, and Ni.

The first compositional maps, displayed in red, show the occurrence of Fe^{2+} (Figure 4.33a) and Fe^{3+} (Figure 4.33b). A concentration of dots within an area, indicate a high proportion of the specific element within an area. Figure 4.33a illustrates the exact grain boundary seen in the greyscale image for Area A, Grain 1. This agrees with the Spectral Analysis section where the same grain was identified as titanomagnetite. The next compositional map, 4.33c, shows the distribution of Ca within the sample. Calcium is indicative of clinopyroxene and plagioclase, and the concentration of the dots follows the grain boundaries of the two mineral species. Compositional map 4.33d shows the occurrence of Ti. The concentration of the dots follows the same grain boundaries of the titanomagnetite. The last compositional map shows the occurrence of Ni throughout the slide. Unfortunately, there was only time for one analysis; as a result, the map shows no high concentrations of Ni. If time permitted,

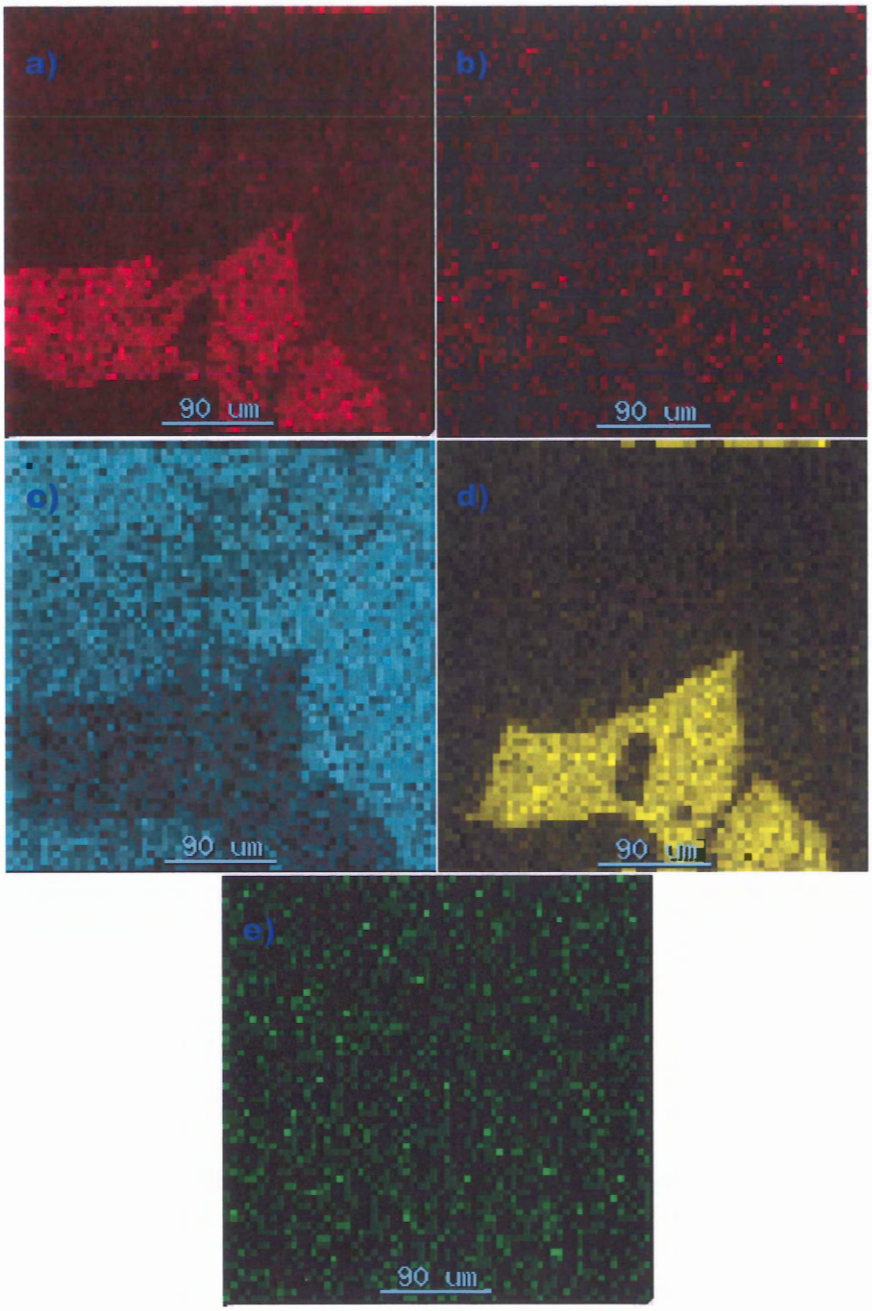

Figure 4.33 - Compositional maps for sample AX03-68 showing the proportion of selected elements and where they occur on the slide, a) Fe^{2+}; b) Fe^{3+}; c) Ca; d) Ti; e) Ni.

other sulphides could have been analyzed; however, the exercise demonstrates the capability of the ESEM.

4.8 Summary

The geological map of the area shows all of the formations and structures that make up the Strand Fiord Area. The faults generally trend east and north and the folds north-south and northwest-southeast. The topography shows a very mountainous landscape with u- and v-shaped valleys.

Dividing the magnetic and gravity rasters into intervals rather than using the colour ramp shows significant breaks between values. The magnetics show a noticeable north-northwest trending linear with a higher magnetic value than surrounding areas of the fiord. The gravity shows a gradual increase from very low negative to low positive moving towards the west within the basin.

Running trends across the fiord show interesting 2D magnetic cross sections. Moving from salt structures (low magnetic signature) to igneous bodies (high magnetic signature) creates a saw-tooth pattern for both magnetic trends. The magnetics can also predict what lies beneath the ice cover. Low negative anomalies occur suggesting the presence of multiple salt structures. Rare high magnetic signatures in this area suggest fewer igneous intrusions. This may prove important if salt structures cap potential gas reservoirs.

The DEMs helped determine geological boundaries and gave a better representation of the formations in conjunction with the aeromagnetics and known geology. DEMs also show the roughness of the land and give absolute heights over important features such as salt diapirs.

LANDSAT images enhance the geological features and structures by displaying colours for different features and allowing for easy identification of geological boundaries. Outlines of the rafted igneous rocks show a definite boundary with the surrounding salt that is not as easily recognized in the air photo or 1:250,000 scaled maps. Knowing where the rafted igneous areas occur within the dome allows for a better representation of the boundaries between the two.

Petrography indicates the basalts of Index Ridge have a fine-grained texture with seriate, hypocrystalline, intergranular, and intersertal textures. The groundmass consists dominantly of plagioclase and clinopyroxene, with minor amounts of olivine, opaque oxides, and devitrified glass. Green clay particles are present in minor amounts and all crystal phases are altered to some extent. Olivine can be partially preserved or pseudomorphed to the brown-red material iddingsite. The Wolf Intrusion is medium-grained with equigranular, holocrystalline, and intergranular textures (Figure 4.XX). The minerals present are plagioclase and clinopyroxene. Some portions of the sill contain up to 5% olivine with smaller amounts opaques. Clinopyroxenes are well preserved, however, olivine is partially altered to iddingsite, and green clay is present.

The ESEM confirmed the presence of olivine, clinopyroxene, plagioclase, and titanomagnetite within AX03-68. Gray scale images obtained from the ESEM display textures and the spectra distinguished between different crystal phases. The spectrum outputs for each of the grains, 1 through 4, are represented in both the EL84050 and AX83-68 samples. The spectrum for each crystal phase may differ slightly in proportions of elements, however due to the composition of the melt, cooling times, and alteration; the spectra may display different values for the elements.

Compositional maps show the presence of Fe2+, Ca, and Ti. Unfortunately, the test for Ni showed no significant results, however only one area was tested and is not representative of the entire Wolf Intrusion. More sulphide tests are needed.

CHAPTER 5 GIS APPLICATIONS

5.1 Salt Structures

5.1.1 Classification

The shapes of the diapirs are very important in terms of the structural relationships with the surrounding formations. There are two distinct shapes of diapirs occurring throughout the fiord, circular and stretched. Figure 4.8 displays the location of each diapir within the Strand Fiord area, while Table 5.1 provides values of length, width, elevation, magnetics and gravity for each diapir appear.

Within the study area, there are 6 circular diapirs, 11 stretched diapirs, and two that express both features. Both types of diapirs intrude Eocene aged sediments particularly the Isachsen and Christopher formations as seen on the geological map (Figure 4.6). The stretched diapirs follow the same north-south and northwest-southeast general trends of folding and occur in vicinity of the Strand Fiord where folding, faulting, and a rugged terrain dominate. Typically the circular diapirs occur in the less mountainous areas where minor folding and faulting occur and have the Mesozoic sediments envelope the boundaries

5.1.2 Characteristics

Due to the poor resolution of the gravity line spacing, the depth of the salt structures could not be determined, however, the intensity of the magnetics can show whether the salt structures have deep or shallow roots. The two trends (Figures 4.10 and 4.11) show two different anomalies for salt structures. The first type of anomaly appears across the Kanguk Diapirs. These diapirs are well exposed on the Kanguk Peninsula with well defined boundaries (refer to

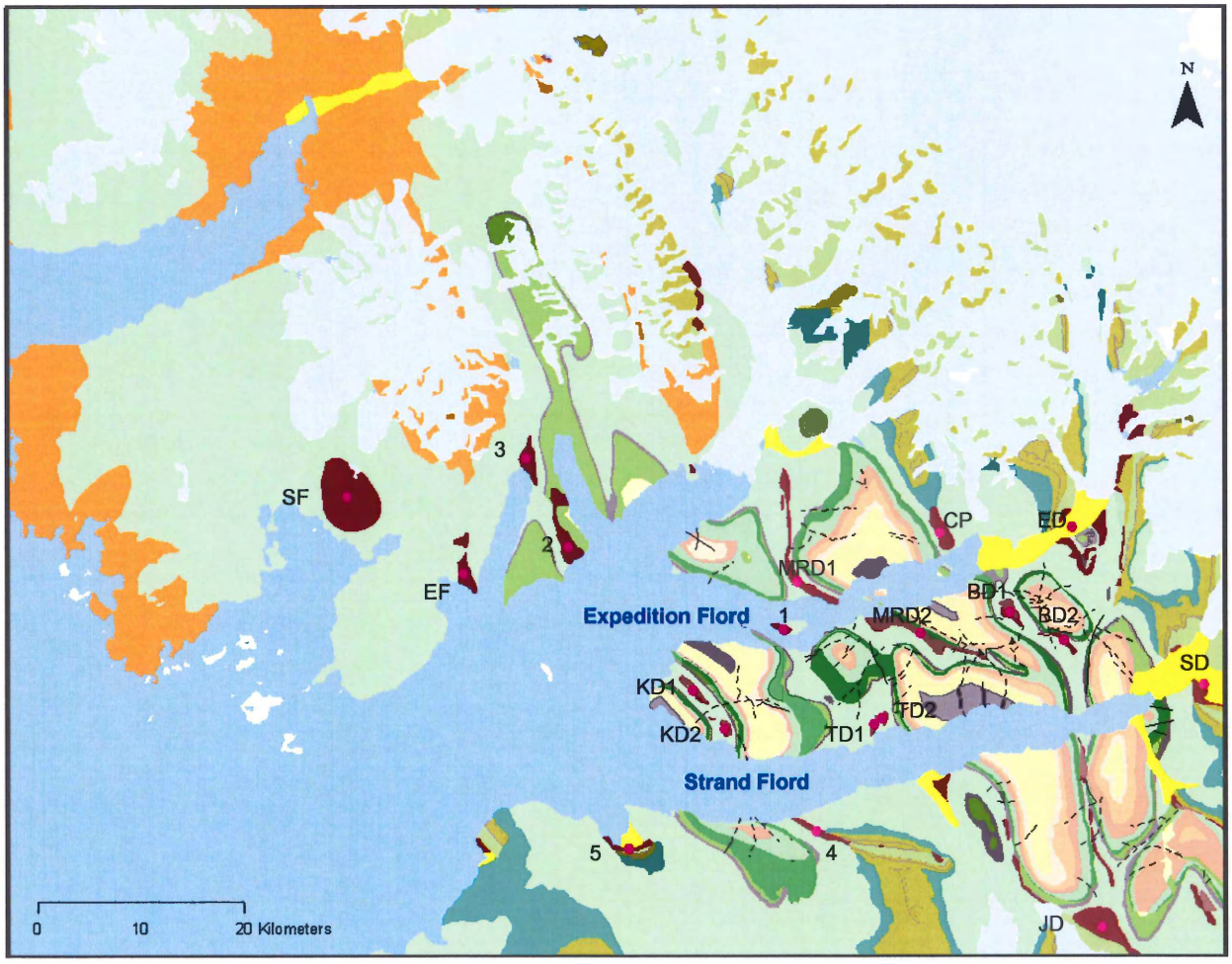

Figure 5.1 – Location of salt diapirs within the Strand Fiord. Refer to Table 5.1 for values of length, width, elevation, magnetics and gravity of each diapir.

Classification of Salt Diapirs of the Strand Fiord Area

Name	Easting	Northing	Length(m) *	Width (m) *	Mag Value Low	Mag Value High	Gravity Value	Topo High **	Topo Low **	Class
South Fiord Dome (SD)	477431.57	8818338	7494.43	5398.21	-457	-1	-19.0183	400	100	Circular
East Fiord (ED)	488988.58	8811571	4045.79	1480.55	-133	62	-24.6471	400	100	Stretched
Kanguk Diapirs (KD1)	510790.14	8799680	3936.99	828.48	-378	-120	-62.2586	300	100	Stretched
Kanguk Diapirs (KD2)	513813.37	8795959	1581.55	755.81	-457	-365	-61.7232	300	100	Stretched
Twin Diapirs (TD1)	528328.84	8796437	1983.69	461.28	-46	70	-63.2044	300	<100	Stretched
Twin Diapirs (TD2)	529156.29	8796975	111.89	453.36	-50	16	-63.2044	100	<100	Stretched
Bastion Diapirs (BD1)	541426.49	8807222	2904.12	1828.64	-199	-55	-65.9888	613	251	Circular
Bastion Diapirs (BD2)	546748.64	8804520	3114.4	627.74	-134	100	-69.9314	577	207	Stretched
Junction Diapir (JD)	550424.1	8776915	7373.95	2911.26	-154	-39	-82.0482	800	500	Circular/Stretched
Expedition Diapir (ED)	547585.6	8815417	6743.59	4585.23	-34	110	-58.2971	694	20	Circular
Colour Peak (CP)	534776.08	8814834	4367.5	1382.85	-134	116	-52.1196	524	54	Circular
Strand Diapir (SD)	560249.6	8800205	7979.45	3347.95	35	70	-82.0631	562	57	Circular
Muscox Ridge Diapir (MRD1)	520947.6	8810104	10723.61	1091.72	-307	333	-58.6786	500	<100	Stretched
Muscox Ridge Diapir (MRD2)	532883.76	8805227	10302.12	1455.63	-319	-26	-61.7833	625	0	Stretched
1	519540.49	8805532	1939.36	1460.12	-199	-96	-58.4417	0	0	Circular
2	498820.73	8813527	7377	2159.89	-337	84	-41.2351	300	100	Stretched
3	494797.9	8821981	4823.21	1571.81	-204	-75	-34.1238	300	100	Circular/Stretched
4	522734.37	8786132	5725.76	1196.17	-162	-24	-54.4277	500	100	Stretched
5	504607.12	8784384	3734.28	598.71	-94	45	-40.1777	100	<100	Stretched

* - distance dependent upon longest length or width possible for diapir

** - exact values taken from DEM where possible, other values taken from contour intervals

Table 5.1 - Values of length, width, elevation, magnetics, and gravity for individual diapirs.

Geological Map Figure 4.6). The Kanguk anomaly shows a drop to -341 nanoteslas over a very steep and fast drop in approximately 2000 metres. In order to achieve a low magnetic value in such a short distance considering the types of rocks surrounding the diapir, a deep rooted salt source must be present. The formations surrounding the diapir are the: Christopher Formation, Hassel Formation, Strand Fiord Volcanic Formation, Kanguk Formation, and Eureka Sound Group. As described in 3.3.4, all of the formations (other than the Strand Fiord Volcanics) contain sandstones, siltstones, and shales; suggesting a 0-0.2 (SI) magnetic susceptibility. The Kanguk Volcanic Formation consists mainly of basalts (described in 3.3.1) implying a magnetic susceptibility of 0.0005-0.18 SI. A study by Prieto (1998) shows various signatures of magnetics for different types of diapirs at depth. An attached salt dome beneath the surface at a depth of 4000 feet (Prieto, 1998), shows a fast drop in the form of a parabola resembling the same shape and values as the Kanguk Diapir. Another example given by Prieto is a salt ridge at a minor depth showing a very steep decline with an even lower magnetic response.

The second type of anomaly is shown with trend B as it runs through the Northern tip of Colour Peak. Colour Peak has an elevation of 524 metres and is another evaporite structure that exists with the surrounding Isachsen Formation, Christopher Formation, Hassel Formation, Strand Fiord Volcanic Formation, and Kanguk Formation. Magnetic values ranging from -134 to 116 nanoteslas occur around the vicinity of Colour Peak and may be caused by the existence of the

formations mentioned above occurring throughout the evaporites of Colour Peak causing a low positive magnetic to prevail.

Ice cover and rugged terrain prevail throughout Axel Heiberg Island causing concealment of geological structures and features. Aeromagnetic images can show the presence of these structures and features that may exist beneath the surface. Figure 5.2a shows the ice cover for Axel Heiberg Island while Figure 5.2b shows the magnetics for Axel Heiberg Island. Even though the ice cover restricts observation of geology in the field, negative magnetic responses indicate that there may be diapirs or a type of salt intrusion below the ice. Salt structures can also exist beneath the surface of the earth and become exposed over time through erosion. An example within the fiord is just north of the Twin Diapirs. While assessing the magnetics, a circular shaped low magnetic anomaly occurs where the Christopher Formation is mapped (Figure 4.6). The Christopher Formation consists of dark shales with minor sandstone, siltstone, mudstone and pyroclastics suggest a 0-0.2 magnetic susceptibility. The centre of the anomaly produces magnetic values ranging from -156 to -180 nanoteslas. The rocks comprising the Christopher Formation theoretically cannot produce such a low magnetic signature because of their positive magnetic susceptibility implying that a salt structure must occur beneath the surface in order for the magnetics to achieve such a low negative magnetic value.

As shown in Chapter 4.6, LANDSAT images enhanced geological features and structures by displaying colours for different features and allowing for easy

identification. Figure 4.17 outlines rafted igneous rocks and show a definite boundary with the surrounding salt that is not as easily recognized in the air photo or 1:250,000 scaled maps. Knowing where the rafted igneous areas occur within the dome allows for a better representation of the boundaries between the two. Also, textures of the image portray a rugged or flat landscape representing how steep slopes are dipping through shadows. Like an air photo, the LANDSAT image gives an idea of geometric features. For example, the South Fiord Dome is oval shaped and is approximately 6 kilometres in width.

5.2 Igneous Rocks

5.2.1 Lithological Data

Through petrography, observations of minerals, textures, and percent cover show what type of rock is present. The basalts of Index Ridge tend to have a fine grained texture with a seriate, hypocrystalline, intergranular, and intersertal textures. Green clay particles are present in minor amounts and all crystal phases are altered to some extent. Olivine can be partially preserved or pseudomorphed to the brown-red material iddingsite. The Wolf Intrusion is medium grained with equigranular, holocrystalline, and intergranular textures. The minerals present are plagioclase and clinopyroxene. Clinopyroxenes are well-preserved, however, olivine is partially altered to iddingsite and green clay is present.

For sample AX03-68, the use of the ESEM confirmed the presence of minerals observed using the optical microscope through grey scale images, spectra, and compositional maps. Using GIS, a link of the observations to the

database highlight the areas of extrusive and intrusive rocks. In the future, if a particular igneous formation is found economically viable, the locations of the formation are easily found within the GIS database and all pertinent information can be accessed.

5.2.2 Future Work

The study is the first to create an interactive compilation of geological and lithological data with observations, images, and preliminary results within a GIS program for the Strand Fiord Area. Limited time prevented the analysis of samples from other areas of the fiord and additional testing such as a geochemical study. Future results can add to the present study with the objective of building a database for Strand Fiord, Axel Heiberg Island and eventually the rest of the Arctic Islands.

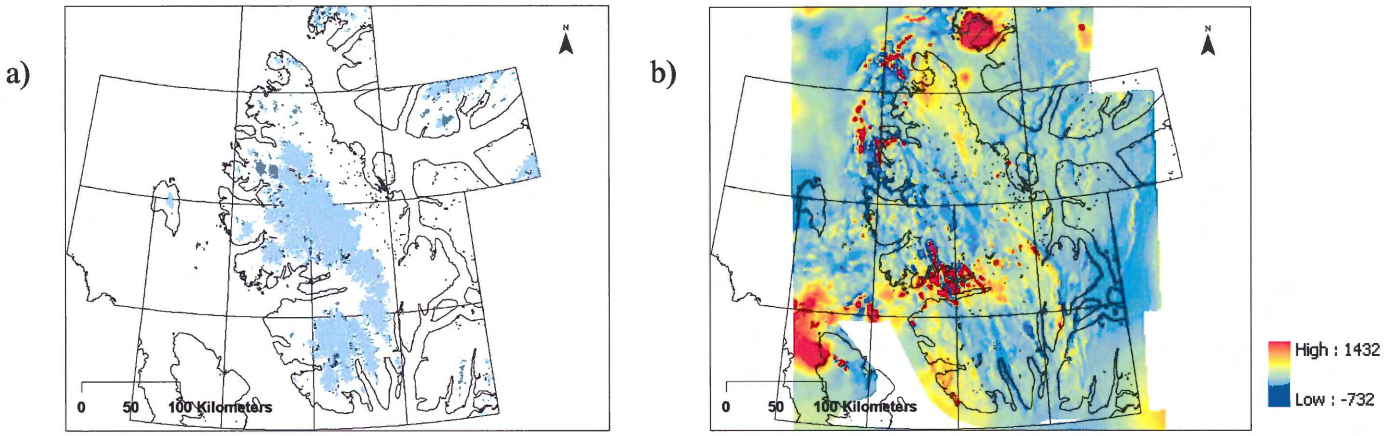

Figure 5.2 a) Shows the amount of ice (blue) that covers Axel Heiberg Island; b) Magnetics for the entire island. Even though the ice cover restricts observation of geology in the field, negative magnetic responses indicate that there may be diapirs or some type of salt intrusion below the ice shown in blue.

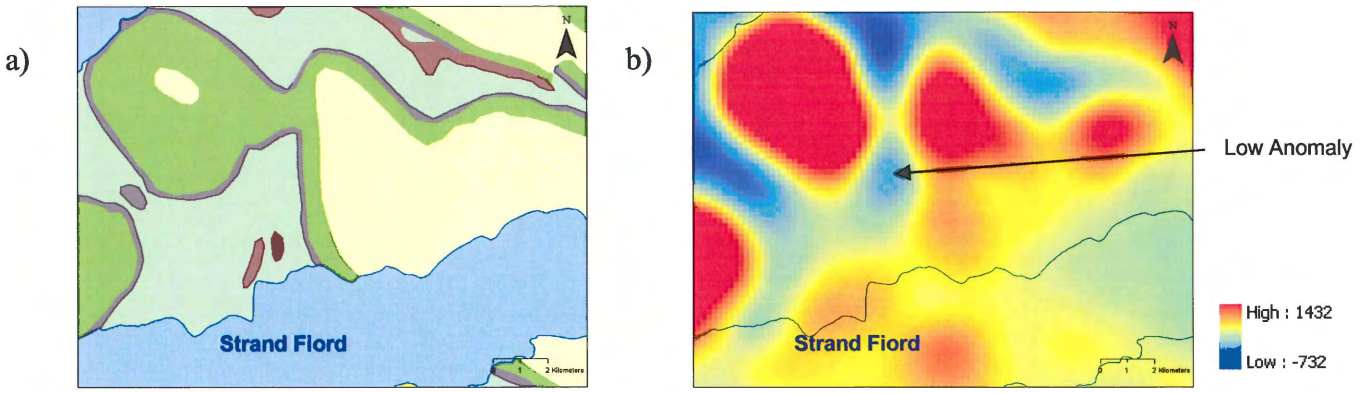

Figure 5.3 a) Shows the mapped geology for area near Bastion Ridge. Refer to Figure 4.7 for legend. b) Shows the magnetics for same area; Note the very low negative magnetic anomaly.

CHAPTER 6 DISCUSSION AND CONCLUSIONS

6.1 Scientific Questions

GIS is a useful tool for managing and interpreting geological databases. It allows for quick viewing and easy access to multiple databases at one time. Throughout the study, the use and application of GIS attempted to answer two questions proposed in Chapter 1.

The following sections examine the two questions in more detail.

6.1.1 Can GIS help assess properties of igneous rocks in the study area?

The magnetic raster can be used to determine properties of igneous bodies. A subtle NNW trend of high magnetic field occurs in the central portion of Strand Fiord following the same NW trend of folds and faults. Due to the high magnetic properties of igneous flows, the trend of intrusion and location of where flows occur is shown within the fiord.

In addition, the DEM combined with the magnetics and known geology can be used to determine geological boundaries and give a better representation of the formations.

LANDSAT images can be used to enhance geological features of large, complex structures such as the South Fiord Dome. Using the image, features and structures displayed as different colours allow easy identification of materials. The outline of the rafted igneous rocks shows a definite boundary with the surrounding salt providing a better representation of the boundary location between the two formations.

6.1.2 Can GIS help determine depth and volume of salt structures in the study area?

The length and width of the diapirs was determined by values outputted by ArcMap. Due to the low resolution of the gravity, an estimated depth and volume of the salt diapirs could not be made. However, the magnetics showed an apparent depth for the diapirs suggesting that some diapirs are in fact deeply rooted and the length and width calculated the area of each diapir. A high resolution gravity survey would give enough data to run 2D cross-sections through the diapirs and determine the depth of the diapirs. This depth combined with the length and width that this study determined would give the volume of the diapir.

6.2 GIS interpretation of Geophysics

6.2.1 Magnetics

Magnetic anomalies occur due to lateral variations in the lithosphere's magnetic polarization and the occurrence of igneous intrusions, metamorphic rocks, and alterations cause local anomalies (Hinze and Hood, 1989). Petrographical and ESEM analysis show the presence of ferromagnetic (titanomagnetite) and nonferromagnetic (clinopyroxene) minerals within the basalts and sills of the study area. In contrast to relatively non-magnetic sedimentary rocks, the highly magnetic basaltic lavas and intrusives generate the highly positive magnetic anomalies for the Strand Fiord region.

The magnetic pattern observed in the Strand Fiord area is suggestive of the geological structures and features present. The magnetic raster displays a

NNW trend of high magnetic values within the central Strand Fiord area (Figure 4.3 and 4.8). As mentioned throughout this study, the Mesozoic strata of the Strand Fiord contain basaltic lavas (which are described as part of mapped formations) and chemically equivalent sills (which were not mapped). On the geological map, there is also a NW trend of abundant igneous intrusions occurring in the most folded and faulted portion of the Strand Fiord. The north westerly trend seen in the magnetic data corresponds with the distribution pattern of the igneous bodies. In addition, moving away from the area shows a decrease magnetic value, igneous intrusions and deformation where Mesozoic sediments dominate. It is possible that the strong folding and faulting of igneous bodies in the Princess Margaret Range impart a stronger and more variable magnetic signature than the same bodies in a horizontal position.

The magnetic raster image combined with the geological data for the study area is very useful for defining geological boundaries and contacts. In the field, outcrop exposure is sometimes limited, leading geologists to predict where the boundaries between different formations occur. Using GIS software, the magnetic raster helps extrapolate lines of known geological boundaries and contacts with a more accurate representation of where the contacts should occur in areas of structural disruption and poor exposure. The reader is referred to Section 5.4 where the use of GIS as a tool in the interpretation of aeromagnetic data at the site of salt domes is described in more detail.

6.2.2 Gravity

The gravity raster displays gravity lows in the highly folded and faulted portion of the eastern Strand Fiord whereas gravity highs predominate in the west moving into the Strand Bay. As mentioned previously, central Strand Fiord contains abundant salt structures. It is suggested that because salt (halite) has a lower density (2.2) compared to the surrounding strata (2.8-3.0), a 'gravity low' results in comparison with the less disturbed and presumably more dense formations to the west. Adjacent to the east of the Strand Fiord is the Princess Margaret Range (PRM), a mountain range running north-south through the centre of Axel Heiberg Island. Throughout the region, the basement rocks are understood to be continental crust. During the Palaeocene-Eocene, compression caused folding, halokinesis, and uplift of the Princess Margaret Range (Miall, 1981). It is believed that this mountain range is cored by salt (M. Zentilli personal communication, 2005) resulting in a gravity low. The geological map (Figure 4.7) shows the intensity of deformation decreases to the west of the Princess Margaret Range into the sea. The above geological setting possibly suggests that the mountain range is underlain by a décollement surface where folds and thrusts overlay relatively undeformed basement.

6.3 Application of Earth Observation to identification, classification and mapping of igneous rocks

LANDSAT images can be used to enhance geological features of large, complex structures such as the South Fiord Dome. Different coloured features and structures

a)

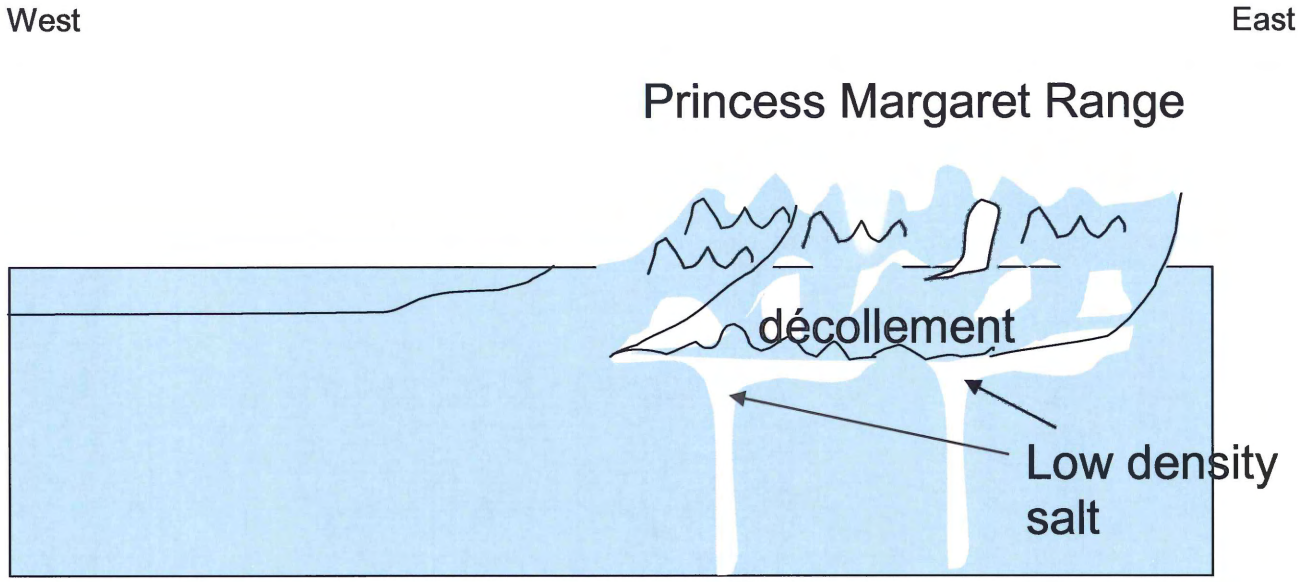

b)

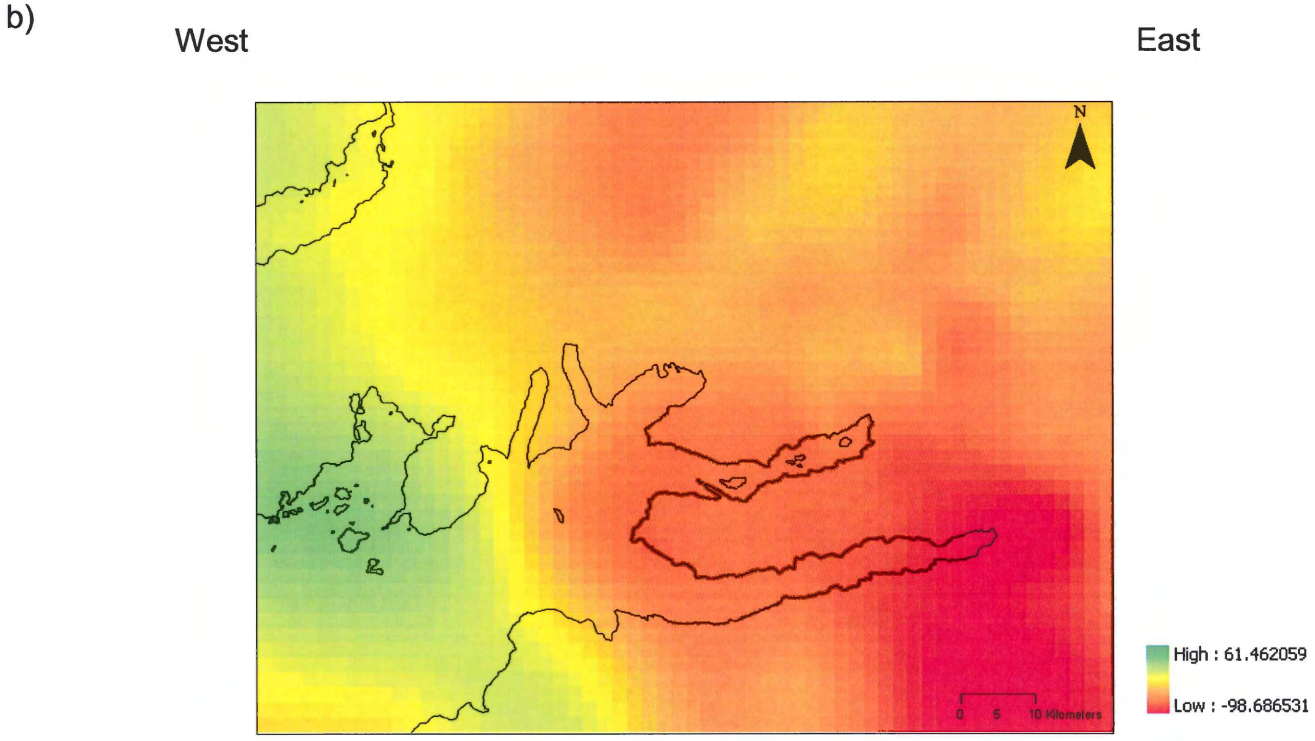

Figure 6.1 - a) Diagram illustrating the landscape of the fiord. Starting in the East, the Princess Margaret Range (PRM) uplifted and influenced faulting and folding adjacent to the mountain range. The mountain itself is believed to be cored by salt (shown in white). The eastern portion of the Strand Fiord has a rugged terrain comprising of igneous and salt bodies with east and north trending faults and north to south trending folds. West Strand Fiord is not as deformed as the eastern portion and is more flat with less deformation; b) the raster image taken from Figure 2.4 shows an east to west transition of gravity lows (in red) to gravity highs (in green).

allow for the differentiation and identification of various landforms. Figure 4.17 shows salt as light cyan, vegetation as green, water as navy blue, ice as blue, Isachsen Formation as brown and rafted igneous rocks as dark brown. Colour, shading, and textures outline rafted igneous rocks showing a definite boundary with the surrounding salt. The new boundary provides a better representation of the contact between the two formations. Remote sensing is therefore very useful in isolated areas where travel is limited by giving quantitative estimates of the aerial extent, volume, shape, and location of diapirs. In areas such as Axel Heiberg Island, satellite imagery can give an idea of the size of structures and the terrain type without stepping foot on land, thus facilitating the planning of field activities or future engineering projects.

Using GIS, a link of the observations to the database highlight the areas of extrusive and intrusive rocks. In the future, if a particular igneous formation is deemed to be of any particular interest, the locations of the formation are easily found within the GIS database and all pertinent information can be accessed.

In addition, any new data that becomes available can easily be added to the existing database.

6.4 GIS interpretation of geological data on salt domes

The way in which a diapir forms influences structural relationships with the surrounding formations, and also the shape and geometry of the diapir. The salt diapirs within Strand Fiord are mostly stretched, elongated, and are associated with faults and isoclinal anticlines (Ricketts, 1987). Throughout the fiord, the occurrence of clustered diapirs and hypersaline springs suggest that originally the Otto Fiord evaporites existed below the Strand Fiord area (van Berkel et al., 1984). Salt diapirs have a specific gravity

of 2.16 (halite), igneous rocks 2.8-3.0, sandstone 2.2-2.8 and shale 2.4-2.8. The exposed cap of diapirs is made of heavier anhydrite (S.G. 2.98) and gypsum (2.32), but the cap is of limited thickness. During inflation, passive growth of salt occurs when the rate of salt flow and sediment-aggradation equal causing vertical movement, or a tongue of salt can form as salt flow exceeds sedimentation causing lateral movement (Rowan et al., 2003). Diapirism keeps pace with sedimentation and causes surrounding sediments to become brushed aside and overturned as sedimentation continues (Rowan et al., 2003). Salt, due to its specific gravity and hydraulic characteristics as a fluid, is squeezed out from the overlying sediments and several workers (e.g. Van Berkel et al., 1984) suggest accelerated diapir emplacement occurred during the Eurekan Orogeny, forming a décollement where the diapirs extruded within the centre of buckle folds.

Section 5.1.1 describes two types of diapirs that occur throughout the vicinity of the fiord, circular and stretched. Arc Map easily displayed distances, magnetic, gravity, and elevation values quickly and easily allowing simple classification. The stretched diapirs follow the same north-south and northwest-southeast general trend of folding and occur where folding, faulting, and rugged terrain dominate. The emplacement of the diapirs occurred prior to the folding and faulting and there elongated shape is a result of tectonic processes taking place around Axel Heiberg Island.

Typically the circular diapirs occur in the less mountainous areas where minor folding and faulting occur and intrude the Mesozoic sediments. These large domes are not influenced by structural processes like the stretched diapirs; however they influence the intruded sediments to envelope around the boundaries of the diapir.

The intensity of the magnetics suggests the depth of the diapirs. The two trends (Figures 4.10 and 4.11) show a saw-tooth pattern as it moves across the diapirs, creating two types of anomalies. The first anomaly is a very steep and fast drop in intensity (approximately 700 nanoteslas) creating a very narrow parabola over a short distance, e.g. Kanguk Diapirs. In order to achieve a low magnetic value in such a short distance with highly magnetic igneous rocks surrounding the diapir, a deep rooted non-magnetic evaporate source must be present. The second type of anomaly shows a very shallow drop (approximately 300 nanoteslas) creating a broad parabola e.g. Expedition Diapir.

The volume of the diapirs could not be determined because the magnetics could only suggest the apparent depth of each diapir. A high resolution gravity survey would give enough data to run 2D cross-sections through the diapirs and determine the depth of the diapirs. This depth combined with the length and width in Appendix C would give the volume of the diapir.

6.5 Integrated geology and geophysics

Throughout Axel Heiberg Island, ice cover and rugged terrain prevail. The presence of salt structures can occur beneath the surface, becoming exposed over time through erosion. Through comparison of the field geology observations and magnetic responses, distinct signatures of certain rock types occur. Using the geology and geophysical data together helps show structures exist beneath the ice or surface where field access may be denied. Magnetics, as shown in Figure 5.2, indicate that there may be some type of salt intrusion occurring beneath the ice. If future studies show potential for oil and gas exploration in and around diapirs throughout Axel Heiberg Island,

knowing where diapirs are concealed by the ice may provide additional sources. Also, there appears to be less igneous intrusions north of the Strand Fiord area. The absence of an intrusion may prove to be an important trait because intrusions may alter any hydrocarbons formed causing overmature hydrocarbon source conditions.

The second example shown in Figure 5.3 shows a circular shaped low magnetic anomaly occurring where the Christopher Formation is mapped. Due to the composition of the Christopher Formation, the low magnetic signature could not normally occur suggesting that a salt structure must exist beneath the surface in order for the magnetics to achieve such a low negative value. This observation may also prove useful in future years if these salt structures are explored for petroleum possibilities.

6.6 Recommendation for Future Studies

For a continuation of this study, a higher resolution gravity survey is needed to calculate the actual depth and volume of the salt diapirs. Further understanding of the petroleum system of Axel Heiberg Island will assess the petroleum potential of the area. Additional data can add to the present database in order to accumulate information for the Strand Fiord and eventually the rest of the Arctic Islands.

Continuing studies by Arctic research scientists, such as Dr. Marie-Claude Williamson and Dr. Marcos Zentilli, will help in the overall understanding and interpretation of the igneous bodies, salt structures and tectonic history of the Arctic Archipelago, and will both make use and update the present GIS.

6.7 Conclusions

GIS is a very important tool for the management and interpretation of data. Northern islands such as Axel Heiberg have limited access throughout the year creating

difficulties while mapping in the field. Through the use of GIS, queries performed on the data allowed for quick and easy interpretation. The study is the first to create an interactive compilation of geological and lithological data with observations, images, and preliminary results within a GIS program for the Strand Fiord Area.

CHAPTER 7 REFERENCES

Andersen, D.T. ,Pollard, W.H. (2002) *Cold springs in permafrost Earth & Mars*. Journal of Geophysical Research, **107**: 10.1029.

Arne, D.C., Zentilli, M., Grist, A.M., and Collins, M. (1998) *Constraints on the timing of thrusting during the Eurekan orogeny, Canadian Arctic Archipelago: an integrated approach to thermal history analysis*. Canadian Journal of Earth Science **35**: 30-38.

Arne, D.C., Grist, A.M., Zentilli, M., Collins, M., Embry, A. & Gentzis, T. (2002) *Cooling of the Sverdrup Basin during Tertiary basin inversion: implications for hydrocarbon exploration*. Basin Research **14** (2): 183-205.

Avison, H. (1987) *Ar-40/Ar-39 age studies of mafic volcanics from the Sverdrup Basin.* Unpub. B.Sc. Honours Thesis, Dalhousie University, Halifax, Nova Scotia, Canada, 88pp.

Balkwill, H.R., and Fox, F.G. (1982) *Incipient Rift Zone, Western Sverdrup Basin, Arctic Canada*: in Arctic Geology and Geophysics; Embry, A.F, and Balkwill, H.R. (eds). Canadian Society of Petroleum Geologists Memoir 8: 171-187.

Balkwill, H.R., Bustin, R.M., and Hopkins Jr., W.S. (1975) *Eureka Sound Formation at Flat Sound, Axel Heiberg Island, and chronology of the Eurekan Orogeny*. Geological Survey of Canada, Paper 75-1, Part B: 205-209.

Budkewitsch P. (2005) Personal Communication. April 26, 2005.

Davies, G.R. and Nassichuk, W.W. (1991) *Carboniferous and Permian history of the Sverdrup Basin*; Chapter 13 in Geology of the Innuitian Orogen and Arctic Platform of Canada and Greenland, H.P. Trettin (ed); Geological Survey of

Canada, Geology of Canada, no.3 (also Geological Society of America, The Geology of North America, v.E): 349-368.

Dawes, P.R., and Christie, R.L. (1991) *Geomorphic Regions*; Chapter 3 in Geology of the Innuitian Orogen and Arctic Platform of Canada and Greenland, H.P. Trettin (ed); Geological Survey of Canada, Geology of Canada, no.3 (also Geological Society of America, The Geology of North America, v.E): 27-56.

Embry, A.F. (1991) *Mesozoic history of the Arctic Islands*; Chapter 14 in Geology of the Innuitian Orogen and Arctic Platform of Canada and Greenland, H.P. Trettin (ed); Geological Survey of Canada, Geology of Canada, no.3 (also Geological Society of America, The Geology of North America, v.E): 369-433.

Embry, A.F., and Osadetz, K.G. (1988) Stratigraphy and tectonic significance of Cretaceous volcanism in the Queen Elizabeth Islands, Canadian Arctic Archipelago. Canadian Journal of Earth Science **25**: 1209-1219.

Embry, A.F. (1982) *The Upper Triassic-Lower Jurassic Heiberg Deltaic Complex of the Sverdrup Basin:* in Arctic Geology and Geophysics; Embry, A.F, and Balkwill, H.R. (eds). Canadian Society of Petroleum Geologists Memoir 8: 189-217.

Fricker, P.E. (1963) *Geology of the Expedition Area: Western Central Axel Heiberg Island Canadian Arctic Archipelago*. Jacobsen-McGill Arctic Research Expedition 1959-1962:156pp.

Fricker, P.E. (1961) *Geological Report*: in Jacobsen-McGill Arctic Research Expedition to Axel Heiberg Island Queen Elizabeth Islands; Müller, B.S. (ed). Mc Gill University, Preliminary Report 1959-1960: 153-159.

Hoen, E.W. (1961) *A study of the gypsum diapirs of Axel Heiberg Island*: in Jacobsen-McGill Arctic Research Expedition to Axel Heiberg Island Queen Elizabeth Islands; Müller, B.S. (ed). Mc Gill University, Preliminary Report 1959-1960: 161-170.

Kranck, E.H. (1963) G*ypsum Tectonics of Evaporite Diapirs on Axel Heiberg Island*: in Jacobsen-McGill Arctic Research Expedition to Axel Heiberg Island Queen Elizabeth Islands. Mc Gill University, Preliminary Report 1961-1962: 133-138.

Kranck, E.H. (1961) G*ypsum tectonics on Axel Heiberg Island*: in Jacobsen-McGill Arctic Research Expedition to Axel Heiberg Island Queen Elizabeth Islands; Müller, B.S. (ed). Mc Gill University, Preliminary Report 1959-1960: 147-152.

Liew, S.C. (2001) *Principles of Remote Sensing.* <www.crisp.nus.edu.sg> (Accessed March 20, 2005).

Miall, A.D. (1981) *Late Cretaceous and Palaeogene sedimentation and tectonics in the Canadian Arctic Islands*: in Sedimentation and Tectonics in Alluvial Basins; Miall, A.D. (ed). Geological Association of Canada Special Paper: 221-272.

Pollard, W., Omelon, C., Andersen, D. & McKay, C. (1999) *Perennial spring occurrence in the Expedition Fiord area of western Axel Heiberg Island, Canadian High Arctic*. Canadian Journal of earth Sciences, **36**: 105-120.

Prieto, C. (1998) *Gulf of Mexico Continental Slope – Understanding the Magnetic Response Due to the Salt Intrusion*: in Geological Applications of Gravity and Magnetics: Case Histories; Gibson, R.I. and Millegan, P.S. (eds). SEG Geophysical Reference Series, No.8: 14-16.

Rickets, B.D. (1991) *Delta evolution in the Eureka Sound Group, Western Axel Heiberg Island: the transition from wave-dominated to fluvial-dominated deltas.* Geological Survey of Canada, Bulletin 402: 72 pp.

Rickets, B.D (1987) *Princess Margaret Arch: re-evaluation of an element of the Eurekan Orogen, Axel Heiberg Island, Arctic Archipelago.* Canadian Journal of Earth Science **24**: 2499-2505.

Rowan, M.G., Lawton, T.F., Giles, K.A., and Ratliff, R.A. (2003) *Near-salt deformation in La Popa basin, Mexico, and the northern Gulf of Mexico: A general model for passive diapirism.* AAPG Bulletin, v. 87, no. 5: 733–756.

Rudberg, S. (1963) *Geomorphological processes in a cold, semi-arid region*: in Jacobsen-McGill Arctic Research Expedition to Axel Heiberg Island Queen Elizabeth Islands. Mc Gill University, Preliminary Report 1961-1962: 139-150.

Stephenson, R.A., van Berkel, J.T., and Cloetingh, S. (1992) *Relation between salt diapirism and the tectonic history of the Sverdrup Basin, Arctic Canada.* Canadian Journal of Earth Sciences **29**: 2695-2705.

Schwerdtner, W.M. (1966) *Identification of evaporite diapirs formed under the influence of horizontal compression.* Bull. CSPG, **34**: 271-278.

Schwerdtner, W.M. and Clark, A.R. (1967) *Structural analysis of Mokka Fiord and South Fiord Domes, Axel Heiberg Island, Canadian Arctic.* Canadian Journal of Earth Sciences **4**: 1229-1245.

Schwerdtner, W.M. & van Kranendonk, M. (1984) *Structure of the Stolz Diapir - a well-exposed salt dome on Axel Heiberg Island, Canadian Arctic Archipelago.* Bull. CSPG, **32**: 237-241.

Thomas, F.C. and Williamson, M-C. (2004) *Imaging and Qualitative Spectral Analysis using the Environmental Scanning Electron Microscope: User Guide for the ESEM Facility at GSC Atlantic.* Geological Survey of Canada, Open File 4599: 24pp.

Thorsteinsson, R. (1971) *Geology, Middle Fiord, District of Franklin.* Geological Survey of Canada, Map number 1299A.

Thorsteinsson, R. (1971) *Geology, Strand Fiord, District of Franklin.* Geological Survey of Canada, Map number 1301A.

Thorsteinsson, R. and Tozer, E.T. (1969) *Geology of the Arctic Archipelago*; Chapter 10 in Geology and Economic Minerals of Canada, Douglas, R.J.W. (ed); Geological Survey of Canada, Economic Geology Report No.1: 548-590.

Trettin, H.P. (1994) *Pre-Carboniferous geology of the northern part of the Arctic Islands.* Geological Survey of Canada, Bulletin 430: 248 pp.

Trettin, H.P. (1991) *Tectonic Framework*; Chapter 4 in Geology of the Innuitian Orogen and Arctic Platform of Canada and Greenland, H.P. Trettin (ed); Geological Survey of Canada, Geology of Canada, no.3 (also Geological Society of America, The Geology of North America, v.E): 57-66.

Trettin, H.P. (1989) *The Arctic Islands*. Chapter 13 in The Geology of North America – An Overview, Bally, A.W., and Palmer, A.R., (eds); Geological Society of America, The Geology of North America, v.A.

van Berkel, J.T., Schwerdtner, W.M., and Torrance, J.G. (1984) *Wall-and-basin structure: an intriguing tectonic prototype in the central Sverdrup Basin,*

Canadian Arctic Archipelago. Bulletin of Canadian Petroleum Geology **32**: 343-358.

Villeneuve, M. and Williamson, M-C. (2003) *$^{40}Ar/^{39}Ar$ Dating of mafic magmatism from the Sverdrup Basin magmatic province*. International Conference on Arctic Margins, Programs/Abstracts:45.

Villeneuve, M. and Williamson, M-C. (In Press) *$^{40}Ar/^{39}Ar$ Dating of mafic magmatism from the Sverdrup Basin magmatic province*.

Williamson, M-C. (1988) The Cretaceous igneous province of the Sverdrup Basin, Canadian Arctic: Field relations and petrochemical studies. Ph.D. thesis, Dalhousie University, Halifax, Nova Scotia, 417 pp.

Zentilli, M. (2005) Personal Interview. March 8, 2005.

Zentilli, M., Williamson, M-C., Mosher, A., and Ferguson, C. (2003) *Thermal effects of basaltic magmatism, salt structures and Tertiary faults on the petroleum system in Strand Fiord, Axel Heiberg Island, Nunavut: A field report*. International Conference in Arctic Margins, Program/Abstracts: p.28.

APPENDIX A ADDITIONAL ESEM DATA

Section 4.5.2.2 describes how the Environmental Scanning Electron Microscope (ESEM) confirmed the presence of four mineral phases within the Wolf Intrusion (sample AX03-68). Using Qualitative Spectral Analysis, a comparison of the AX03-68 to a fresh, unaltered sill, EL84-50 showed similar spectrums. As mentioned previously, sample EL-84-50 is a well-preserved, unaltered portion of basaltic sill from northern Ellesmere comprising of similar mineralogy to volcanic and intrusive rocks in the Strand Fiord area (Williamson, 1988).

A quick inspection of EL84-50 showed an area consisting of three mineral phases. The area, referred to as Area A of (Figure A.1a), shows three phases as light, medium, and dark grey. Qualitative spectral analysis provided spectrum for each mineral grain. The first grain is very light grey and has a subhedral shape. The spectrum, Figure A.1b, shows a high proportion of iron with titanium present suggesting titanomagnetite is present. The second grain is medium grey displaying a subhedral shape. High values of silica with calcium and iron occur as the major peaks on the spectrum (Figure A.1c) signifying a clinopyroxene composition. The third grain is dark grey and has high silica values with aluminium, calcium, and minor iron (Figure A.1d); suggesting a composition of a feldspar, particularly that of plagioclase.

Analysis of another area consisting of the same mineral phases confirmed the above identifications (Area B). The grey scale image of Area B (Figure A.2a) shows the same mineral phases (light, medium, and dark grey) as Area A of EL84-50. The first grain, yields the same spectrum as Area A showing high values of iron and titanium verifying titanomagnetite is present (Figure A.2b). The second grain of Area B shows

peaks of silica, calcium, and iron confirming a clinopyroxene composition (Figure A.2c). The last grain, displays aluminium, calcium, and minor iron (Figure A.2d); suggesting plagioclase is present.

A third and last area generates spectra for an olivine grain. The grey scale image, Figure A.3c, shows a cracked grain (labelled 4) with alteration around the cracks. The spectrum outputs a high silica value with iron and oxygen. This proves an olivine composition, primarily that of the iron rich fayalite.

Using the above preliminary analysis as a guide for the chemical compositions, the testing of the sample AX83-68 produced similar spectrum. The results for the Qualitative Spectral Analysis for sample AX83-68 are located in Section 4.5.2.2.

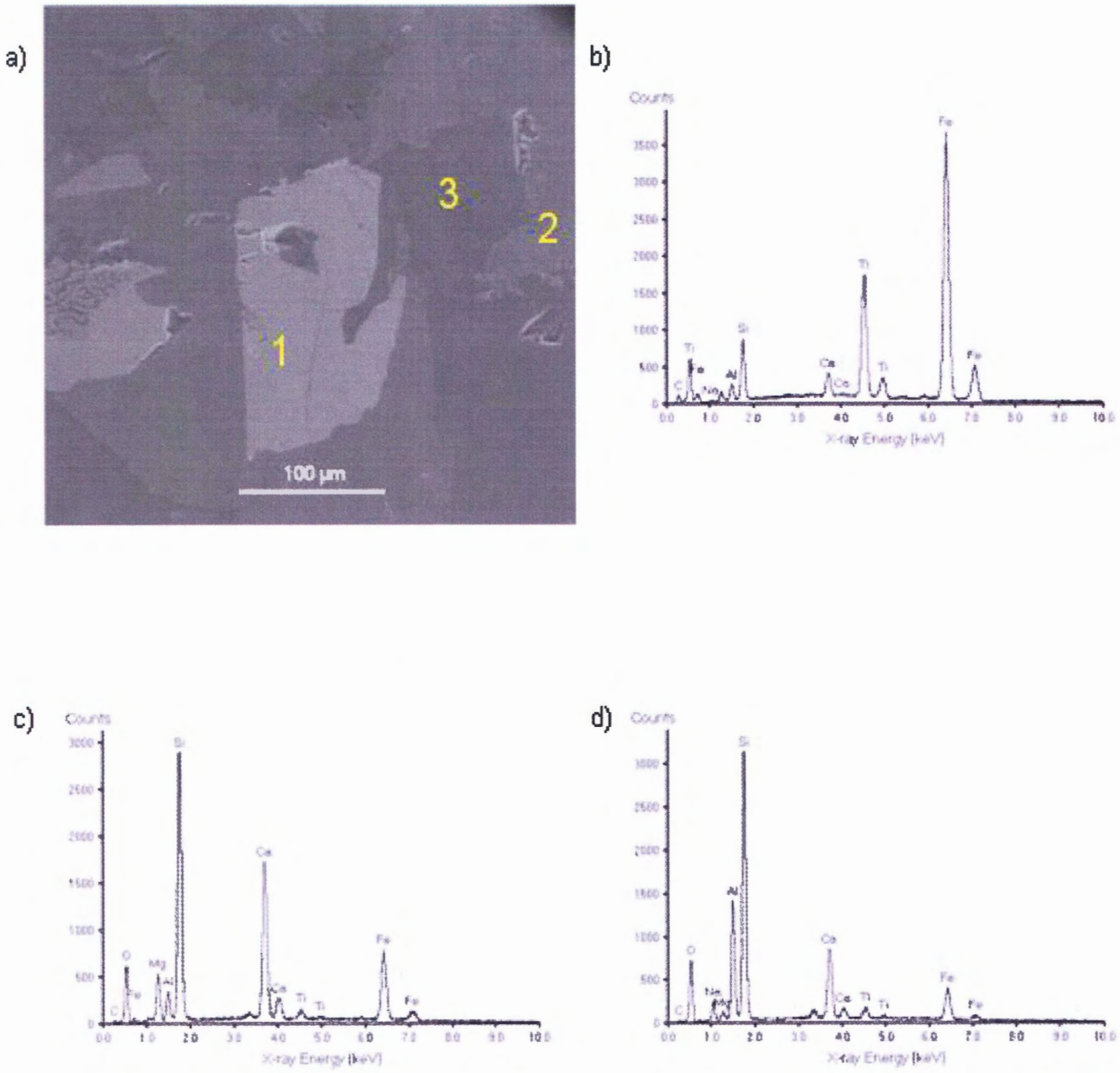

Figure A.1 - a) Area A gray scale image displaying three mineral phases, light, medium, and dark for EL84-50; b) Spectrum analysis for grain 1; c) Spectrum analysis for grain 2; d) Spectrum analysis for grain 3. The above analysis confirms the identification of the mineral phases described during petrography.

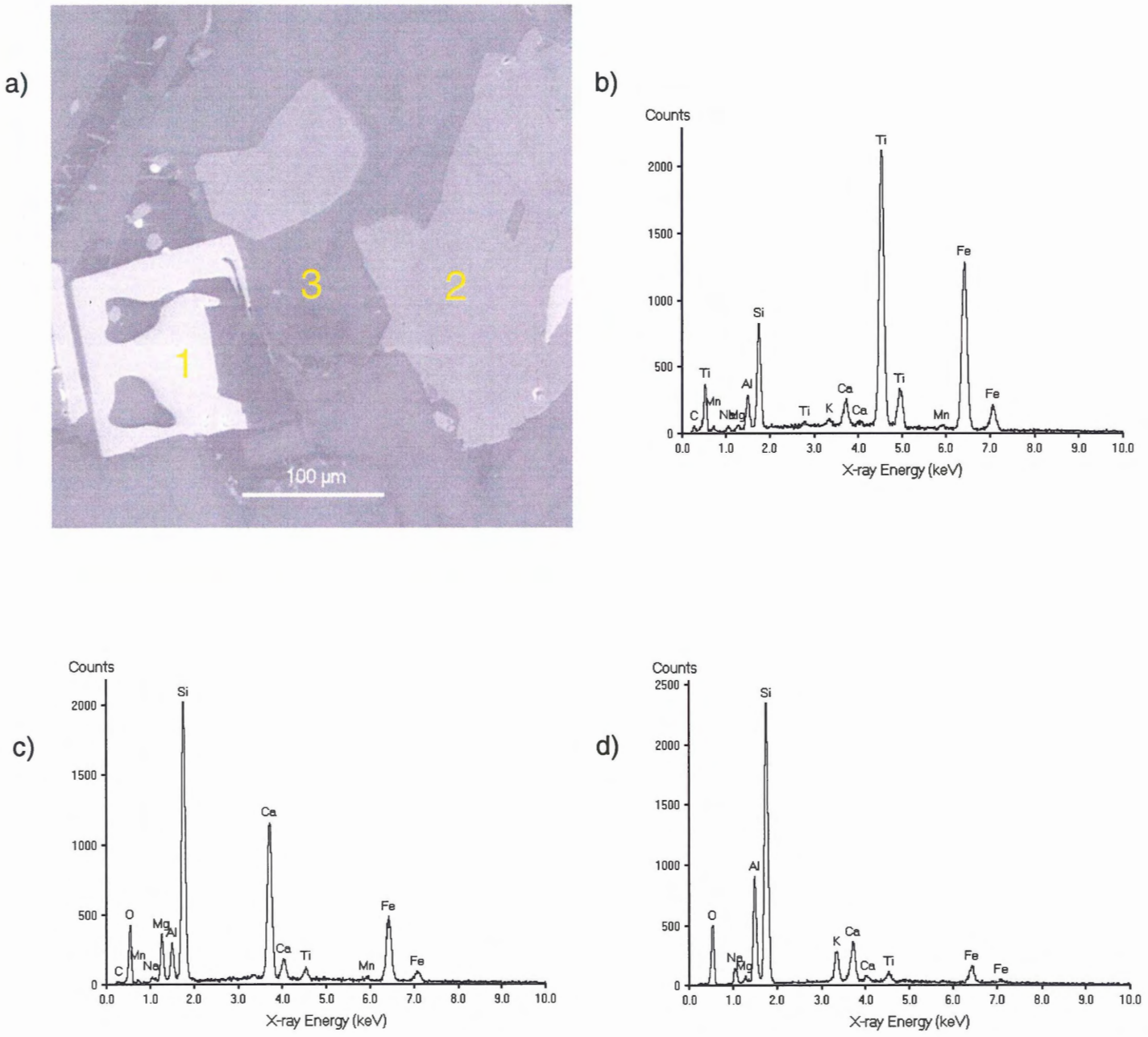

Figure A.2 - a) Grey scale image of Area B displaying the three mineral phases, light, medium, and dark for EL84-50; b) Spectrum analysis for grain 1; c) Spectrum analysis for grain 2; d) Spectrum analysis for grain 3. The above analysis confirms the identification of the mineral phases present in Area A.

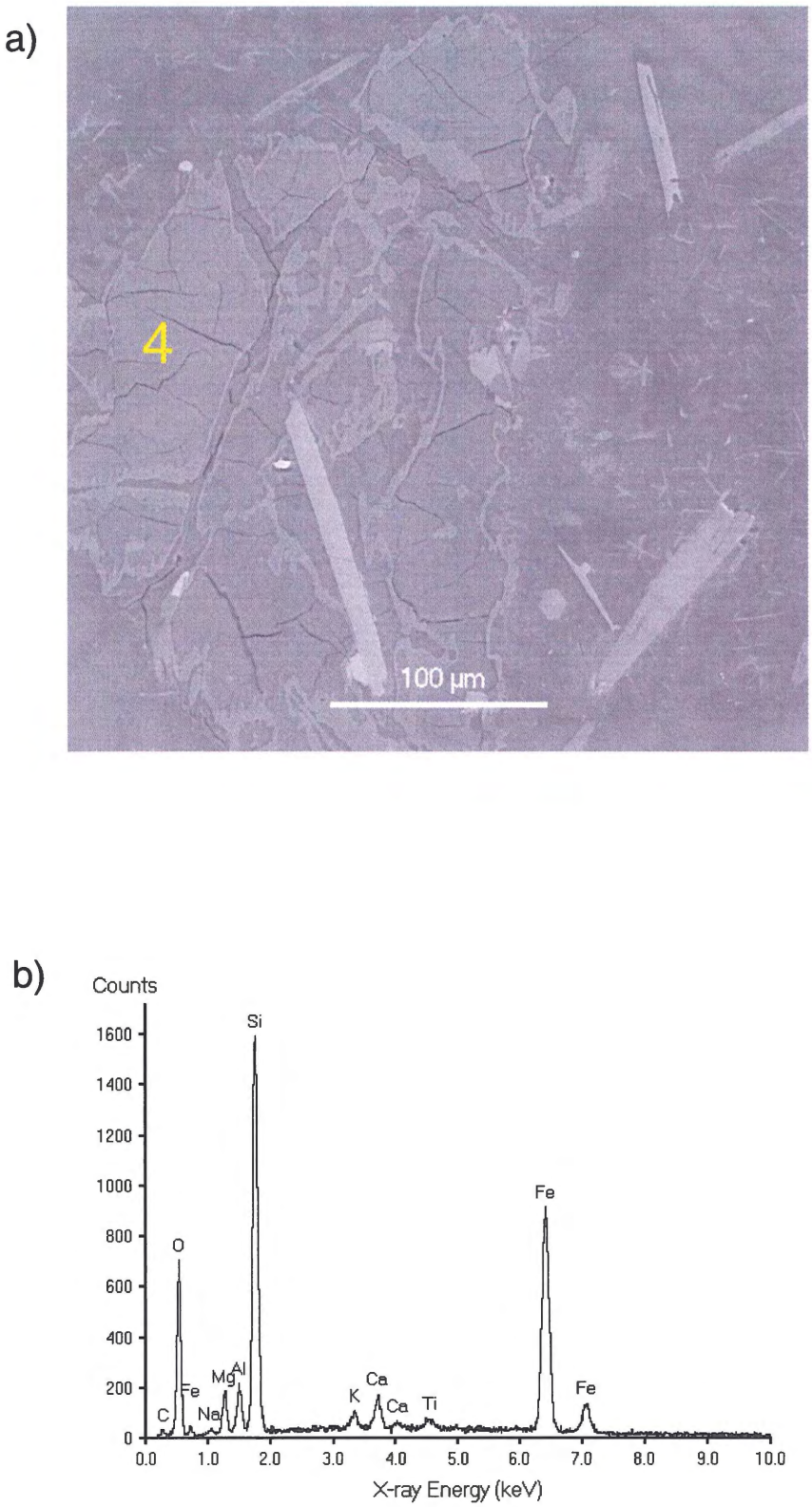

Figure A.3 - a) Grey scale image of Area C displaying a cracked olivine grain for EL84-50; b) Spectrum analysis for grain 4 confirms the presence of olivine.